AN ABSTRACT OF THE THESIS OF

Keith E. Williams for the degree of Master of Science in Civil Engineering

presented on June 1, 2012.

Title: Accuracy Assessment of LiDAR Point Cloud Geo-Referencing

Abstract approved:

_____

Michael J. Olsen

Three-dimensional laser scanning has revolutionized spatial data acquisition and can be completed from a variety of platforms including airborne (ALS), mobile (MLS), and static terrestrial (TLS) laser scanning. MLS is a rapidly evolving technology that provides increases in efficiency and safety over static TLS, while still providing similar levels of accuracy and resolution. The componentry that make up a MLS system are more parallel to Airborne Laser Scanning (ALS) than to that of TLS. However, achievable accuracies, precisions, and resolution results are not clearly defined for MLS systems. As such, industry professionals need guidelines to standardize the process of data collection, processing, and reporting. This thesis lays the foundation for MLS guidelines with a thorough review of currently available literature that has

been completed in order to demonstrate the capabilities and limitations of a generic MLS system.

A key difference between MLS and TLS is that a mobile platform is able to collect a continuous path of geo-referenced points along the navigation path, while a TLS collects points from many separate reference frames as the scanner is moved from location to location. Each individual TLS setup must be registered (linked with a common coordinate system) to adjoining scan setups. A study was completed comparing common methods of TLS registration and geo-referencing (*e.g.,* target, cloud-cloud, and hybrid methods) to assist a TLS surveyor in deciding the most appropriate method for their projects. Results provide insight into the level of accuracy (mm to cm level) that can be achieved using the various methods as well as the field collection and office processing time required to obtain a fully geo-referenced point cloud.

Lastly, a quality assurance methodology has been developed for any form of LiDAR data to verify both the absolute and relative accuracy of a point cloud without the use of retro-reflective targets. This methodology incorporates total station validation of a scanners point cloud to compare slopes of common features. The comparison of 2D slope features across a complex geometry of cross-sections provides 3D positional error in both horizontal and vertical

component. This methodology lowers the uncertainty of single point accuracy statistics for point clouds by utilizing a larger portion of a point cloud for statistical accuracy verification. This use of physical features for accuracy validation is particularly important for MLS systems because MLS systems cannot produce sufficient resolution on targets for accuracy validation unless they are placed close to the vehicle.

Accuracy Assessment of LiDAR Point Cloud Geo-Referencing

by
Keith E. Williams

A THESIS

submitted to

Oregon State University

in partial fulfillment of
the requirements for the
degree of

Master of Science

Presented June 1, 2012
Commencement June, 2012

Master of Science thesis of Keith E. Williams presented on June 1, 2012.

APPROVED:

_____

Major Professor, representing Civil Engineering

_____

Head of the School of Civil and Construction Engineering

_____

Dean of the Graduate School

I understand that my thesis will become part of the permanent collection of Oregon State University libraries. My signature below authorizes release of my thesis to any reader upon request.

_____

Keith E. Williams, Author

ACKNOWLEDGEMENTS

I would first like to thank my committee members David Hurwitz, John Sessions, and Robert Schultz for their time and assistance in reviewing this document.

A big thanks to Prof. Schultz for enlightening me to the world of surveying; without this enlightenment I would have never sat down to my first PLSO student appreciation dinner. At this dinner I just happened to sit down next to Scott Ashford and Mike Olsen…both of them asking, “so have you thought about grad school?”

I cannot extend enough appreciation for all the help and guidance Mike Olsen has given me over the last couple of years. I was initially a little nervous, wondering if grad school was the right choice for me, but thanks to Dr. Olsen’s mentoring it has been nothing but a pleasure. My only disappointment was that I never got to witness M$lice perform in front of an audience!

Thanks to Abby Chin, Kris Puderbaugh, Hamid Mahmoudabadi, Jeremy Conner, John Raugust, Mahyar Sharifi, Rubini Santha, and Shawn Butcher for all the assistance and collaboration within the office.

I would like to also thank the many organizations who have made this research possible through equipment, software, training, and experience:

Leica Geosystems, Maptek I-site, David Evans and Associates, Oregon DOT, and the Transportation Research Board (NCHRP 15-44). Additionally, thank you to Gene Roe, Craig Glennie, and Marcus Reedy for providing feedback and expert guidance on the NCHRP project.

Finally, thanks to all my family for their support in whatever I decide to do, and thank you to Shawna Zimmerman for always being there by my side.

CONTRIBUTION OF AUTHORS

Dr. Michael Olsen has provided input and direction on all projects presented herein and has assisted with the format and editing of this document.

Abby Chin, Shawn Butcher, and Kris Puderbaugh assisted with data collection for Accuracy Assessment of Geo-Referencing Methodologies for Terrestrial Laser Scan Site Surveys.

TABLE OF CONTENTS

Page

TABLE OF CONTENTS

Page

TABLE OF CONTENTS

LIST OF FIGURES

LIST OF FIGURES

LIST OF FIGURES

LIST OF TABLES

1 INTRODUCTION

Light Detection And Ranging (LiDAR) has experienced explosive growth over the last decade with new possibilities continuously being realized. In engineering applications, this field has branched into three distinct divisions: 1) Airborne Laser Scanning (ALS), 2) Static Terrestrial Laser Scanning (TLS), and more recently 3) Mobile Laser Scanning (MLS). Many similarities exist between these different platforms; however, differences in these platforms provide varying levels of precision, accuracy, and resolution that can be obtained with current methods (Vosselman and Maas, 2010).

Significant research has been accomplished to develop and calibrate these systems for accurate surveying (*e.g.*, Barber *et al*., 2008; Cahalane et al., 2010; Glennie 2007a, 2007b, 2009; Glennie and Lichti, 2010; Haala et al. 2008; Rieger et al., 2010). Evidence that these systems can be used for accurate surveying has led to many applications including earthwork quantities, slope stability, pavement analysis, urban modeling, infrastructure analysis and inventory (Grafe, 2008), coastal erosion (Olsen et al., 2009), feasibility studies, route alignment, environmental assessments, 3D visualizations, noise assessment, vegetation management planning, and accident investigation (Duffell and Rudrum, 2005).

1.1 THESIS FORMAT

This thesis has been formatted to follow the manuscript document format.

Chapter 2 provides a thorough review of key literature pertaining to the technology, techniques, and applications of mobile laser scanning (MLS). Research documents were obtained from industry magazines and websites, technical reports, peer-reviewed journals, and conference presentations produced by industry leaders across the globe.

Chapter 3 presents a technical manuscript that has been published in the ASPRS Sacramento 2012 Proceedings titled *Accuracy Assessment of Geo-Referencing Methodologies for Terrestrial Laser Scan Site Surveys*. The purpose of this study was to compare geo-referencing methods for terrestrial laser scanning (TLS) and to document information regarding time, accuracy, and possible introduction of error to assist a TLS surveyor in deciding which method is most appropriate for their projects.

Chapter 4 focuses on the fundamental concern of how to verify horizontal accuracy of a point cloud, which arises in ALS, MLS, and TLS systems. Resolution of this issue comes by way of a methodology that has been designed to compare against total station point measurements in order to verify proper horizontal and vertical alignment of a scan point cloud.

Chapter 5 provides overall conclusions of this thesis, and provides insight regarding potential future research.

The appendices contain the glossary of terms developed for chapter 2 (Appendix A), individual target transformation parameters for chapter 3 (Appendix B), condensed procedures for the spreadsheet discussed in chapter 4 (Appendix C), and the digital spreadsheet used to develop the methodology in Chapter 4 (Appendix D).

1.2 BASICS OF LIDAR

Light detection and ranging (LiDAR) is an active (*i.e.* energy is emitted) method for remotely sensing distant objects. It can be used to generate 3D models. Coordinates of the reflected object are determined by the angle of the emitted pulse and the range to the object. The range measurements are determined by one of two methods, (1) time-of-flight or (2) phase shift. Time-of-flight scanners precisely record the time it takes for an emitted laser pulse to reflect off of remote objects and return to the scanner, while phase shift scanners emit a sinusoidally modulated laser pulse, and calculate distance using the phase shift principle. This method can be used to more precisely calculate the distance over short intervals (typically up to 75m), consequently resulting in a higher level of positional accuracy and much faster data acquisition rate. These benefits, however, come at the expense of range. As

such, time-of-flight systems (typical range: 100 – 1000 m) are generally more common for civil engineering and transportation applications.

Most time-of-flight and phase shift systems are able to distinguish multiple returns from a single pulse, known as echoes, which provide useful information for filtering data. For example, in the case of a forest (Figure 1), part of the emitted laser beam will strike the top of the trees (first return), part will strike the branches (intermediate returns), and part will (hopefully) return from the ground (last return).

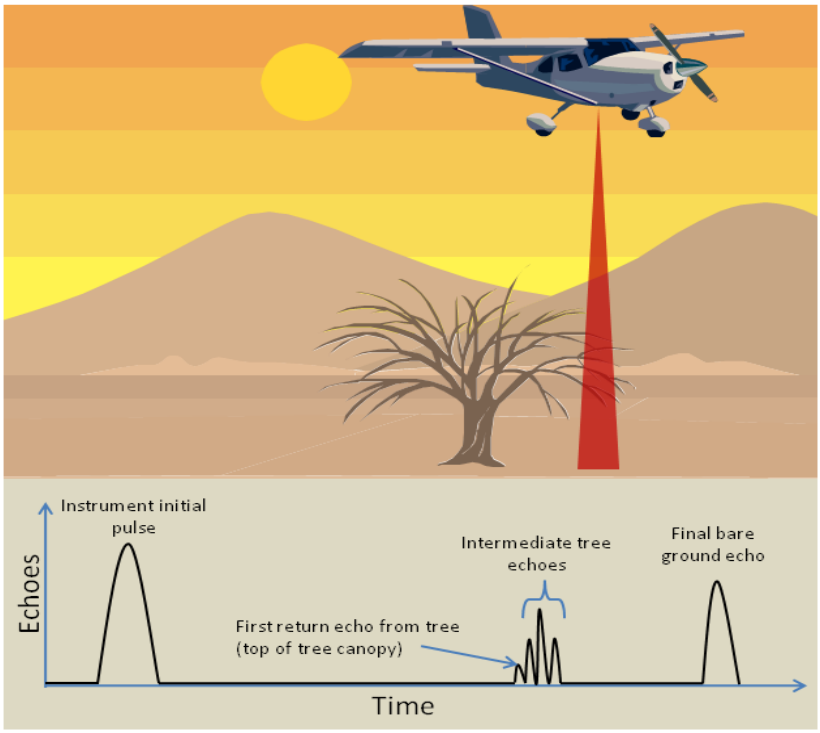

Figure 1. Example illustrating concept of multiple returns from a single LiDAR pulse.

To distinguish each echo, the distance between them must be greater than half the pulse length (Vosselman and Maas, 2010). For example, if the pulse width is 8ns, objects must be greater than 1.2m apart to be distinguished (assumed speed of light is 3 x 10^8 m/s and refractive index is 1.0). This can be calculated by:

$$\text{pulse length} = \text{pulse width} \times \frac{\text{speed of light}}{\text{refractive index}} \quad (1)$$

The amplitude of returned echoes can be recorded, and are based primarily on the reflectance of the object returning the echo. This amplitude of returned echo, called intensity, can be used to assist in distinguishing between different objects in the scan view. Vosselman and Mass (2010) discuss how intensity values can be used to distinguish between objects at similar elevations, such as a manhole cover on a street, or painted street markings (Figure 2).

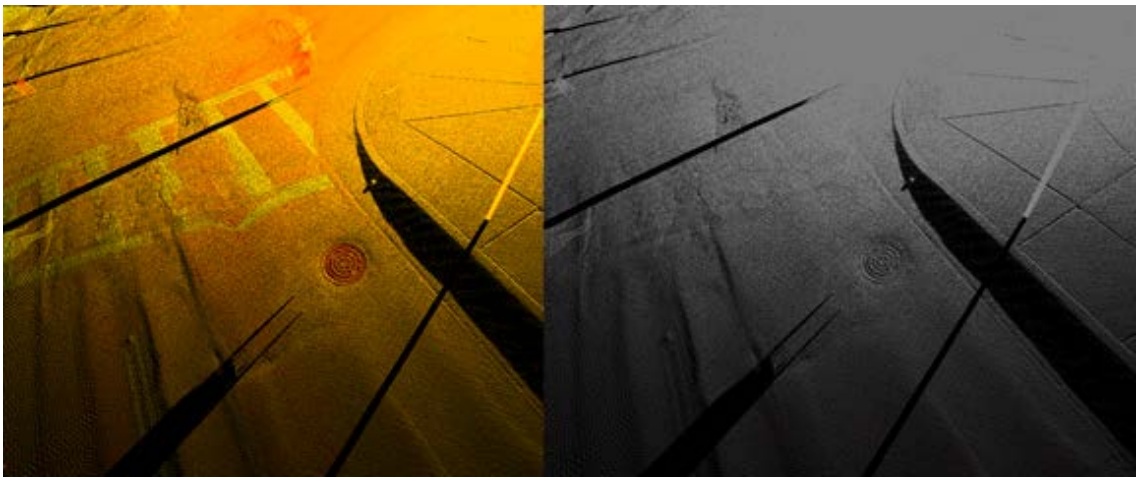

Figure 2. Painted street markings and manhole cover can be better distinguished in the intensity return image on the left.

How intensely a laser pulse is returned to the scanner is determined by many factors such as range, angle of incidence, atmospheric conditions, and the material properties of the object being scanned. Some of these factors are normalized so that a consistent intensity value can be obtained from the same object at different locations (Soudarissanane *et al.*, 2011). For example, objects closer to the scanner will have a more intense return than objects further away; this can be normalized so that range does not contribute to the difference in intensities.

Scanning sensors can record returning echoes from a single pulse in one of two ways, discretely, and full-waveform (Figure 3). In the discrete mode, the scanning sensor records the returns as a binary result (yes, there is

a return or no, there is not a return). Full-waveform scanning sensors are able to record the entire backscattered waveform (Vosselman and Maas, 2010).

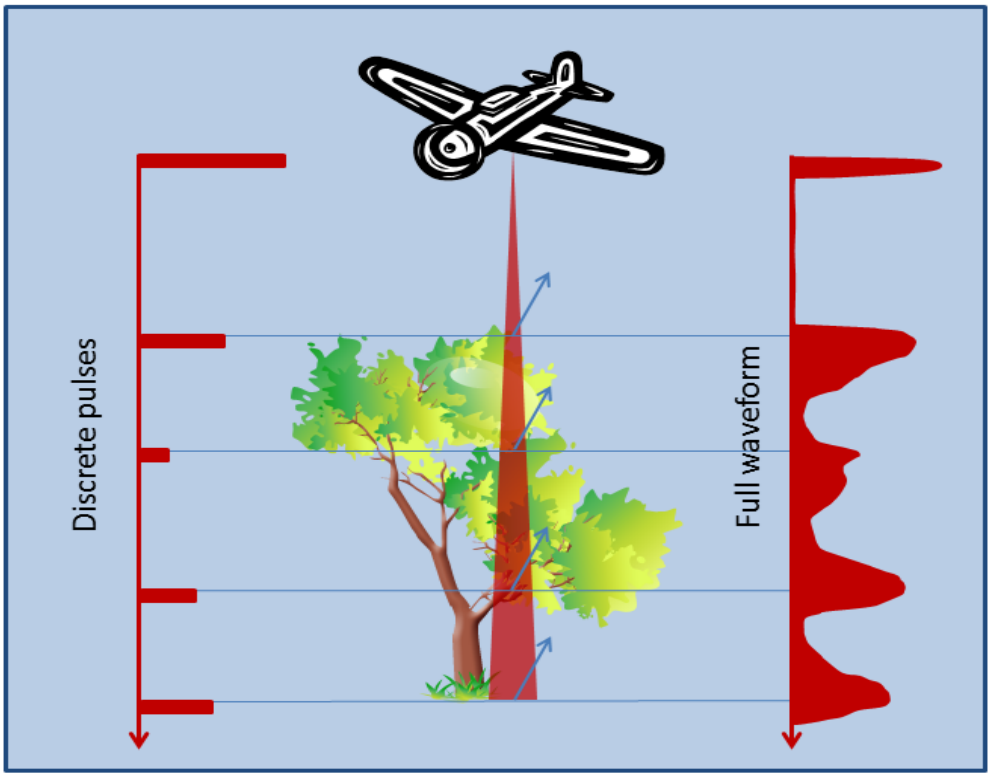

Figure 3. Discrete pulses vs. full-waveform returns.

The return of the full-waveform allows for advanced determination of the peaks, which may indicate additional returns that were not recorded in the discrete analysis. Further, material properties and geometry are generally better distinguished by a full-waveform scanner. For example, scanning at an oblique plane (Figure 4) will return a pulse width greater than the initial scanner pulse width; whereas a flat plane would return the same pulse width.

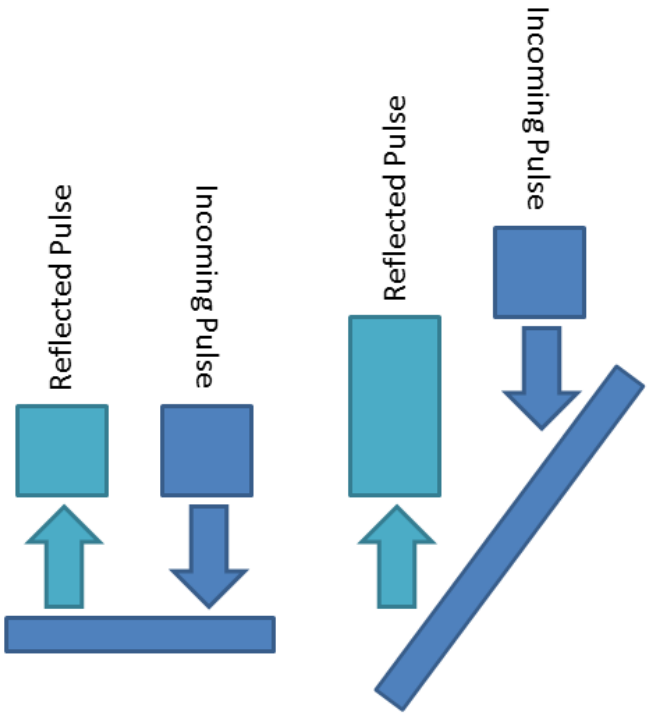

Figure 4. Increase of pulse width on oblique surface.

Remote assessment using LiDAR (Duffell and Rudrum, 2005) can provide high speed data collection in areas with restricted access and/or safety concerns. Particularly, use of MLS on transportation corridors can minimize roadway delays. LiDAR sensors have been equipped on static ground-based platforms, and mobile platforms such as airplanes, vehicles (Figure 5), boats, helicopters, UAVs, etc. Much work has been done to develop and calibrate these devices for accurate surveying (*e.g.*, Barber *et al.*, 2008; Cahalane *et al.*, 2010; Glennie 2007a, 2007b, 2009; Glennie and Lichti, 2010; Haala *et al.* 2008; Rieger *et al.*, 2010). The primary focus of this review

pertains to mobile vehicular scanning, as opposed to airborne, railway, terrestrial, and other platforms. Although airborne scanning has become more mainstream since the 1990's (Duffell and Rudrum, 2005), often increased visibility, accuracy, and resolution needs require a ground-based scanning solution, particularly in transportation engineering applications. Because static scanning has efficiency limitations, mobile scanning has become an effective solution to rapid data collection in recent years with advancements in scanning speed and accuracy, global positioning systems (GPS), and inertial measurement units (IMU).

Figure 5. MLS system (TITAN, courtesy of DEA).

2 REVIEW OF APPLICATIONS OF MLS IN TRANSPORTATION

2.1 MLS SYSTEMS

2.1.1 Background and history

Prior to LiDAR based mobile mapping, other systems used a nearly identical setup but relied on photogrammetric methods. The first fully functional system, GPSVan, was created by the Center for Mapping at Ohio State University. It utilized GPS, gyro, DMI, two CCD cameras, and a voice recorder (Burtch, 2006).

Glennie (2009) recounts the history of the first MLS system, constructed in 2003, which was a helicopter based LiDAR setup turned on its side and mounted onto a vehicle. The system was used to survey Highway 1 in Afghanistan, which was potentially hostile for helicopter based scanning. This initial system had many downfalls; primarily the limited field of view that accompanies airborne systems. However, this system proved successful and demonstrated the potential value of MLS, upon further refinement. Currently, there are several MLS systems available through commercial vendors. Yen et al. (2010) provides a comparison of many available mobile scan systems.

2.1.2 Components

Even though there are many MLS mapping systems, most systems consist of five distinct components:

1. the mobile platform
2. positioning hardware (*e.g.*, GNSS, IMU)
3. 3D laser scanner(s)
4. photographic/video recording, and
5. computer and data storage.

2.1.2.1 Mobile platform

A mobile platform connects all data collection hardware into a single system. The platform is usually a rigid platform, precisely calibrated to maintain the positional differences between the GPS, IMU, scanner(s), and imaging equipment. It also provides a means to connect to the vehicle being used in the data collection process (Figure 6).

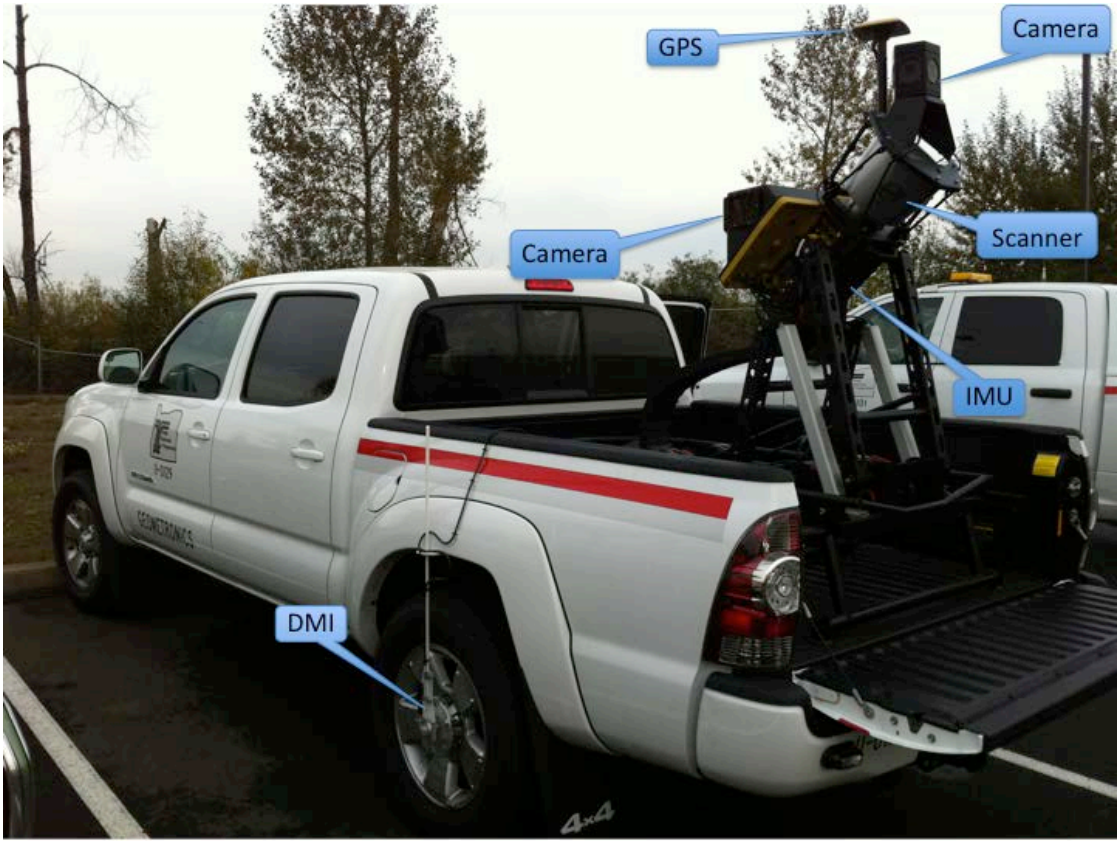

Figure 6. MLS system components (Topcon IP-S2 HD system owned by ODOT).

2.1.2.2 Positioning hardware

Positioning hardware varies significantly from system to system. However, at a minimum most systems incorporate at least one GPS/GNSS receiver and an inertial measurement unit (IMU). The GPS/IMU system work together to continually report the best possible position. In times of poor satellite coverage, the IMU manages the bulk of the positioning workload.

However, when satellite coverage is ideal, the IMU's positional information is then updated from the GPS (Schwarz *et al.*, 1993; Barber *et al.* 2008). In addition to augmenting the GPS in periods of poor satellite coverage, the IMU must continually fill gaps between subsequent GPS observations. Typical GPS receivers report positioning information at the rate of 1 Hz (*i.e* one measurement per second). However, during the course of a second, a vehicle will experience substantial movement, particularly when traveling at high speeds. The IMU records positional information at a much higher rate, typically around 100 Hz, or 100 times per second (Shan and Toth, 2009; Yousif *et al.*, 2010). GPS/IMU data quality is typically the primary factor in gaining the best accuracy for a LiDAR point cloud (Ussyshkin and Boba, 2008). Barber *et al.* (2008) explain how detailed route planning and satellite almanac checks can greatly improve accuracy with better satellite coverage.

More complex MLS systems will utilize multiple GPS receivers, an IMU, and also a distance-measuring instrument (DMI) for improved positioning. The DMI, a precise odometer, reports the distance traveled to improve GPS/IMU processing. DMI's provide direct distance traveled by measuring distance along the ground path, typically by mounting to one of a vehicles rear wheels. In some MLS systems the DMI may be used only to trigger image capture at fixed distances (Kingston *et al.*, 2006).

2.1.2.3 3D laser scanner

Many different types of 3D laser scanners are well suited for setup on a mobile platform. These scanners are set to operate in a line scan (or planar) mode, where the scan head stays fixed and only internal mirror movement takes place. Yoo *et al.* (2010) demonstrate how scanner orientation on the mobile platform can have drastic effects on the quality of data captured. In order to minimize the number of passes necessary to fully capture data, most platforms utilize more than one scanner with view orientations at different angles.

2.1.2.4 Photographic/video recording

Photographic and video recording provides greater detail than the laser scan alone (Toth, 2009). The primary reason for this equipment is to color individual scan points in the point cloud to the representative real world color. This is done by recording a red, green, blue (RGB) value to the geo-referenced point location. This point coloring can make a highly dense point cloud appear as if it were a photograph. Also, visual record provided by this equipment can assist users in determining abnormalities in the scan data.

2.1.2.5 Computer and data storage

Advancements in computer processing speed and data storage capabilities have lowered the cost, and increased the efficiencies of working with LiDAR data (Vosselman and Maas, 2010). Mobile systems need to be capable of processing and storing large quantities of data from many sources. The data includes: the point cloud, IMU data, GPS data, DMI data, and all photographic and video data which must then all be connected with a common, precise time stamp.

2.1.3 System calibration

Accurate location of a ground coordinate from a mobile laser scan requires finding the value of 14 (or more, depending on the number of scanners) parameters for single scanner systems, each with a certain level of uncertainty. These parameters are the X, Y, Z location of the GPS antenna, the roll, pitch, and yaw angles of the mobile platform, the three boresight angles from each individual scanner, the X, Y, Z lever arm offsets to the IMU origin from each scanner, and the scanner scan angle and range measurement (Glennie, 2007).

Various methods can be used to help pare down some of the uncertainty of the individual values. Barber *et al.* (2008) discuss a calibration procedure

used to determine lever arm offsets, which consists of multiple passes over the same section of roadway. The lever arm offsets will be propagated thorough the data set, and can be reduced by analyzing differences between the separate passes.

Boresight errors can also be determined by performing multiple passes over a region. Glennie (2007) discusses how these boresight values can be determined using a least squares adjustment to align the overlapping point clouds. Rieger *et al.* (2010) also describe how boresight alignment of 2D laser scanners on a mobile platform can be determined by comparing to a reference 3D point cloud of the same region. Rieger *et al.* (2010) also describe a method of using multiple passes of an area to determine lever arm offsets between the IMU and measurement axis of the scanner.

2.1.4 Software and data processing

The point cloud (Figure 7) consists of raw data points collected by the scanner, these data points are referenced from the scanner origin. For most uses of MLS data, several processing tasks need to be completed:

1. Geo-referencing the data,
2. Mapping color information,
3. Filtering\cleaning of points, and
4. Generating models or extracting features from the point cloud.

Aside from geo-referencing the data, most processing tasks are similar between airborne, static TLS, and MLS systems.

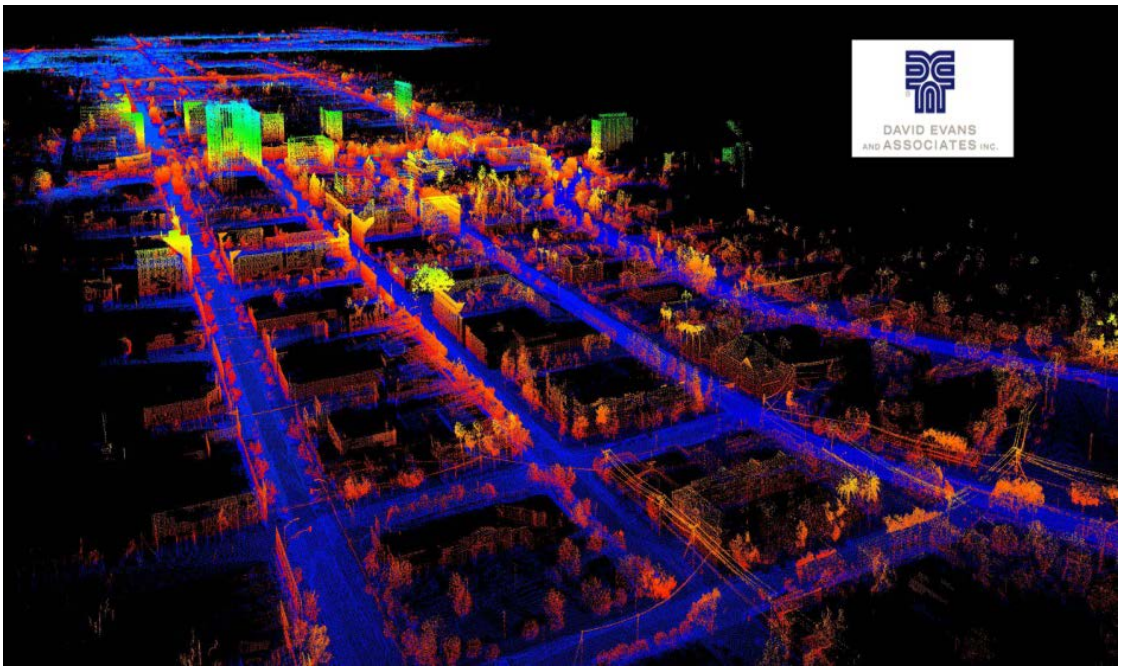

Figure 7. Point cloud data obtained through MLS (Courtesy of DEA).

2.1.4.1 Geo-referencing the data

A prime interest in software processing is to register, or combine, many independent 3D point clouds into a single data set referenced in a single coordinate system with minimal error (Brenner, 2009). Point cloud data must undergo several software processing procedures to accurately position the point cloud in the selected coordinate system. Components of the MLS system simultaneously collect and store data (*e.g.*, the GPS stores location,

the scanner collects point locations relative to its origin, the IMU provides location corrections, and the color information is collected by photographic or video methods). This data must be precisely time-stamped for integration (Rieger *et al.*, 2010). RTK GPS or post processed kinematic (PPK) GPS are the primary methods employed to geo-reference the MLS data; however, other methods (Barber *et al.*, 2008) can be utilized such as alignment to targets, high resolution TLS data, or ground control points surveyed through traditional methods. Often, alignment to high resolution TLS data and/or ground control points are used as a post-processing validation step to provide a measure of how accurately the MLS system has performed. In areas where the GPS/IMU system did not collect accurate geo-referencing data, the MLS point cloud may be adjusted to ground control through a least squares adjustment. Data processing can also introduce additional errors into a point cloud, but generally it will bring a point cloud into a much higher level of accuracy than the originally captured point cloud, depending on the applied processing procedures (Ussyshkin and Boba, 2008).

2.1.4.2 Mapping color information

As a LiDAR scanner collects data, a precisely calibrated image recording system collects color information to map to each individual point in the point cloud (Vosselman *et al.*, 2010). This color information is stored as a

numerical value (*e.g.*, 0-255) in the red, green, and blue spectrum (RGB). This color mapping is typically tagged to the individual points in a point cloud so that a location given as X, Y, Z is then amended to include R, G, B values (*i.e.* X,Y,Z,R,G,B). In some instances, calibrated images can be overlaid on a point cloud adding X, Y, Z data to a 2D image. This provides users more accustomed to working in a 2D environment the ability to transform 2D drafting into a 3D environment (Knaak, 2010).

2.1.4.3 Filtering of points

Following registration, point cloud data is typically filtered to eliminate unwanted features, including pits and birds, objects passing in the scanner view, unwanted vegetation, or, more generally, anything that is not needed by the end user. Filtering is also commonly done to reduce the file size of the deliverable point cloud since the full dataset can require intense computational power and data storage. Some common filtering techniques include: first, intermediate, and last returns, selection of every i^{th} point, minimum separation between points, octree, k-d tree, elevation, range, and intensity (see Vosselman *et al.*, 2010, for examples of filtering algorithms). Note that octree and k-d tree structures are also generally used as data organization schemes to improve interactivity of the dataset.

2.1.4.4 Generating models from the point cloud

Mathematical computations are not easily performed on point cloud data. Typically, these point clouds are modeled using triangulation or gridding techniques for bare earth models, or by applying least square fitting of geometric primitive shapes (*e.g.*, planes, squares, rectangles, cylinders, spheres, etc.) to the structures found in the point cloud. Typically, modeling of features in a point cloud incorporate an automated or semi-automated segmentation algorithm; this algorithm predicts points that can be modeled to a real world object, permitting extraction of the modeled structure (Vosselman and Maas, 2010). Various calculations and analyses can then be applied to these models to permit complex calculations such as volume change (*e.g.*, Olsen *et al.*, 2009).

2.1.4.5 Software considerations

In general, the requirements for software packages used for analyzing MLS datasets vary with respect to the final application of the dataset, and the variety of sensor data collected during the survey. However, as a baseline, Rieger *et al.* (2010) describe four tasks that should be possible in various point cloud software programs:

1. All data should be organized into one project where it can be processed and archived.
2. The data should be viewable on different scales, such as micro-scale point clouds and a full project area (*e.g.*, as a rasterized data set).
3. The software should allow for calibration of the various sensors via a strip adjustment.
4. The data should be able to be exported in many different formats, including standardized formats such as LAS and E57, to be compatible with other software.

2.1.4.6 Data exchange formats

A standard data format is crucial to avoid data loss between software packages and data transfer between organizations (*e.g.*, ASPRS LAS, ASTM E57). In addition, conversion between different formats may consume significant time and resources, adversely impacting productivity and delivery schedules. Mobile scanning systems record data from GPS, IMU, laser scanners, images, and video sensors (Glennie, 2009). These data need to be linked through complex file formats that can optimally store the data while maintaining appropriate links. Basic data transferred between applications consists of XYZ position, RGB color, and intensity (I) data, at a minimum.

2.1.4.7 LAS format

ASPRS developed the LAS format for airborne sensors (ASPRS Standards Committee, 2010) which has been successfully integrated into several software platforms and has become the standard in the ALS industry. The LAS file, an open format, allows various LiDAR software tools to export data in a common format that can be utilized across a wide range of platforms, with minimal data loss. The LAS format also enables binary compression of the data to reduce file size and ease transfer. The format provides storage for data classification and identification (*e.g.*, ground, building, vegetation, etc.) of each point in the point cloud. The latest versions of LAS enable full-waveform support, and support classification of features. Important information and metadata related to the dataset including date of acquisition, hardware type, processing information, and projection and coordinate system can be stored in the file. Version 1.4 has been released, and the ASPRS LAS committee is working on version 2.0 (ASPRS Press Release, 2011).

2.1.4.8 E57 format

Recently, the ASTM E57 committee developed specifications for 3D imaging systems, including terrestrial laser scan data. The ASTM E57 file format is designed to be flexible in storing data across a broad range of applications. Externally, it incorporates much of the same data as the LAS

format, but internally the data is stored significantly different. For example, the E57 format enables a user to specify the number of bits to be used to represent the captured data, in addition to the ability to select additional information that is associated with the 3D points. The LAS format, in contrast, only allows the user to select various pre-configured formats. The maximum file size of E57 data is 10 orders of magnitude larger than that of LAS, adding additional flexibility to data management (Huber, 2011). The E57 format also stores ancillary imagery and associated calibrations with the scan data. However, either of these formats would require some modification and testing to fully support mobile scanner data.

2.1.5 Scan deliverables

Common deliverables following laser scan projects include point clouds, CAD models, DTMs, etc. The options, advantages, and disadvantages of each deliverable type can be confusing for someone without substantial laser scanning experience. Guidelines for accuracy reporting have been developed by ASPRS (2005) for airborne LiDAR, and many commonalities can be associated to MLS.

Providing adequate metadata on employed processing and filtering methods can be a challenge. Additionally, because the technology and hardware evolve rapidly, it is difficult for software development to keep pace.

In conventional surveying, a point is tagged with a code for identification during acquisition. In mobile scanning, however, the collected points no longer are individually tagged with specific reference information; additional reference information must be added to individual points through semi-automatic or manual methods.

2.1.5.1 Metadata and specifications

There is currently no standard for reporting instrument specifications (*e.g.*, POB, 2010 lists specifications for current systems, but varying techniques are used to determine the specifications) for static and kinematic laser scan systems, leading to potential confusion when comparing models and systems. Additionally, because the specifications are developed in carefully controlled laboratory testing, they can create unrealistic expectations for data acquired in the real world, which varies significantly based on the application and materials to be scanned. For example, some scanners are better suited for short vs. long-range applications, topographic vs. metal surfaces, etc. Many factors influence overall accuracies and resolution including: range from the vehicle, objects blocking view, material, and speed of the vehicle. The ASTM E57.02 subcommittee is currently working on developing standardized test methods for medium-range 3D imaging systems. Glennie (2007) recommends that at a minimum a boresight calibration report,

and any confidence statistics should be included in the standard deliverables for a survey.

2.2 APPLICATIONS

MLS systems have been utilized along navigable corridors for a variety of applications including earthwork quantities, slope stability, infrastructure analysis and inventory, pavement analysis, urban modeling, and railways (*e.g.*, Grafe, 2008). Ussyshkin (2009) presents additional potential applications of MLS derived from existing airborne applications, such as topography, utility transmission corridors, coastal erosion (*e.g.*, Olsen *et al.*, 2009), flood risk mapping, watershed analysis, etc. Duffell and Rudrum (2005) discuss additional applications of ALS, which are applicable to MLS, such as feasibility studies, route alignment, environmental assessments, 3D visualizations, noise assessment, vegetation management planning, and accident investigation. Olsen *et al.* (2012, In Press) discuss general applications of LiDAR from various platforms in transportation. In addition, the following applications demonstrate some more specific uses of MLS and the types of vehicles that these systems have been employed on. These applications are far from exhaustive, especially as new applications of MLS systems are being realized on a frequent basis. Figure 8 provides a graphical representation of many of the discussed applications.

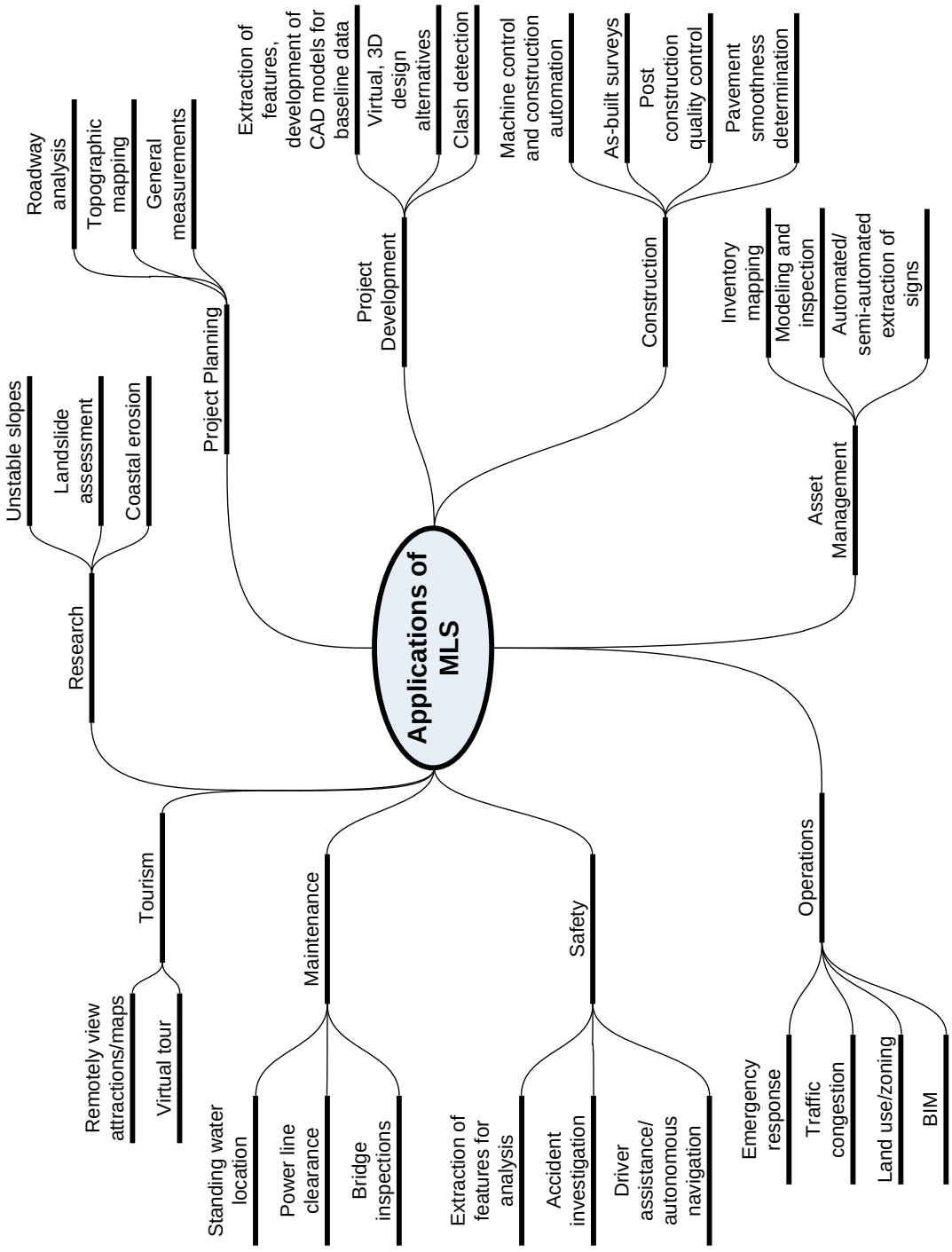

Figure 8. Graphical representation of common applications of MLS.

2.2.1 Project planning

2.2.1.1 Roadway analysis

Grafe (2008) provides examples of a roadway digital surface model, cross sections, and a highway interchange that have all been surveyed using MLS. Additionally, Grafe (2008) demonstrates how a controlled and guided roadway milling machine can be set to automatically cut the road using the digital surface model. Olsen *et al.*, (2012, In Press) show an example of how a vehicular model derived from a static scan can be used to evaluate its ability to navigate through a highway system that has been digitally captured through mobile, prior to travel.

2.2.1.2 Topographic mapping

As in ALS and TLS, topographic mapping is an important application of MLS, including earthwork computations. Jaselskis *et al.* (2003) performed a comparative study of total station and LiDAR based volume calculations from TLS. In this study, a 1.2 percent difference was calculated between the different methods, demonstrating that LiDAR can be a very efficient method of volumetric determination.

Vaaja *et al.* (2011) researched the feasibility of using MLS to monitor topography and elevation changes along river corridors. The vehicles used in

this study were a small, rigid hull, inflatable boat, and a handcart designed to be pulled along by an individual. Results showed that MLS provides accurate and precise change detection over the course of the study (one year), however, very careful control of systematic errors need to be accounted for. Vaaja *et al.* (2011) note that the scanning field of view was often parallel to the topography, resulting in lower accuracy than scanning conducted more perpendicularly to the topography.

Yen *et al*. (2010) evaluate the quality of DTMs of pavement created from MLS data. They determined that although the technology does not currently meet CALTRANS specification requirements, additional refinement of the technology should overcome this limitation in the near future.

2.2.1.3 General measurements

MLS systems provide a permanent record of site conditions that can be measured at any time after the initial collection of point data. This allows users to remotely measure length, volume, elevation, deflection, smoothness, camber, curvature, and others (Jaselskis *et al.*, 2005). Figure 9 demonstrates how linear measurements in a point cloud can be used to find lane width, sidewalk width, and building dimensions.

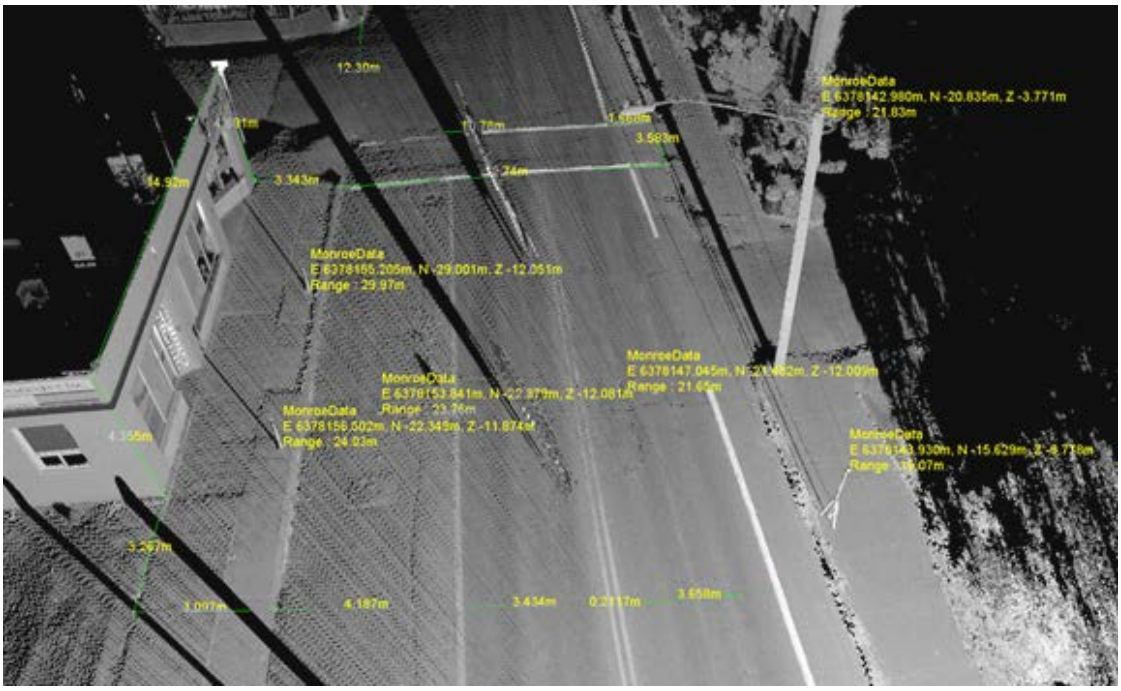

Figure 9. Linear measurements and point coordinates in a dataset.

2.2.2 Project development

2.2.2.1 Extraction of features, development of CAD models for baseline data

Novak (2011) discusses the use of MLS to extract streetlights in El Paso, TX, and store them in a database managing light bulb replacement. Due to an increase in worker safety and a faster rate of completion, MLS was chosen for the project. Jacobs (2005) provides many examples of how this baseline data can be used for further construction development; these include:

slope stability near the roadway, intersection improvement projects, pavement quality monitoring, pavement volume calculation, roadway milling settings, and pre-accident condition data. Figure 10 provides an example of how reflective signage can be semi-automatically detected for extraction and cataloging.

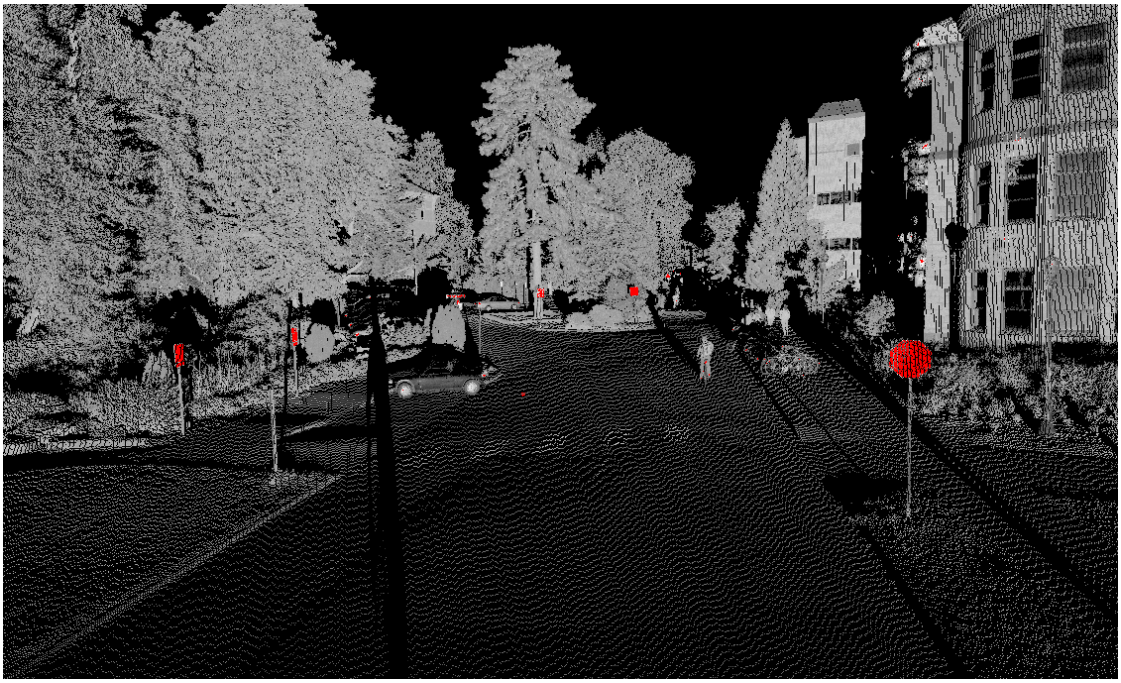

Figure 10. Reflective signs (red) extracted from a point cloud at the Oregon State University campus.

2.2.2.2 Virtual, 3D design of alternatives

A LiDAR point cloud allows designers to test various configurations in a virtual world that recreates the real world in high accuracy. The University of Wisconsin—Madison has utilized MLS to create a virtual world of the

roadways surrounding the campus which is used in their driving simulator, allowing the simulator's users to intimately connect the simulated environment with the real world (Mandli Communications, 2011).

2.2.2.3 Clash detection

MLS systems are capable of providing clearance data (Figure 11) for highway overpasses, bridges, traffic signs, and even roadside high power lines. In many of these instances the georeferencing accuracy of the point cloud is less important than the relative accuracy provided by the scanner (Clancy, 2011). Olsen *et al.*, (2012, In Press) provide examples of bridge height clearances over roadways and waterways. These height clearances can be used to determine if a modeled object can navigate through the section.

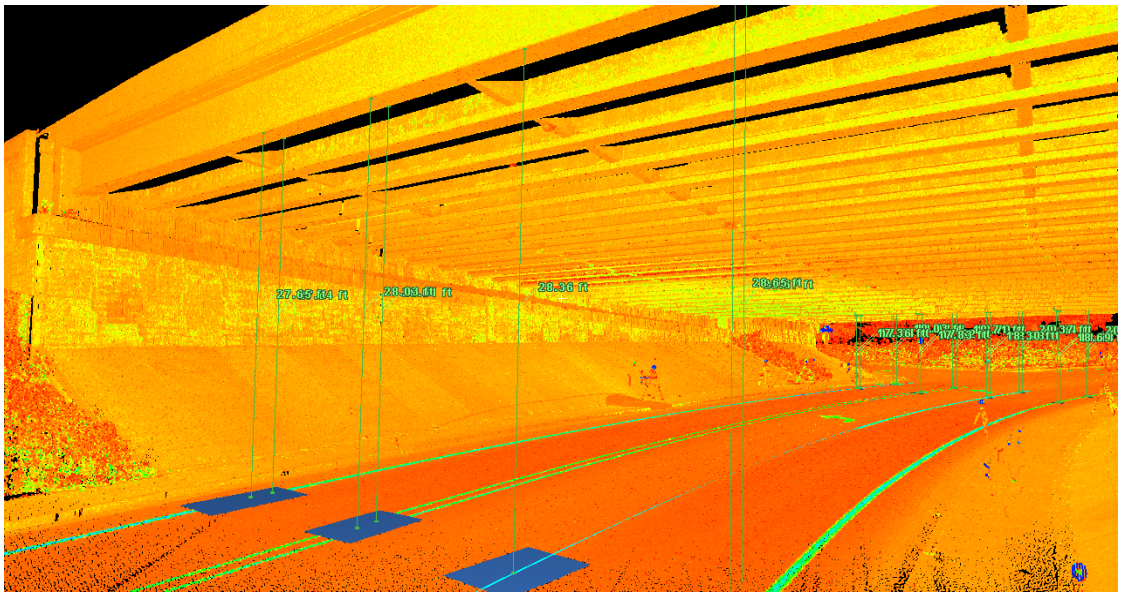

Figure 11. Clearance values measured from point cloud perpendicular to roadway surface (Courtesy of Oregon DOT).

2.2.3 Construction

2.2.3.1 Machine control and construction automation

Singh (2009) discusses the role of laser scanning in machine automation for transportation applications, and how this use enhances efficiency. Rybka (2011) demonstrates an entirely digital site planning project. Periodic scans with a MLS permit initial design, estimates of percent completion, project compliance, and as-builts at project completion. Rybka (2011) also discusses “Design to Dozer” a demonstration of construction automation hosted by Oregon DOT and the PPI Group depicting how MLS

data can be used to create a DTM for machine control and construction automation to grade a site without ever having to drive grade stakes. All grading is done entirely through equipment guided by GPS and a base model created from the 3D point cloud. This presents a cost savings, time savings, and improves site safety.

2.2.3.2 As-built surveys

Singh (2009) discusses the role of a living survey database through all stages of the infrastructure life cycle through planning, design, construction, and maintenance. In addition, digital, as-built records provided by LiDAR can provide significantly more detail than traditional methods (Su *et al.*, 2006).

2.2.3.3 Post construction quality control

In addition to providing high accuracy as-built records, MLS can provide quality control on the construction process. Tang *et al.* (2011) discuss the use of algorithms for determining the flatness of concrete providing permanently documented results of the flatness defects, and permits users to remotely access the surface. Kim *et al.* (2008) verify superelevation slope values, curb design, and soundproofing wall design by creating cross sections of a roadway at 5m intervals.

2.2.3.4 Pavement smoothness determination

The data collected for roadways can be used for several geometric analysis including stopping sight distances, adequate curve layouts, slope, super-elevation, drainage properties, lane width, pavement wear. Chin and Olsen (2011) have shown that TLS data has potential for pavement smoothness evaluation, which determines significant financial incentives/disincentives for contractors on highway construction projects. Potentially, scanner intensity information could be usable to determine the reflectivity of painted stripes, signs, and more. Scanner intensity information can also be used to highlight damaged sections of concrete (Figure 12) or asphalt pavement, which reflects light differently. Herr (2010) presents several examples of how MLS data can be used to evaluate pavement condition including rutting, ride quality, rehabilitation, texture, and automated distress. He emphasizes that the acquisition of all of these data from a single, integrated point cloud represents a major paradigm shift for the industry where these data are acquired from a variety of sources. Chang *et al*. (2006) performed tests to compare the use of static 3D laser scanning, Multiple Laser Profiler (MLP), and rod and level surveys and found significant correlation. As MLS accuracies increase, it may provide the ability to provide detailed roughness data, which are important to evaluate new pavement smoothness quality, resulting in significant incentives and disincentives for contractors.

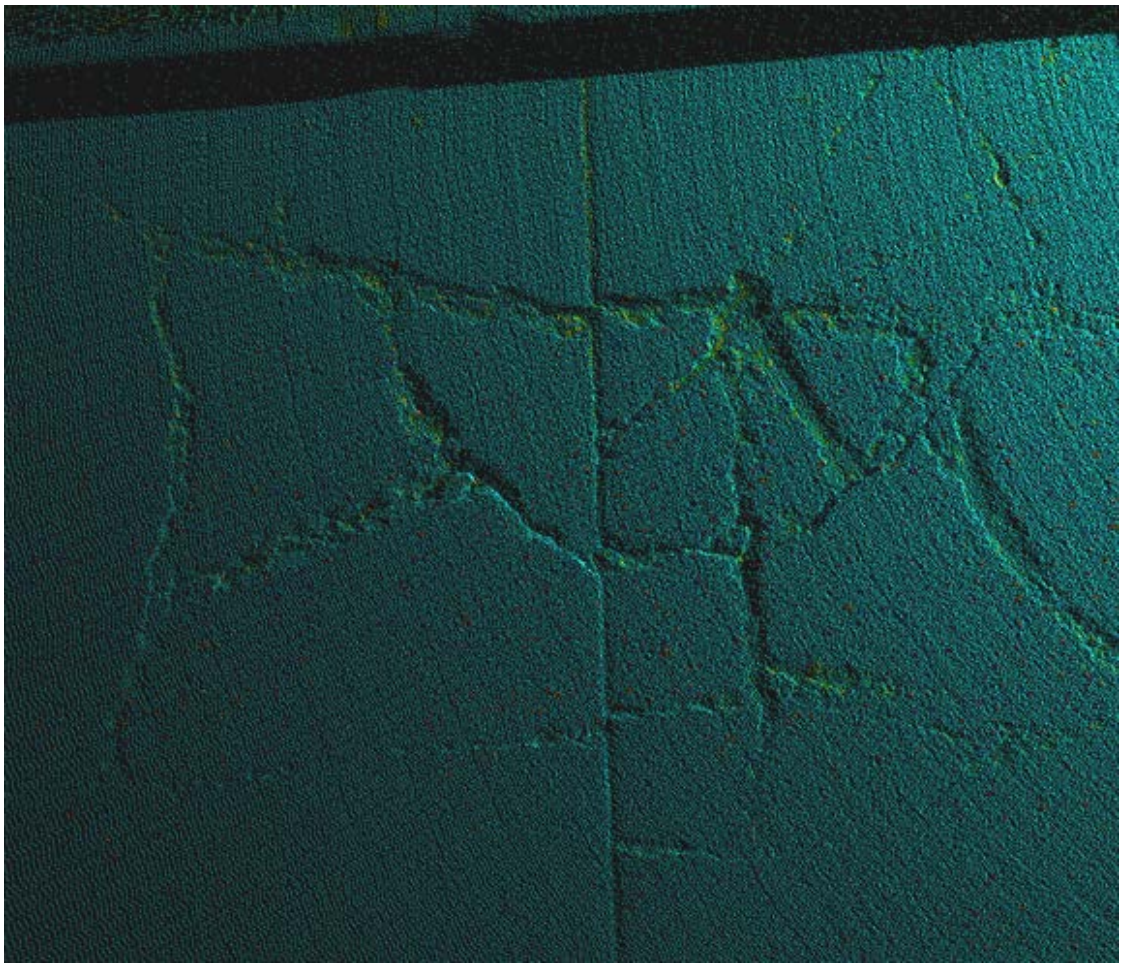

Figure 12. Intensity return used to highlight concrete cracking.

2.2.4 Operations

2.2.4.1 Traffic congestion

Traffic congestion typically results from human error, and automakers are researching methods to remove much of the human component from driving. BMW has been working on a system called Traffic Jam Assistant to

take over driving tasks when vehicle speed is lower than 25 mph. The system relies on GPS and LiDAR along with other components to perform steering, braking, and acceleration (Barry, 2011).

2.2.5 Safety

2.2.5.1 Extraction of features for safety analyses

Lato *et al.* (2009) demonstrate how rock fall hazards along transportation corridors can be monitored using MLS. For this study, the monitoring took place from both railway and roadway based MLS systems. In both situations, MLS provided increased efficiency and also the ability to monitor hazards in real-time. The safety benefits from real-time monitoring also extend beyond locating unstable rock hazards. Figure 13 demonstrates the use of LiDAR along an unstable portion of highway.

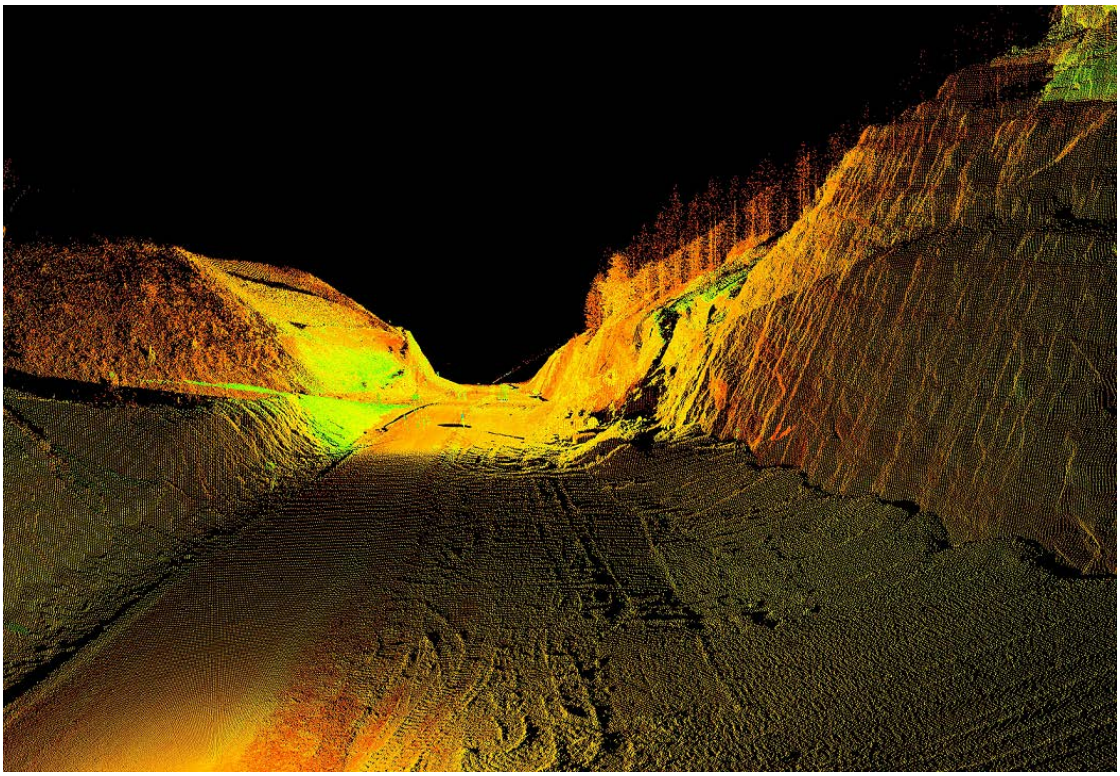

Figure 13. Landslide on newly cut roadway. Courtesy of Oregon DOT.

2.2.5.2 Accident investigation

TLS systems have been used to document accident scenes, permitting the accidents to be moved off the roadway sooner, and allowing investigators to continue the investigation after all physical evidence has been removed from the scene. 3D Laser Mapping (2011) reports that accident scene investigation can be 50% faster than total station surveying, resulting in a 1.5 hour reduction in roadway closure. According to Duffell and Rudrum (2005) and Mettenleiter *et al.* (2008), MLS has begun to play an important role in

documenting pre-accident conditions, and also, a much faster means of documenting long accident scenes which typically occur in high speed crashes. Jacobs (2005) discusses that laser scanning may also be used to analyze structural damage caused by vehicular impact on bridge overpasses due vehicle height exceeding the bridge clearance.

MLS systems can rapidly scan networks of tunnels for damage inspection. Rapid deformation analysis enables highway crews to safely open a tunnel soon after a problem is resolved. However, the resulting accuracy using MLS will depend heavily on the length of the tunnel and quality of the IMU because GNSS data will not be available in the tunnel. Figure 14 shows an example of an intensity shaded TLS dataset obtained for a tunnel damaged by fire.

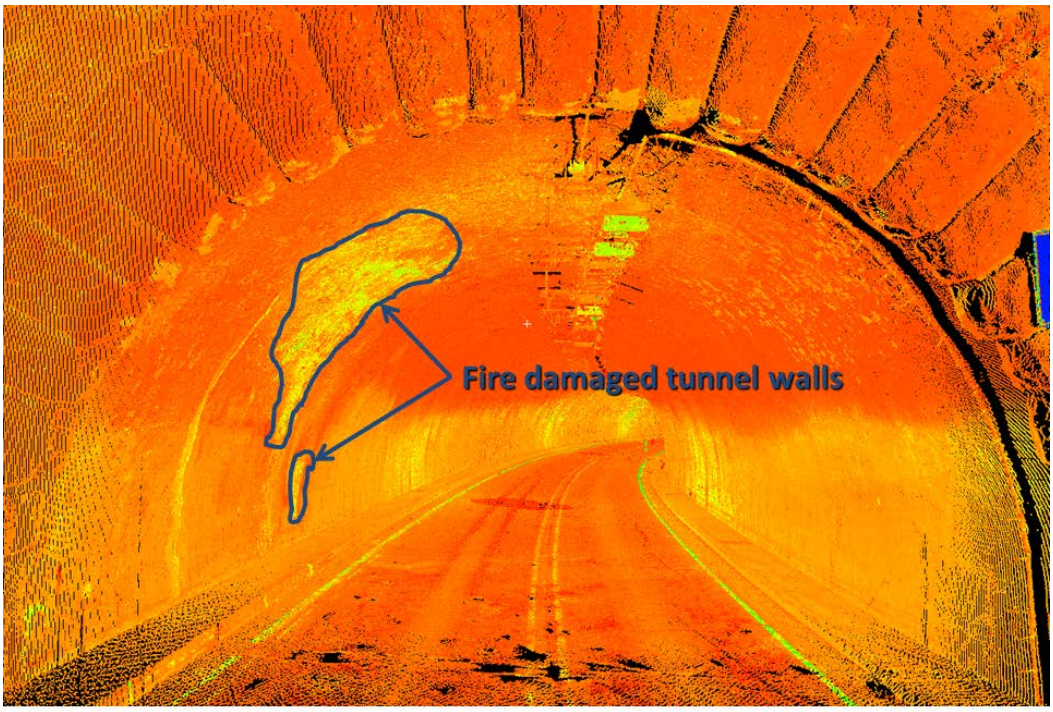

Figure 14. Close examination of the intensity shaded point cloud shows additional, minor damage to concrete in a tunnel in Oregon. (Courtesy of Oregon DOT).

2.2.5.3 Driver assistance/autonomous navigation

Brenner (2009) and Toth (2009) discuss how MMS's have begun to shape the research track of the autonomous vehicle navigation field. Toth (2009) predicts that autonomous vehicle navigation could be operational within the next decade. Brenner (2009) tests a simulated car, designed to model what a fully autonomous vehicle would be able to sense from a position on the roadway. This is done by automatically extracting poles (any vertical narrow

structure), and then allowing the autonomous vehicle to calculate positioning based on the constellation of the poles. Pole extraction is performed on an already geo-referenced point cloud, and vehicle positioning calculated along the roadway based on referencing to the located poles.

2.2.6 Research

2.2.6.1 Unstable slopes, landslide assessment

Su *et al.* (2006) describes the use of LiDAR data for geotechnical monitoring of excavations, particularly in urban areas. In these urban excavations, real time monitoring of the excavation site as well as surrounding infrastructure is critical in maintaining integrity. Miller *et al.* (2008) demonstrate the use of TLS in assessing the risk of slope instability, and provide two examples along transportation corridors. The authors note the challenge and safety issues that arise from setting up a stationary TLS instrument along the side of a busy transportation corridor. Figure 15 demonstrates how LiDAR can be used to highlight localized slope failures. Olsen *et al.* (2011) developed an algorithm that permits real-time detection of changes that have occurred over a region of previously collected LiDAR data. This allows field crews to immediately see where changes have taken place so that any additional measurements can be made at the site with no need for office processing of the point cloud.

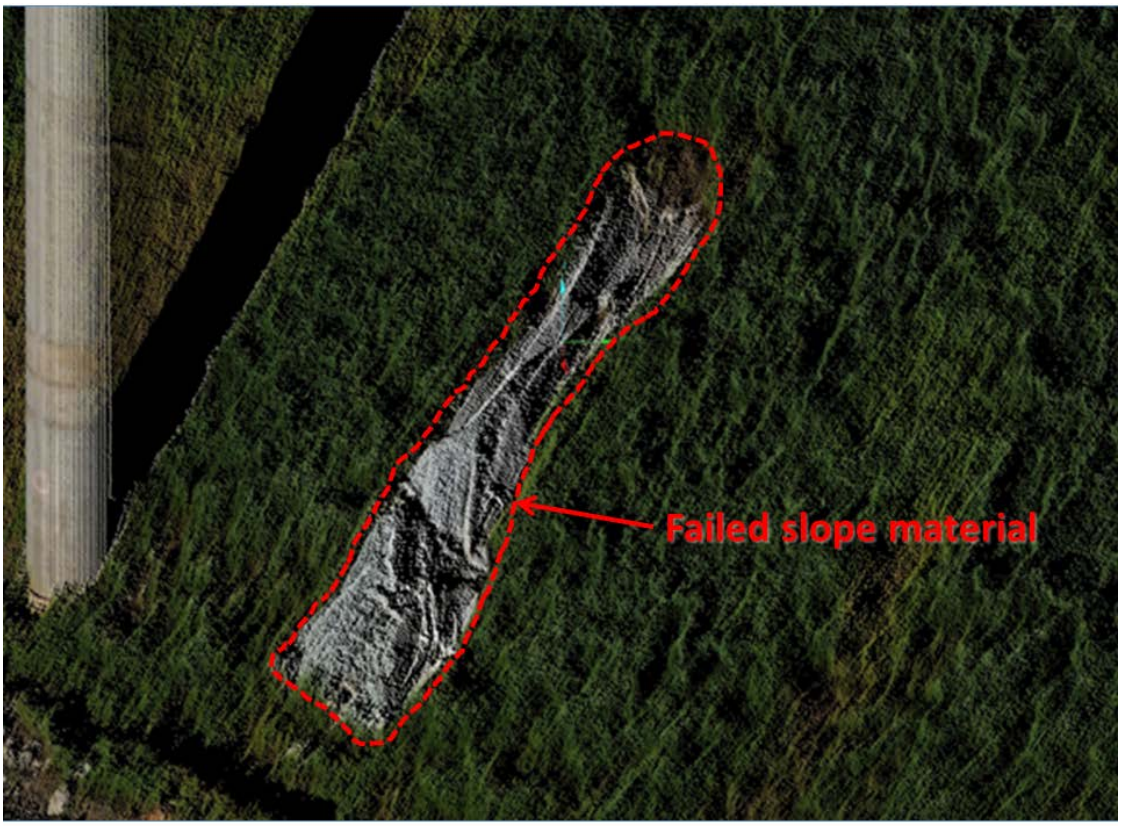

Figure 15. Surficial slope failure along highway embankment at the US 20 Pioneer Mountain to Eddyville re-alignment project in Oregon (Failure scarp is covered by a white tarp to prevent sediment from entering nearby water).

2.2.6.2 Coastal erosion

Olsen *et al.* (2009) provide background on TLS of long coastal cliff sections. TLS provides many advantages over traditional methods of monitoring coastal erosion, these advantages primarily coming from the

density of the data points collected on the cliff faces. This allows for in-depth monitoring of accretion and excretion along the cliffs, as well as monitoring of large land mass movements. Olsen *et al.* (2009) discuss one of the challenges of working with TLS along these coastal sections is the necessity to time the ocean tides to prevent equipment and users from being submerged. Young *et al.* (2010) compare ALS and TLS for quantifying sea cliff erosion. The TLS data enables detection of small-scale changes, however coverage is limited. In many areas, MLS systems can rapidly obtain these small-scale changes over a much larger region; this is important for coastal highways such as Highway 101 on the West Coast.

2.2.7 Asset management

2.2.7.1 Inventory mapping

Duffell and Rudrum (2005) discuss inventory mapping as a secondary benefit that can be utilized from a point cloud. Inventory mapping can include any structure, pavement, signage, traffic signaling devices, etc. that can be extracted from a point cloud. Kingston *et al.* (2006) focus on both manual and automated feature extraction. In addition to feature extraction, they also demonstrate the ability of software to automatically detect road signs and classify them by shape as defined by the Manual on Uniform Traffic Control Devices (MUTCD).

2.2.7.2 Modeling and inspection

Becker and Haala (2007) emphasize the need for detailed 3D modeling of urban landscapes for city planning. They demonstrate an automated façade grammar building tool that can model building facades beyond the line-of-sight of the scanner by hypothesizing further facades based on the adjoining style. Jochem *et al.* (2011) also proposes using MLS to model building facades; however, the focus is to select the facades with the highest solar potential. The goal is to extract individual structures from a point cloud and assign solar potential ratings to the various facades of the structure. This would allow individuals to easily see where the most appropriate placement for solar panels would be on their building.

2.2.7.3 Automated/semi-automated extraction of signs

Semi-automatic or fully automatic extraction of signs is necessary to efficiently locate signs in a large point cloud such as that provided by MLS. Brenner (2009) discusses a method of pole extraction by use of cylindrical stacks; these stacks contain a core that must contain data surrounded by a ring that contains no data. McQuat (2011) discusses several different structures (signs, facades, bays, automobiles, curbs, *et al.*) and how they can be automatically detected. McQuat also provides insight on how these structures can then be converted to useful shapes for use in a GIS.

2.3 DATA QUALITY CONTROL

2.3.1 Accuracy and precision checks

Each component of the MLS setup requires careful calibration to ensure accurate data. Calibration errors are additive in the scanning platform, each portion of the system that is not well calibrated propagates errors to the final point cloud.

2.3.1.1 Laser scanning errors

System specification sheets provide a basic idea of scanner performance; however additional factors need to be considered that are well beyond the scope of the specification sheet (Ussyshkin and Boba, 2008). These include the material properties of the scanned objects, inconsistencies in scanner manufacturing, the geometric configuration of the object to the scanner, and GPS errors.

- **Material Properties:** White surfaces will provide very intense laser returns, while black surfaces will return a much less intense value (Boehler *et al.*, 2003). System performance varies greatly, and consideration needs to be taken for the objects being scanned, such as low reflectivity asphalt in many DOT applications. Highly reflective surfaces (*e.g.*, traffic signs, retro-reflectors) may produce additional

distortion effects such as saturation and blooming (Vosselman *et al.*, 2010). Saturation (Figure 16) is caused by too much energy being returned to the scanner and appears as points spread out along the line of sight of the scanner. Blooming (Figure 17) is a similar effect that occurs perpendicular to the line of sight of the scanner. Blooming appears as an enlargement of the reflective surface due to excessive energy being returned to the scanner.

- **Inconsistencies in scan manufacturing:** Boehler *et al.* (2003) warn that many scanners are built in small quantities and individual errors vary significantly between units. Careful care and inspection of equipment, in addition to periodic calibration checks are necessary to maintain the best possible accuracy from hardware.

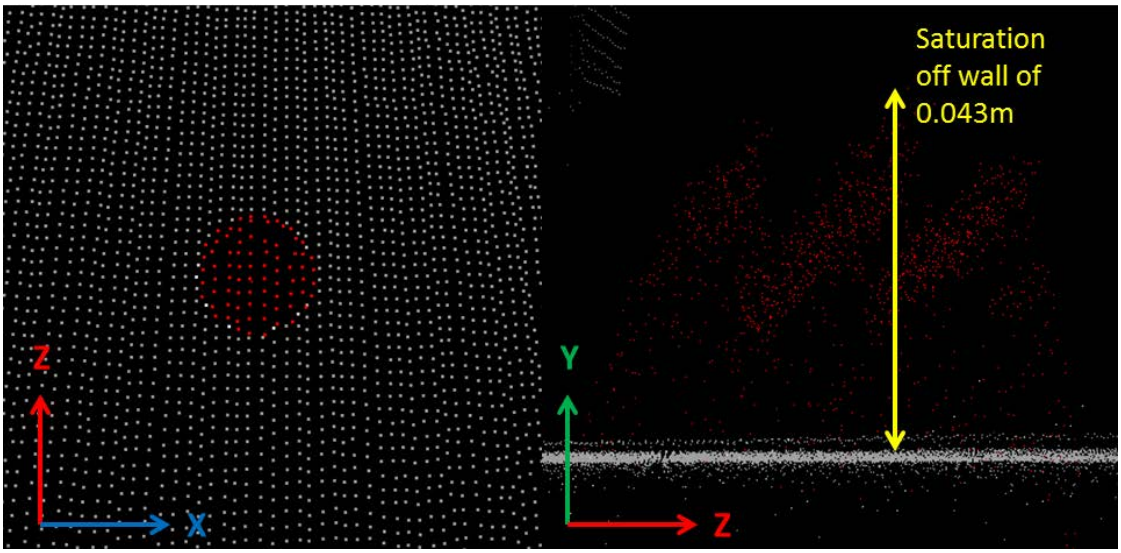

Figure 16. Saturation of a flat, 5cm retro-reflective target is seen as the target extending 4cm off of the wall. Left image is a straight on view (down on Y-axis), and right image is a side view along plane of wall that target is affixed to (along X-axis).

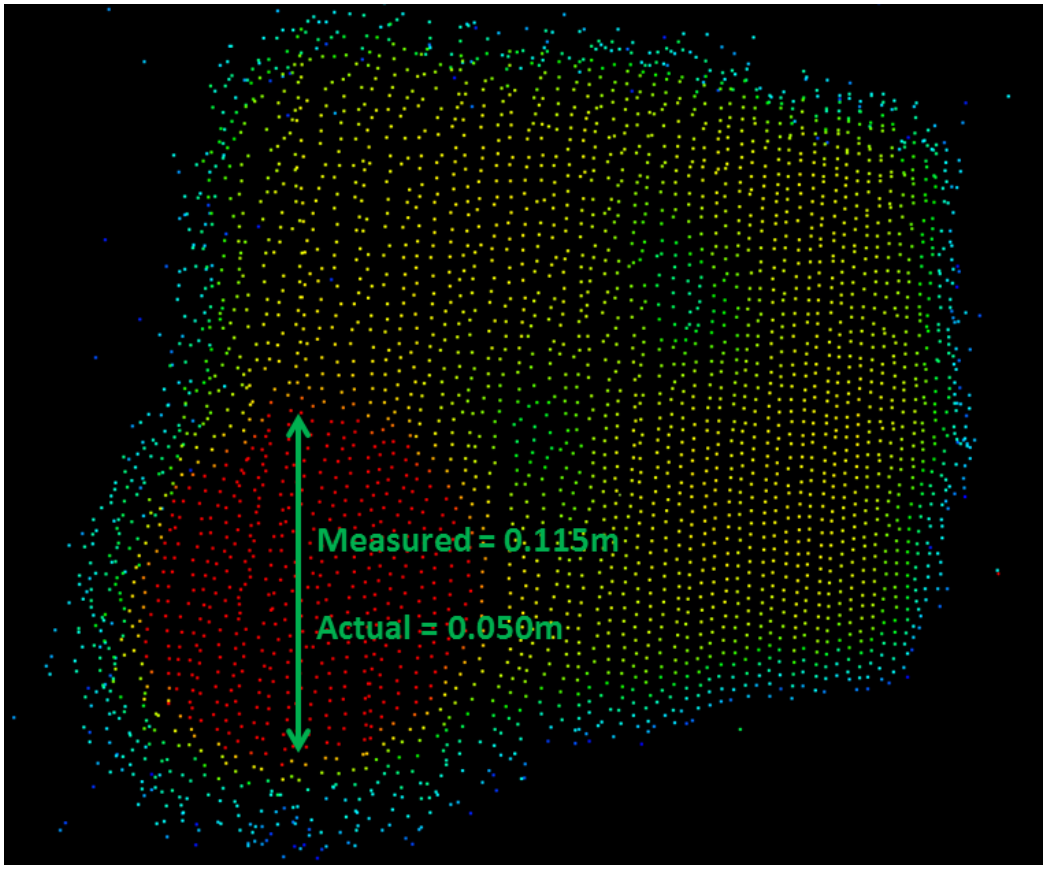

Figure 17. Blooming of a flat 5cm retro-reflective target. (See Figure 22b for image of the actual target).

- **Geometric configuration:** The size of the laser footprint is important in understanding the final data accuracy. The uncertainty of point location due to divergence of the laser beam adds additional random error (Barber *et al.*, 2008 and Ussyshkin and Boba, 2008). Boehler *et al.* (2003) state that it is possible to record the same object multiple times using multiple passes of the scanner, however, due to the beam

width uncertainty the exact same point cannot be measured precisely. The obliquity of how the laser pulse strikes the surface can result in significant positioning error (Laefer *et al.*, 2009 and Olsen *et al.* 2011). If two surfaces are placed less than half a pulse width apart, along the line of sight, a mixed pixel (Figure 18) discrepancy may result (Vosselman *et al.*, 2010). This discrepancy can be seen as an extension of points off of the edge of the closer object, extending back to the further object.

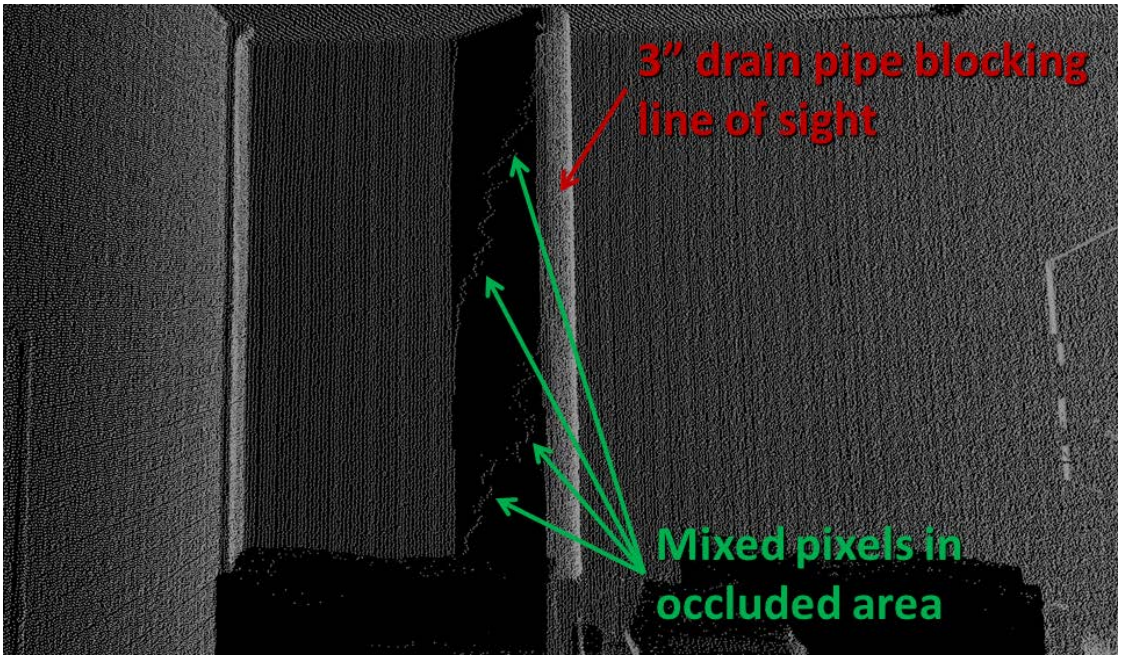

Figure 18. Mixed pixels appear in an area occluded from the scanners line-of-sight.

- **GPS source errors:** Factors that affect the accuracy of GPS include: multipath, shading by buildings and trees, loss of satellite lock, atmospheric conditions, and poor satellite geometry (Glennie, 2007 and Haala *et al.*, 2008). GNSS systems combining GPS, GLONASS, Galileo, and Compass (when available) will help improve accuracy results (Chiang *et al.*, 2010).

2.3.2 Procedures for measurement quality control

Many different methods have been employed to verify the accuracy of the final point cloud. Commonly, ground control points, or an already geo-referenced TLS point cloud are used to verify accuracy of the MLS data. Ussyshkin (2009) discusses geo-referencing mobile scan data using a system of six base stations and ground control points spaced every 50-80 meters throughout the survey extents in order to achieve 1-2cm accuracy (*e.g.,* CALTRANS specifications call for these validation points every 500ft ~152m). Barber *et al.*, (2008) state automated validation to compare MLS data to survey control high resolution terrestrial laser scans, or target matching in real-time is greatly needed. Hiremagalur *et al.*, (2007) provide “best practices” to ensure the proper registration of MLS data and recommend target redundancy (if target registration is to be used), examination of overlapping point clouds, and comparison of point cloud coordinates to check point coordinates

surveyed using traditional methods. A report of the RMS error of the point cloud to the ground control coordinates should be a standard deliverable in addition to an RMS error report of overlapping point clouds. Points to be used for an RMS evaluation should be spatially distributed throughout the entire dataset. Additionally, Graham (2010) recommends that final quality control be performed by someone other than those involved in registering the dataset.

2.3.3 Level of detail concept

When assessing the quality of a mobile mapping system point cloud, many factors contribute to the final accuracy and precision values. The ASPRS Mobile Mapping Committee (2011) and Hiremagalur *et al.* (2007) have recommended that final point cloud quality be assigned a rating based on the quality of data. For example, an end user may be in need of a point cloud to inventory roadway signs along a corridor. The user is not concerned about the geo-referencing accuracy of these signs; they are using the data solely for the purpose of counting the number of signs along this corridor. In this example, the user would not want to pay a premium for positional survey quality of data, and a lower level of data would be appropriate. However, this user still needs high enough resolution in the point cloud to be able to extract signs. This creates a two-fold level of data that needs to first address the accuracy of the data, and also the resolution of the data (ASPRS Mobile Mapping Committee,

2011). Accuracy tends to have a higher impact on project cost, since higher resolution can be more easily obtained with slower vehicle speeds, or multiple passes through the corridor. According to Barber *et al.* (2008), positioning is not affected by vehicle speed, however higher speeds lead to a lower point density.

Boehler *et al.* (2003) describe that various jobs will require various levels of data. Figure 19 demonstrates this concept, high resolution and accuracy would be designated 1A whereas low resolution and high accuracy would be designated 1C. If instruments and methods are taken to obtain data well beyond the needed standard, too much additional cost and time may be put into a project. Duffell and Rudrum (2005) argue that the over-collection of data may not always be a negative, because data can often be reused for many different tasks. One data cloud could be made available to many end users who can mine the data source for several different job tasks. In addition, extra detail could allow the reuse of archived point clouds for base data in accident investigations, hazard identification, and future project planning.

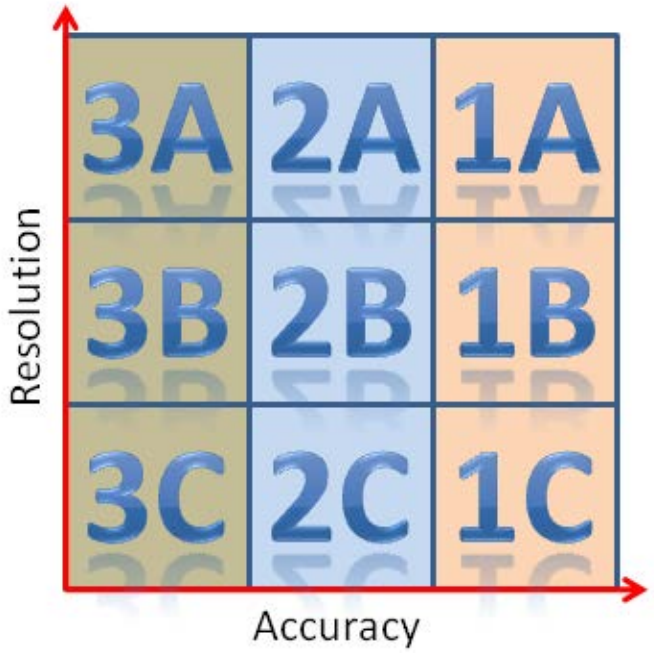

Figure 19. Conceptual level of detail dual rating chart, including resolution and accuracy requirements.

2.4 MOBILE SCANNING ADVANTAGES

2.4.1 Safety

Yen *et al*. (2011) show that MLS technology presents multiple benefits, including safety, efficiency, accuracy, technical, and cost. Mobile mapping has increased safety benefits over traditional survey techniques and static TLS (Glennie, 2009), including safety and logistic improvements because nearly all work is performed from within the vehicle. There are various reasons why this

is beneficial: 1) Drivers become distracted by survey instruments, often observing the equipment and not paying attention to the actual surveyor. 2) Traffic often needs to be stopped or re-routed to allow the surveyor to make the necessary measurements. 3) Surveyors may have no other option but to place themselves in precarious situations to acquire the necessary measurements, whereas mobile mapping requires little or no need for surveyor and vehicular interaction. 4) The vehicle generally can move with the flow of traffic, eliminating the need to divert traffic or close roadways.

2.4.2 Efficiency

Glennie (2009) provides an example of MLS efficiency over a four mile section of a busy interstate section. Washington DOT specifically requested that the roadway remain fully open for the duration of the survey, leaving MLS as the logical data collection method; total scanning time was 1.5 hours. Mendenhall (2011) gives details about the cost and time savings of performing a MLS in San Francisco over 15 miles of roadway from the Golden Gate Bridge to the Palace of Fine Arts. The cost saving on this project was estimated at $200,000 to $300,000 while the physical survey time was reduced by six to eight weeks further reducing management time by four weeks.

2.4.3 Comparison with airborne systems

Airborne and MLS share a number of similarities in the data processing workflow as both systems require the processing of positional data in tandem with LiDAR data (Ussyshkin and Boba, 2008). Airborne LiDAR is significantly more costly than mobile based LiDAR, and does not provide the same level of detail from the ground plane. On demand data capture can be provided by MLS, as well as capture of building facades and tunnels that are not available from airborne LiDAR (Barber *et al.*, 2008 and Haala *et al.*, 2008). However, airborne systems can cover larger portions of the terrain and are not limited to ground navigable terrain.

2.4.4 Comparison with static scanning

Zampa and Conforti (2009) provide data showing that MLS can be significantly more efficient than TLS. For example, in 2007 an 80km stretch of highway was scanned using TLS, and in 2008 60km of similar highway was scanned using MLS. The field time required to collect the TLS was 120 working days, while the MLS was able to capture all the data in three hours.

2.5 CURRENT CHALLENGES

Several difficulties exist when performing mobile scans (*e.g.*, Glennie, 2009). Measurements are performed from a moving platform, requiring high

precision GPS/IMU readings for accurate data georeferencing. Typically it is not feasible to close down a section of highway for scanning, so neighboring vehicles can block data collection. Additionally, the vehicle must be moving at a safe speed (with the flow of traffic) while simultaneously collecting data. In some cases, a rolling slow down can be used to avoid these problems.

Further, the size and complexity of the laser scan data presents immense challenges. Sensors collect data at very high speeds (typically 100k to 1 million points per second) and at very high point densities (typically >100 points per m^2) at close ranges (typically < 100m). This creates large datasets that can be difficult to work with on typical computing platforms and software. The wealth of data collected also requires a substantial amount of data storage and backup during a project. Following completion of a project, care must be taken to ensure proper data archival. The large size also makes web, DVD, or other common media difficult to use for data transfer. The complexity of data and minimal availability of software also presents challenges to end users such as DOTs in actually being able to use the data. Currently, most consultants subsample and filter the data to reduce size. They also process the data in small sections because computing resources limit their ability to work with the entire dataset. The final data typically transferred to the end user represents a fraction of the original data obtained. Ussyshkin (2009) discusses limitations on the number of points that can be imported into

common software packages. While manufacturers of GIS and CAD software have recently been integrating point cloud support, many challenges remain to make this process seamless for the end user. Further, point cloud processing usually requires working between multiple software packages where information can be lost on imports and exports through the process. The ASTM E57.04 (2010) subcommittee on data interoperability was formed, in part, to help resolve these data transfer issues.

Unfortunately, many of these challenges, lessons learned, and user experiences are disseminated verbally at conferences or other events but currently have not been adequately integrated into a citable document.

Knaak (2012b), after a conversation with Florida DOT personnel, discusses problems with MLS technology adoption by DOT and offers suggestions including:

1. Avoid the “WOW” factor of point clouds. Often this results in incomplete projects where consultants do not provide DOTs with something they can actually use,
2. Agree on a QA/QC procedure, including a lineage from the point cloud to the final product and metrics to evaluate that lineage. The QA/QC should be done by an independent contractor,

3. Identify the model needs first so that the point cloud requirements can be determined easier, and
4. Define the respective responsibilities of the customer and consultant in the process.

Knaak (2012b) also explains problems in current payment and procurement standards that are focused on time in field work and minimal office processing time. The key factor with MLS technology is that it reduces field time dramatically (80-90%) but shifts loads to processing. Under current payment schemes, these current payment schemes reduce the contractors pay substantially because they are paid based on field time.

2.6 BEST PRACTICES AND LESSON LEARNED

Missouri DOT (Vincent and Ecker, 2010) evaluated the accuracy, cost and feasibility of airborne, mobile, and static terrestrial laser scanning for typical projects. They determined that all systems met their accuracy requirements. The report also highlights current hurdles including software and computing challenges. The authors also conclude that traditional surveying and/or static scanning may still be required to fill in gaps from mobile scanning. Yen *et al.*, (2011) provide an in-depth evaluation of MLS technology in Washington State. They show that maintenance, asset management, engineering, and construction programs all incur cost savings, time savings, and safety

improvements. This evaluation also demonstrates the needs of national standards and best practices as well as a common data exchange platform to improve data interoperability.

2.7 EXISTING GUIDELINES

Many other agencies (FAA, 2011; FGDC, 1998; NDEP, 2004; NOAA, 2008; USGS, 2010) have provided recommendations, guidelines, or standards that must be met for geospatial data. Some of these (FGDC, 1998 and NDEP, 2004) are broad specifications that pertain to all remotely sensed data while others pertain more directly to LiDAR data (FAA, 2011; NOAA, 2008; USGS, 2010). The ASPRS Standards Committee (2005) has produced "Guidelines Vertical Accuracy Reporting for LiDAR Data," and "Guidelines Horizontal Accuracy Reporting for LiDAR Data" which more specifically declares reporting standards (*e.g.*, fundamental vertical accuracy (FVA), consolidated vertical accuracy (CVA), supplemental vertical accuracy (SVA)). A summary of these guidelines can be seen in Table 1.

Common trends can be seen in the various LiDAR specifications:

1. Standardize accuracy reporting methods
2. Requirements for ground point density
3. Requirements for scan overlap
4. Number of control/check points for accuracy verification

5. Deliverables

Although these guidelines are currently focused on aspects of ALS, many of their fundamental principles could be adapted to produce guidelines more relevant to MLS. However, these documents do not adequately address the needs of many DOT applications. For example, the accuracy, resolution, coverage, and look angle of MLS data varies significantly from that achieved with airborne LiDAR. Particularly, true 3D error vectors are important for many applications that cannot be evaluated by focusing on vertical error only.

Recently, Chapter 15 of the California Department of Transportation (2011) Surveys Manual is one of the first developed set of specifications that explicitly addresses the required information and data quality that should be provided with a MLS survey. This chapter also covers static TLS. These specifications contain a two part classification system for MLS surveys. Type 'A' is a higher accuracy hard surface survey used for engineering applications and forensic surveys. Type 'B' is used for lower accuracy earthwork measurements (*e.g.*, asset inventory, erosion, environmental and earthwork surveys). These specifications are broad enough to not limit vendor equipment and technology but provide details regarding data acquisition and processing procedures, including the minimum overlap between scans, maximum PDOP, minimum number of satellites, maximum baseline, validation

point accuracy requirement, IMU drift errors, and others pertaining to the georeferencing accuracy of the point cloud. Knaak (2012a) has developed a set of best practices based on experience; this document defines three distinct levels of data as well as requirements for: vehicle trajectory, point cloud, file management, and images.

Table 1. Summary of existing LiDAR guidelines.

Existing Guidelines		
General Geospatial		***Key Points***
	FGDC 1996	95% confidence evaluation, 20 control points, methodology on how to compute accuracy statistics
	NDEP 2004	DTM certification, reporting of accuracy across many different remote sensing platforms
Mobile LiDAR (Current)		
	CALTRANS Chapt. 15 Survey Manual 2011	TLS and MLS specifications, various classes of data (Type A-high accuracy, Type B-lower accuracy), requirements for: mission planning, control placement, system calibration, overlap requirements, QA/QC
Mobile LiDAR (Development)		
	TxDOT	In Development
	ASPRS Mobile Mapping Committee	At outline stage
	MoDOT 2010	Evaluation of MLS usage for DOT activities
Airborne LiDAR		
	FAA 2011	Airport surveys
	NOAA 2009	Shoreline mapping
	USGS 2010	Rev. 13 still in draft phase
	ASPRS Vertical	
	ASPRS Horizontal	Draft phase
	ASPRS Geospatial Procurement Guidelines	Draft phase
	FEMA Guidelines	Flood plain mapping

2.8 MOTIVATION AND KEY NEEDS FOR NATIONAL GUIDELINES

MLS data provides many benefits when processed and used appropriately. Ussyshkin (2009) states that the underlying technical details

(*e.g.*, applications, procedures, benefits) need to be well understood in order to prevent disappointments and misunderstandings when using MLS data. Guidelines need to incorporate and integrate fundamental principles of quality control and performance to result in the desired deliverable. Optimally, end users such as engineers and designers should have a strong understanding of MLS, so that the data can be utilized effectively and to its full potential. However, because of the wide variety of applications and quality needs, many personnel within a DOT can effectively use MLS without being experts in the details of the technology once the appropriate guidelines are in place. Simple yet powerful guidelines focused on performance evaluation will enable them to adequately integrate MLS into their operations. National guidelines will ensure that DOTs do not duplicate efforts in producing similar documentation. The consistency provided through national guidelines will also enable improved communication between vendors and DOTs.

2.9 CONCLUSION

The Transportation Research Board (TRB), NCHRP 15-44 has provided funding for this research and has a desire to develop guidelines for using MLS in transportation applications to enable DOTs to make informed decisions when procuring MLS services (Transportation Research Board, 2011). The TRB states that MLS “promises many benefits to transportation agencies as a

tool for project planning, project development, construction, operations, maintenance, safety, research, and asset management." Key findings from this review show that the transportation industry has a strong desire for:

- Standardized accuracy reporting methods,
- Data interoperability,
- Control/check requirements,
- Various levels of data quality (*e.g.,* asset management vs. engineering),
- And more familiarity with the technology.

Finally, there is a lot of discussion in the industry regarding WHAT is being done with MLS, but not a lot of HOW and HOW WELL it is being done. Many people are willing to summarize projects being completed, but few are documenting the methodologies used and results achieved. More research is needed regarding the actual capabilities of the systems on transportation projects and methodologies used for collection and processing of data. It is important to realize that MLS is a tool in the DOTs toolbox, which sometimes may be the best tool for a job, and sometimes may not be.

3 MANUSCRIPT CHAPTER

Accuracy Assessment of Geo-Referencing Methodologies for Terrestrial Laser Scan Site Surveys

Keith E. Williams[1], Michael J. Olsen[2], and Abby Chin[3]

1. Graduate Research Assistant, School of Civil and Construction Engineering, Oregon State University, 220 Owen Hall, Corvallis, OR, 97331, williamsfabrication@gmail.com
2. M.ASCE., PhD. Assistant Professor, School of Civil and Construction Engineering, Oregon State University, 220 Owen Hall, Corvallis, OR, 97331, michael.olsen@oregonstate.edu
3. Graduate Research Assistant, School of Civil and Construction Engineering, Oregon State University, 220 Owen Hall, Corvallis, OR, 97331, chinab@onid.orst.edu

ASPRS – American Society for Photogrammetry and Remote Sensing

http://www.asprs.org

Williams, K., M.J. Olsen, A. Chin, (2012). Accuracy Assessment of Geo-Referencing Methodologies for Terrestrial Laser Scan Site Surveys, ASPRS Sacramento 2012 Proceedings.

3.1 ABSTRACT

Achieving accurate geo-referencing of 3D point clouds from terrestrial laser scanning depends on both the data quality as well as the registration procedures used to align the data. This paper presents a comparison of several common geo-referencing techniques for a limited number of scans across a site. The first approach performs resection of the scanner position and orientation from black and white targets printed on paper. The target centers are surveyed using a total station. Similarly, the second approach uses retro-reflective targets whose coordinates are also established using a total station. Software-based (Cloud-to-cloud) registration through surface feature matching of the point clouds is used for the third approach. This approach first matches scans on a pair-wise basis and then performs a global adjustment. The fourth approach (*PointReg*) constrains scanner orientation parameters to surveyed origins and internal inclination sensors. It then employs a least-squares, surface-matching adjustment to determine the azimuth of the scanner for each scan position. For comparison, scan origin positions are obtained (a) through a total station and (b) through RTK GPS.

A detailed comparison of the registration methods shows the time required to perform the data acquisition and geo-referencing, overall quality of the alignment, and comparison of the variability of scan transformation

parameters (translations and rotations) for each method. The time required for alignment consists of: field time to collect the data, user-interactive processing time, and automated processing time. Quality of the alignment is assessed by comparing the accuracy of the target positions and the RMS values calculated for adjacent scans for each methodology. Overall, the methodologies compare well with one another in regards to accuracy. However, there are significant differences in time requirements and distribution between field and office processing time.

Finally, this paper can inform persons performing laser scans of the benefits, efficiencies, and limitations that exist when employing different geo-referencing methods in terrestrial laser scanning. One primary consideration for selecting an appropriate method for a project is the amount of available field versus processing time.

3.2 INTRODUCTION

Multiple methods of terrestrial laser scan (TLS) collection and geo-referencing exist. Olsen (2011) provides an overview of several scan alignment approaches and quality control procedures. This paper provides a comparison of three of these techniques and variations, including:

1. Target registration
    a. Black and white paper targets

   b. 5 cm, retro-reflective, stick-on targets
2. Software based registration
   a. Cloud-to-cloud
3. *PointReg* hybrid registration
   a. Total station acquired scan origins
   b. GPS acquired scan origins

For all methods outlined, seven degrees of freedom need to be solved in order to accurately geo-reference the scans using a similarity coordinate transformation. Providing scaling corrections for the atmospheric conditions lowers this to six degrees of freedom: translation in X, Y, and Z, and rotation about the X (roll), Y (pitch), and Z (yaw) axis. Silvia and Olsen (In Press) performed analyses related to the data quality provided by scanner inclination sensors (roll and pitch) and their utility in scan geo-referencing, particularly in validating control coordinates. The following methods were implemented to solve for these parameters:

- The first method, target resection, uses identifiable objects scanned at high resolution to provide common matching points between scans. The first variant uses black and white targets printed on paper to perform resection to determine the scanner position and orientation. The target centers are surveyed using a total station.

Similarly, the second variation uses retro-reflective 5cm flat disk targets whose coordinates are also established using a total station.

- The second method, utilizing software registration, will simultaneously solve for four degrees of freedom after the operator provides a close approximation of the initial alignment. Two degrees of freedom, roll and pitch, will be provided by the scanners internal inclination sensors. This method first matches scans on a pair-wise basis and then performs a global adjustment.

- In the last method, *PointReg* (Olsen *et al*. 2009, 2011), translation (X, Y, and Z) will be provided by (a) total station and (b) RTK GPS. In addition, the use of the scanner's internal inclination sensors will result in only the unknown yaw value to be adjusted through least-squares.

3.3 PURPOSE

The aim of this research is to compare geo-referencing methods for terrestrial laser scanning and to document information regarding time, accuracy, and possible introduction of error to assist a TLS surveyor in deciding which method is most appropriate for their projects.

3.4 METHODOLOGY

A test site was selected to evaluate the laser scan techniques. For efficiency, data required for all methodologies were collected simultaneously rather than completing multiple surveys of the site. Documentation of the time required for each process was recorded to allow a close approximation of the time that each individual geo-referencing method would have taken if performed individually.

3.4.1 Site Location

Reser Football Stadium (Figure 20) on the Oregon State University campus in Corvallis, OR was selected as the test site for three primary reasons:

- It provided a large test area with very little disturbance due to pedestrian or vehicular traffic.
- There were no overhead GPS obstructions, which allowed the use of RTK GPS using the ORGN (Oregon Real-time GPS Network).
- Most of the site consisted of hard surfaces, eliminating registration uncertainty that can arise due to vegetation. The field itself is an artificial turf.

3.4.2 Field collection

Data were acquired from four scan positions (Figure 20) using a Riegl VZ-400 scanner, with each scan origin's coordinates determined by (a) setting up over a control point (whose coordinates were obtained from a total station) and (b) RTK GPS with a GPS unit mounted above the scanner, with appropriate height corrections. Three independent, one minute GPS observations were recorded at each scan position for data quality assessment purposes. For all point sets, horizontal observations did not vary by more than 1 cm, and vertical observations did not vary by more than 2 cm. Averages of the three observations were reported as the final GPS location. Twelve target locations were used throughout the stadium; five located behind each end zone, and one on each side of the 50-yard line (Figure 20). These targets were staggered at various elevations providing complex target geometry to aid in scan alignment. Each target location consisted of an 8 ½" X 11" black and white paper target with a 5cm flat disk retro-reflective target placed in the lower left corner of the paper (Figure 22).

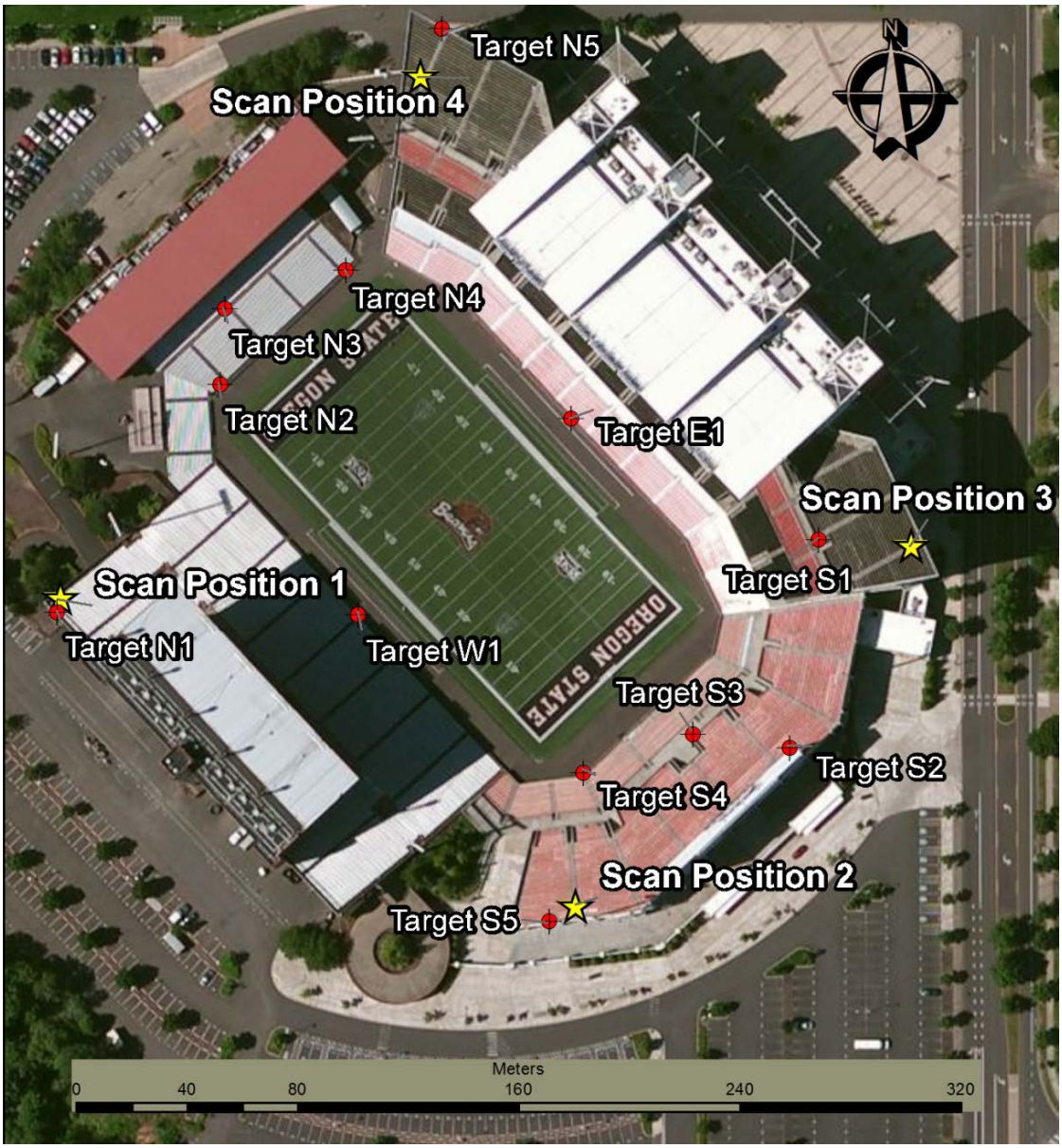

Figure 20. Scanner location and target layout, Reser Stadium. Background image provided by 2010 Microsoft Corporation and its data suppliers through ESRI.

360° overview scans at each setup location were collected using a 0.03° angular increment (each requiring five minutes of scanning time to complete), collecting nearly 15 million points per scan. After completion of the overview scan, targets were acquired through two techniques. The first was a semi-automated approach, which located the retro-reflective targets and scanned them at a higher resolution with a window large enough to also capture the black and white paper targets. The second method required the scanner operator to provide a scan window for a high-resolution scan and select the target centers from within this window. The second method was needed because reflective targets at a distance greater than approximately 200m from the scan origin were not always detected automatically. Finally, a total station was used to find the center of the 24 targets, as well as to establish control points below each of the scan setup locations.

3.4.3 Office processing

Figure 21 outlines the processing workflow and data coordination for each method. In order to geo-reference the total station data (collected in a local coordinate system) for each scan position and target location, the total station coordinates were adjusted to the RTK GPS coordinates through a least squares adjustment using the 4 control points. This adjustment enables the total station data to maintain its high relative accuracy. The adjustment only

allowed the data to translate in X, Y, Z, and rotate about the Z-axis only. Rotation about X and Y-axes was constrained so that the data did not become unleveled from the adjustment. Additionally, scaling was constrained because the total station data was previously corrected for environmental conditions (temperature, pressure, and relative humidity). The resulting RMS of this least squares fit (total station to GPS) was 0.017m. Once the adjustment was completed, all total station target values were imported into the laser scan software and assigned as control targets.

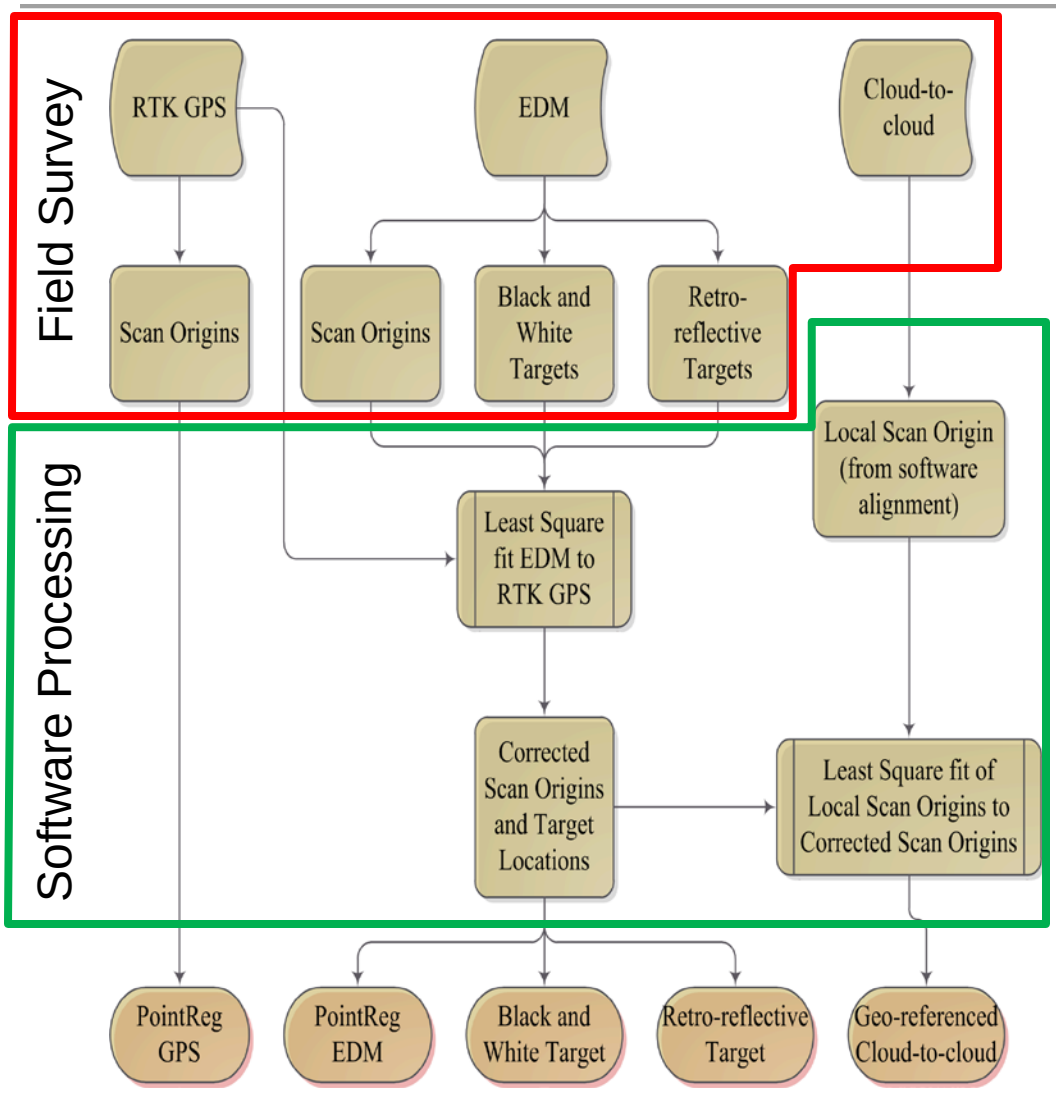

Figure 21. Flowchart depicting the acquisition and processing procedures necessary for geo-referencing techniques.

3.4.3.1 Target Registration

Target processing was very similar for the retro-reflective targets and the black and white paper targets. The key difference was that the black and white paper targets required that the target center was manually selected, and the retro-targets were automatically selected using Riegl's RiSCAN software. Leica Cyclone software provides the ability to auto-extract black and white paper targets; however, since the data was acquired from a Riegl VZ-400 scanner, the auto extraction was unsuccessful. After all centers had been selected in the high-resolution target scans, a registration was performed to match corresponding targets between scans. Figure 22a depics how a typical target appears in a high resolution scan at a distance of approximatly 150m. Note that the center of the retro-reflector (red points) is automatically selected in the software, while the user must manually decide the best point representing the center of the black and white target. The scanner used in this study has a beam divergence of 0.3mrad, which results in an approximate beam width of 60mm at a target 200m from the scanner. At 200m the beam width is larger than the retro-reflector, when a small portion of this beam strikes the retro-reflector and the remaining larger portion strikes the surronding paper a blooming effect is seen in the size of the reflector, Figure 22a (Vosselman and Maas, 2010). Due to the symmetric nature of blooming effects, the target center can still be reliably found.

Pesci and Teza (2008) determined that retro-reflective targets should only be used at normal incident angles, and at longer distances from the scanner. Beyond 200m the retro-reflectors are still detected, while the centers of the paper targets can no longer be determined, this is seen as a drop in the corresponding number of points for scan positions 2 and 4 in Table 2. The manufacturer of the scanner used in this study specifically warns the user to not scan retro-reflective targets at a distance less than 50m from the scanner. Scans of paper targets are much improved at closer distances; hence, they are typically used for close range (<50m) scanning.

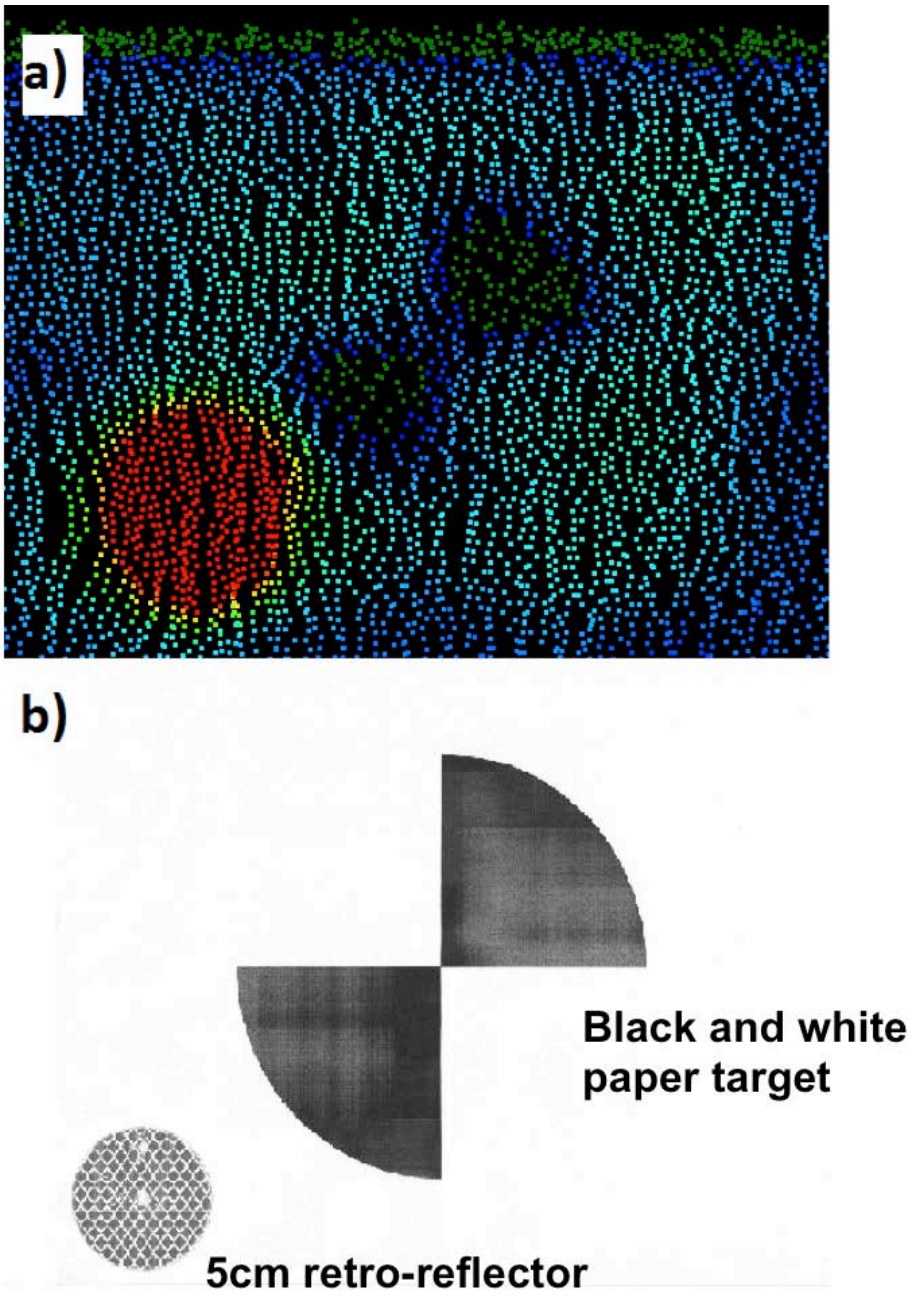

Figure 22. 8 1/2" X 11" target with retro-reflector in lower left corner. (a): Point cloud of target at approximately 150m from the scan origin. (b): Image of actual targets used in study.

Table 2. Target alignment results

Target alignment statistics				
	Retro-reflective target		Black and white paper target	
Scan Position	Overall Std. Deviation (m)	Number of corresponding points	Overall Std. Deviation (m)	Number of corresponding points
1	0.0033	5	0.0077	5
2	0.0048	6	0.0116	5
3	0.0028	6	0.0066	6
4	0.0036	6	0.0093	5

3.4.3.2 Cloud-to-Cloud Registration

This method used a cloud-to-cloud alignment technique, through an iterative closest point (ICP) algorithm. However, the exact variant (Rusinkiewicz and Levoy, 2001) is unknown because it is included in proprietary software. This variant samples the point clouds at random, selecting a subsampled set (~2,000) of points for determining the alignment to increase efficiency. Point density is typically much higher closer to the scan origin. Hence, a random sampling will likely sample more points close to the scan origin. Additionally, slight error between these point pairs found closer to the scan's origin will have significant influence on an accurate scan alignment, particularly rotation. To avoid this problem, one can either (a) remove points within a certain range of the scan origin, or (b) provide a minimum separation filter so that all points are separated by the given minimum value (any closer points are removed). For this study a minimum separation filter was set to

0.01m. Points outside of the study area were manually cropped. The four scans were imported into the alignment software with only the scanners roll and pitch values applied, all other transformation parameters remained zero.

One scan was selected to be the reference surface. The remaining scans were then manually moved until a close visual alignment was achieved for an initial approximation to seed the ICP surface match. Each scan was aligned, pair-wise, to the reference scan. This was then followed by a global, cloud-to-cloud adjustment that adjusts all scans simultaneously. Because the data were on a local coordinate system for the surface registration, all scan origin coordinates obtained through the surface matching were then adjusted, using least squares, to the geo-referenced total station coordinates. Assessment of this fit (cloud-to-cloud to geo-referenced total station) produced a RMS of 0.053m.

3.4.3.3 PointReg Registration

The *PointReg* method was specifically developed for dynamic environments where traditional controls, such as targets, were not a feasible option (Olsen *et al*., 2009) due to spatial and temporal limitations. Olsen *et al*. (2011) provides an in-depth description of the *PointReg* algorithm. *PointReg* constrains translation parameters as well as leveling information to avoid error propagation. It then finds matching points that are spatially distributed and

implements a point to plane distance minimization approach to determine the optimal azimuth adjustment of each scan in the alignment. One of the key differences between *PointReg* and other techniques is that during a pair-wise adjustment, both scans are able to rotate simultaneously. Most cloud-to-cloud methods require that one of the scans remain fixed as a reference for the adjustment. The freely available program utilizes a CSV file containing the scanner origin coordinates and the scanner's internal roll and pitch values, and an estimated yaw value, within a couple of degrees. This estimated yaw value is determined by manually aligning the scans until an approximate visual fit is found. It can also be estimated through a digital compass or directly acquired if the scanner has the ability to perform back sighting.

3.4.3.4 Accuracy Assessment

The resulting scan data from all five methodologies and variants were run through a RMS calculation mode (where the scans remain fixed) of *PointReg* to produce an RMS accuracy report of the alignment. This process uses a CSV file setup with the X, Y, and Z scan origin values, the yaw value, and the roll and pitch values. Note that the roll and pitch values were acquired from the scanners internal inclination sensor for all cases except the target registration, where they were found through resection. *PointReg* then outputs a report stating the RMS, number of points used to calculate the RMS, and the

distances between scan origins for all scan combinations. A distance threshold value of 0.1m was used for the analysis (points were not considered matching if they were greater than 0.1m apart).

3.5 RESULTS

The quality of alignment can be analyzed through RMS values (Table 3 and Table 4). The results of transformation (translation and rotation) for all scans and methods can be seen in Table 5. For this analysis, it is difficult to determine which coordinates would be the most accurate. If the scanner origin could be obtained directly using a total station, *PointReg* EDM in Table 5 would provide the most accurate translation values; however, because the scanner was setup over a point on the ground, the coordinates contain centering and height measurement errors. It is also possible that the target alignments may provide a better measure of the true scanner origin due to redundancy of target placement, and the target centers being measured directly with the total station. For comparison of rotation values, the values measured from the scanners internal inclination sensor (used in the cloud-to-cloud and *PointReg* methods) are reported to have an accuracy of ± 0.008 degrees. In the target methods, these values are obtained through resection, using the total station derived control to establish the level plane. For short range scanning, inclination sensors can be more reliable, due to the precision

at which target centers can be determined. However, properly placed targets and control may achieve improved results for leveling compared to inclination sensors at longer distances. In Table 4, the bold items represent the best RMS achieved between the adjoining scans.

The scan data from each alignment were analyzed visually for quality control, as well as the quantitative analyses discussed previously. Figure 23 demonstrates a visual technique used to help verify that scan geo-referencing has been successful. Each scan has been colored differently allowing a user to see each point cloud as an individual entity, therefore making it possible to see gross misalignment errors, or un-level setup errors. Along flat surfaces there should be a smooth blending of colors with some amplification of individual scan color as viewed closer to the scan. In addition, viewing geometric primitive shapes that are centered between scans should result in the geometric primitive shape with the individual scan colored points blending around the perimeter of the shape.

In addition to the RMS report (Table 4) generated by *PointReg,* target registration provides statistics (Table 2) of how well target locations correspond between adjoining scans and the control, empowering the user with an additional technique to evaluate scan geo-referencing performance.

Table 6 summarizes the total time required, divided into field time, manual (user interaction required) time, and automated (no user interaction required) time.

Table 3. Average RMS values for each method.

Average RMS (m)	
Retro Target	0.033
Paper Target	0.034
PointReg GPS	0.035
PointReg EDM	0.033
Cloud-to-Cloud	0.052

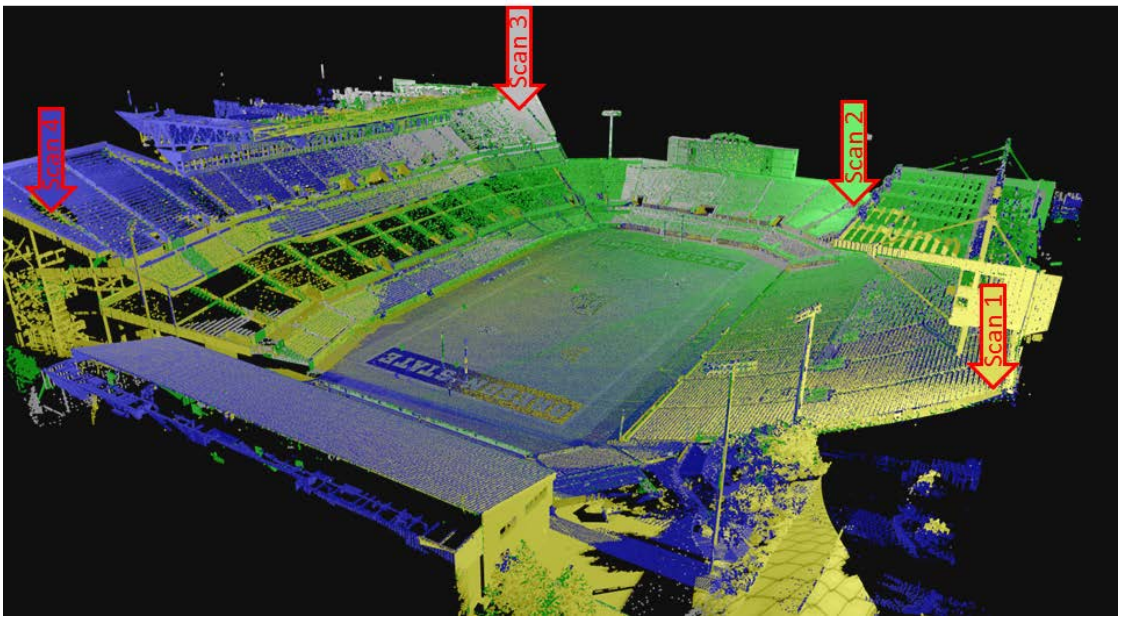

Figure 23. Geo-referenced point clouds of Reser Stadium with each scan shown in a different color.

Table 4. RMS comparison values (bold values indicate best results).

Comparison of scan 1 and scan 2			
Method	RMS (m)	Number of point pairs	Distance between scans (m)
Retro Target	0.036	272616	154.114
Paper Target	0.034	273740	154.123
PointReg GPS	0.034	275720	154.087
***PointReg* EDM**	**0.032**	**276788**	**154.112**
Cloud-to-Cloud	0.037	274559	154.047
Comparison of scan 1 and scan 3			
Method	RMS (m)	Number of point pairs	Distance between scans (m)
Retro Target	0.035	198184	225.568
Paper Target	0.036	196597	225.576
PointReg GPS	0.039	198140	225.542
***PointReg* EDM**	**0.033**	**200186**	**225.565**
Cloud-to-Cloud	0.066	115089	225.509
Comparison of scan 1 and scan 4			
Method	RMS (m)	Number of point pairs	Distance between scans (m)
Retro Target	0.033	275659	171.068
Paper Target	**0.032**	**276817**	**171.070**
***PointReg* GPS**	**0.032**	**276833**	**171.058**
PointReg EDM	0.033	275081	171.066
Cloud-to-Cloud	0.052	258841	171.042
Comparison of scan 2 and scan 3			
Method	RMS (m)	Number of point pairs	Distance between scans (m)
Retro Target	**0.031**	**248084**	**128.705**
Paper Target	**0.031**	**248297**	**128.709**
PointReg GPS	0.034	247423	128.678
***PointReg* EDM**	**0.031**	**248360**	**128.692**
Cloud-to-Cloud	0.051	134497	128.663
Comparison of scan 2 and scan 4			
Method	RMS (m)	Number of point pairs	Distance between scans (m)
Retro Target	**0.034**	**221586**	**217.267**
Paper Target	0.036	219773	217.291
PointReg GPS	0.036	222829	217.233
PointReg EDM	0.036	220280	217.263
Cloud-to-Cloud	0.059	205041	217.214
Comparison of scan 3 and scan 4			
Method	RMS (m)	Number of point pairs	Distance between scans (m)
Retro Target	**0.029**	**244318**	**175.662**
Paper Target	0.034	240269	175.689
PointReg GPS	0.034	241456	175.645
PointReg EDM	0.031	242874	175.668
Cloud-to-Cloud	0.045	235968	175.644

Table 5. Scan transformation parameters (translation and rotation) determined by the different methods.

Scan Position 1						
Method	X (m)	Y (m)	Z (m)	Roll	Pitch	Yaw
Retro Target	2278972.026	103001.052	93.438	-0.051	-0.007	134.413
Paper Target	2278972.021	103001.043	93.448	-0.051	-0.008	134.414
PointReg GPS	2278972.036	103001.048	93.433	-0.062	-0.008	134.413
PointReg EDM	2278972.025	103001.054	93.447	-0.062	-0.008	134.409
Cloud-to-Cloud	2278972.060	103001.043	93.482	-0.062	-0.008	134.416
Scan Position 2						
Method	X (m)	Y (m)	Z (m)	Roll	Pitch	Yaw
Retro Target	2279103.254	102920.242	81.775	-0.011	0.093	113.920
Paper Target	2279103.262	102920.237	81.766	-0.019	0.091	113.926
PointReg GPS	2279103.248	102920.263	81.763	-0.012	0.086	113.917
PointReg EDM	2279103.253	102920.248	81.767	-0.012	0.086	113.918
Cloud-to-Cloud	2279103.238	102920.279	81.812	-0.012	0.086	113.911
Scan Position 3						
Method	X (m)	Y (m)	Z (m)	Roll	Pitch	Yaw
Retro Target	2279197.490	103007.903	107.887	-0.032	0.186	-143.870
Paper Target	2279197.492	103007.911	107.918	-0.027	0.195	-143.865
PointReg GPS	2279197.474	103007.896	107.921	-0.029	0.192	-143.880
PointReg EDM	2279197.486	103007.894	107.907	-0.029	0.192	-143.879
Cloud-to-Cloud	2279197.465	103007.889	107.839	-0.029	0.192	-143.891
Scan Position 4						
Method	X (m)	Y (m)	Z (m)	Roll	Pitch	Yaw
Retro Target	2279077.231	103135.945	103.730	0.022	0.014	117.928
Paper Target	2279077.200	103135.959	103.696	0.037	0.019	117.941
PointReg GPS	2279077.235	103135.934	103.749	0.011	0.009	117.925
PointReg EDM	2279077.228	103135.946	103.746	0.011	0.009	117.926
Cloud-to-Cloud	2279077.231	103135.930	103.736	0.011	0.009	117.931

Table 6. Time requirements for each method.

Acquisition and processing time (minutes)				
Method	Field time	Office Manual	Office Automated	Total Time
Retro Target	170	35	11	216
Paper Target	170	45	11	226
***PointReg* GPS**	**60**	**30**	**24**	**114**
PointReg EDM	80	55	24	159
Cloud-to-Cloud	60	80	61	201

3.6 DISCUSSION

The RMS values produced through the various methods were very similar with the exception of cloud-to-cloud registration. In general, a user should feel comfortable with the results achieved by either target registration or the *PointReg* method. For similar and larger sites and when scanning at longer ranges, the cloud-to-cloud registration may not be suitable as the primary technique. However, it would still be useful as a back-up option for small sections in the event that field collection data was lost or misreported. This correlates with the findings of Olsen *et al*. (2011) who determined that significant error propagation could occur when using cloud-to-cloud alignments along extended, linear segments. Bae and Lichti (2006) note that variants of the ICP algorithm, like that used in cloud-to-cloud, will produce different results. These algorithms are tailored to work with specific datasets. It is

anticipated that the cloud-to-cloud method would likely have performed better if there had been more scans in closer proximity to each other, providing denser data and more overlap. Hence, there are many cases where it might be an appropriate technique.

Target resection bases the transformation on a limited number of points (3 or more) that are generally more precisely defined that pick points in a point cloud. The cloud-to-cloud method typically uses around 2,000 points for determining the coordinates. The *PointReg* method uses substantially more points by default (*i.e.*, tens to hundreds of thousands). However, should a user desire it to run faster, they could limit the number of point pairs used.

A user should also consider many factors about the equipment that they are using before selecting any of these methods. For example, if the scanner has poor, or no, inclination sensors, then the *PointReg* method would not be an acceptable registration technique. If target geometry is poor (linear target setup allowing rotation about the line) then the *PointReg* method could provide better results. A user will need to carefully consider scanning conditions prior to deciding which method to use.

Consideration should be made with regards to how much time can be allotted to field processing and office processing (manual and automatic). For TLS, more time spent in the field typically equates to less time spent in the

office and vice versa (Table 6). Total station usage adds a significant amount of additional time, and has the potential to introduce error with additional processing steps. The total station, however, generally will provide improved accuracy across a site, and may be necessary in cases where RTK GPS is not available due to forest or urban canopy. Most cloud-to-cloud processing techniques require significant manual user interaction time to permit the algorithm to work correctly. This includes filtering the point cloud to eliminate erroneous points, and applying a minimum separation between points. However, work is underway to develop automated procedures to estimate a scan's initial pose. Field time can also vary significantly depending on the conditions encountered. In the case of this study, many targets were not automatically detected, which required the user to manually find them within the point cloud. In some cases, more closely placed targets may be initially scanned at high enough resolution to not require any human intervention to extract them. This can significantly reduce acquisition time, with target setup being the only additional time required.

3.7 CONCLUSION

With the exception of cloud-to-cloud registration, all methods provide similar RMS results. Total time to geo-reference a point cloud varies significantly, with external surveying (*e.g.*, total station) adding the bulk of time.

PointReg using RTK GPS provides the overall most efficient method and greatly lowers the possibility of introduced error. This method, however, can only be as accurate as the RTK GPS coordinates, and is not possible where RTK GPS is not feasible. *PointReg* using EDM scan origins eliminates the RTK GPS requirement, and also requires less field time than target methods. A key point to remember with the *PointReg* method is that geo-referencing accuracy is also related to the accuracy of the scanners internal inclination sensors. Target registration eliminates the need for inclination sensor values, but requires significant field time, as well as pre-planning, to ensure that required target correspondence is met between scans. Cloud-to-cloud provides an acceptable means of geo-referencing a scan that has a pair of adjoining scan neighbors, but may require additional accuracy verification if it is used as the primary registration technique when limited scans are obtained across a large site. In this case, all scans were at a long distance from each other, which is not ideal for the cloud-to-cloud method as it tends to work better with many scans situated closer together. Different scanners will also have varying influential effects on the alignment methods due to variations in beam divergence, range, pulse repetition rate, and the overall accuracy of the scanner. The user will have to choose the most appropriate method based on the variety of factors discussed in this paper as well as the requirements of the final geo-referenced point cloud (Figure 24).

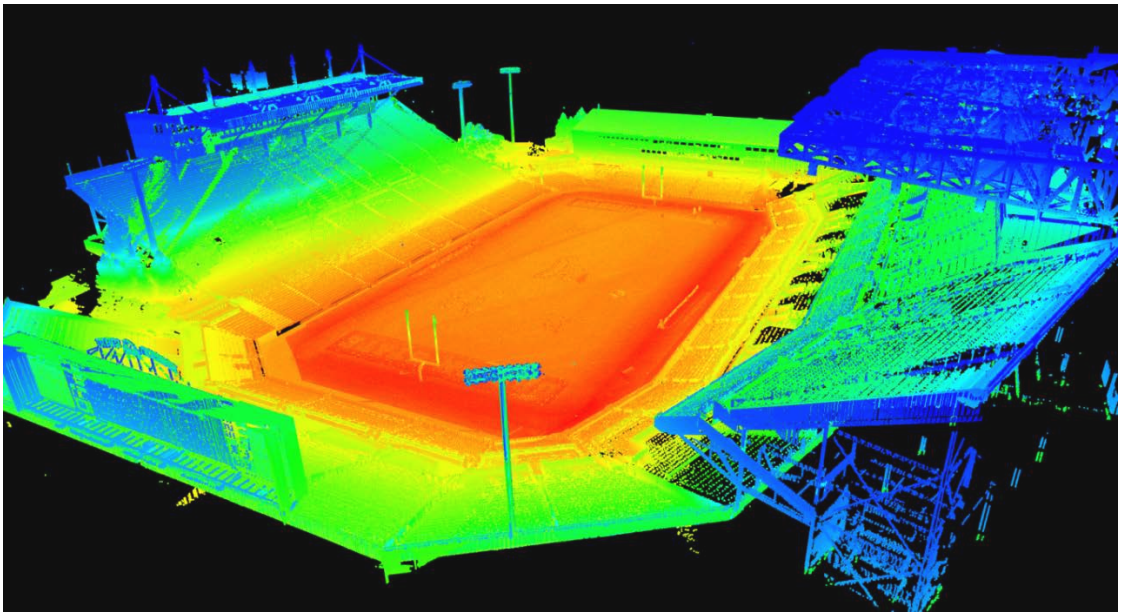

Figure 24. Geo-referenced point clouds colored by elevation values.

3.8 ACKNOWLEDGEMENTS

The authors would like to thank Leica Geosystems, David Evans & Associates, and Maptek I-site for their generous donations of training, equipment, support, and software to Oregon State University. Much thanks to Shawn Butcher and Kris Puderbaugh for assisting with data collection, which involved more stairs running than expected!

4 3D POSITIONAL ERROR AND 2D SLOPE EVALUATION FOR LIDAR DATA USING NATURAL FEATURES

4.1 INTRODUCTION

Accuracy verification of a LiDAR point cloud faces a number of challenges. First, there is no guarantee that the laser will strike the center of a target or control point; the user merely selects a scan window and angular sampling increment. Second, the laser spot size increases with distance from the scanner, and can be a few centimeters in size at far distances; hence, it is uncertain where the pulse returned from within the spot on the surface. Third, the accuracy of every point will vary depending on the scanning geometry, laser properties, and properties of the material being scanned. Finally, error sources are propagated from the initial collection of LiDAR data and can be additive or reductive through each processing stage (Vosselman and Maas, 2010). The accuracy of a point cloud can be described in terms of relative (*i.e.*, how accurately the points are measured relative to one another or the scanner origin) and absolute (*i.e.*, how accurately the point cloud is positioned in a coordinate system) accuracies.

Currently, a common practice of scan validation compares check points (points within the point cloud, collected independently of the scan) with the approximate same point in the point cloud. This comparison faces the

uncertainty of whether the point selected in the point cloud actually corresponds to the check point (Figure 25). To lower this uncertainty these check points are typically placed where they can be readily distinguished in a point cloud (*e.g.,* the tip of a turn arrow or end of pavement striping). However, as the resolution of scan data decreases, the ability to select appropriate scan points to match to the check points also decreases.

An accuracy estimate of LiDAR data can be divided into both a vertical component and a horizontal component. However, the vertical accuracy of a LiDAR point cloud is typically easier to determine than the horizontal. Figure 25a demonstrates that the vertical component of accuracy can be defined well due to the relation of control points to a plane created through three scan points. Figure 25b demonstrates that, in this same situation, the horizontal component faces uncertainty of which scan point the control point should be matched to, or if it should even be matched to one of these scan points.

Ray and Graham (2008) propose a method of verifying horizontal accuracy in ALS data by utilizing the intensity of returning scan pulses to extract linear feature such as pavement markings; these features are then adjusted to orthophoto control. Unfortunately, using orthophoto control does not permit the horizontal accuracy of the LiDAR data to exceed the horizontal accuracy and resolution of the orthophoto, which does not permit use for TLS

or MLS, which provide data of much higher accuracies and resolutions. Meade (2008) discusses methods to verify horizontal accuracy including, LiDAR intensity return on sloped surfaces (*e.g.*, metal roofs, concrete vs. asphalt), LiDAR intensity overlaid on orthophotos, and comparison of cross-sections between different flight lines of the scan data. In all instances, multiple passes are used as a check to insure that both passes align with each other well.

MLS and TLS typically require a much higher level of accuracy than what can be provided by the methods discussed in the preceding paragraph. Another difficulty for accuracy verification of these technologies is that devices used to establish a reference are usually at least an order of magnitude improved in accuracy are used for validation. However, TLS and total station data have similar precision capabilities (~2mm to 5mm nominally).

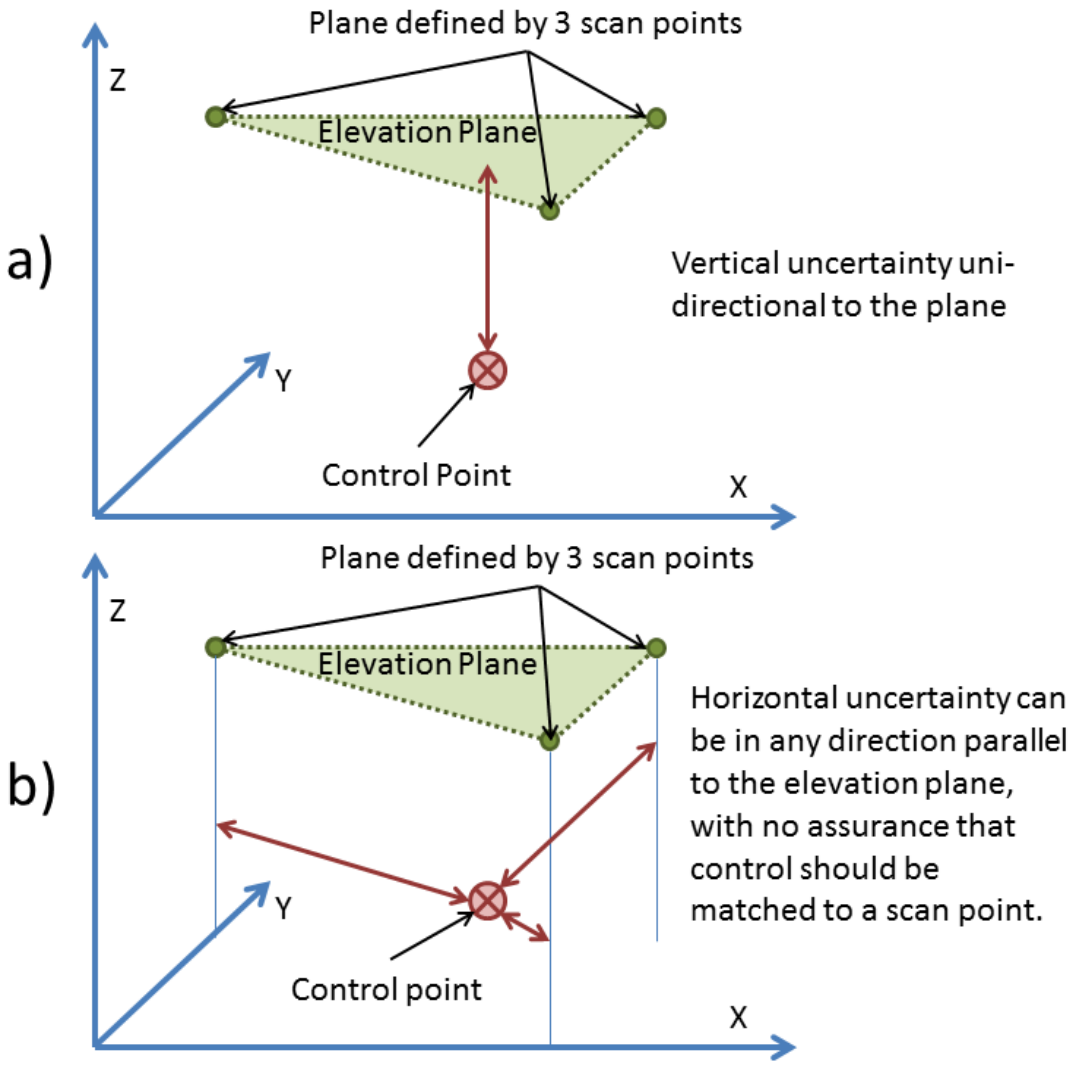

Figure 25. Uncertainty of accuracy based on a) vertical measurement and b) horizontal measurement

4.2 PURPOSE

The goal of this methodology is to provide a means to verify (in 3D) the accuracy of scan geo-referencing; this is done by comparing a series of 2D

cross-sections from the scan data with those from a total station. The use of cross-sections throughout the scanned area enables a larger portion of the scan to be verified, and can provide advanced determination of individual components of error in roll, pitch, yaw, and translations in X, Y, and Z.

4.3 METHODOLOGY

4.3.1 Field Collection Procedures

This methodology was developed to function for any form of collected scan data (*e.g.*, ALS, MLS, or TLS). Therefore, this section is focused solely on the collection of total station data since it focuses on the validation of the scan data rather than the collection process. Cross-sections are collected at an intersection for two reasons. First, the geometry of an intersection allows the use of 2D cross-sections at each leg to be used to find a representative 3D offset in the data. Second, an intersection typically has built crosswalks (at approximate data collection path) and lower vehicular speeds, creating a safer environment for a surveyor to collect these points.

The total station should be setup so that the all cross-sections within the intersection can be collected from a single setup. At least three control points should be established to geo-reference the total station data. The total station can either be setup over a control point and back-sighted to another control point, or geo-referenced through resection to the control points. The

control points for resection of the test dataset consisted of five temporary markers with RTK GPS coordinates, situated well outside of the bounds of the intersection (Figure 26). Coordinates were then collected with the total station for each control point and then along each cross-section.

Considerations for selecting the most appropriate cross-sections will vary greatly depending on site conditions. For optimal results, smooth, clean, minimally rutted, and minimally patched sections should be used. In addition, the presented methodology provides improved statistics when a defined crown can be extracted from the road; for this reason it is recommended that cross-section point collection be located an adequate distance along each leg of the intersection to avoid slope transitions that take place within the physical intersection. Cross-section points should then be collected at each of the four legs of the intersection. These cross-section points should be linear and closely spaced (0.3 m was used for the test data). To obtain a linear collection of points along the road surface a string, chalk line, or laser line should be laid across the roadway. Figure 26 shows the topographic points collected along the cross-sections of the test intersection. The total station points, if collected on a local coordinate system, should then be geo-referenced to the control points (with coordinate system defined by that of the scan) through a least-squares coordinate transformation.

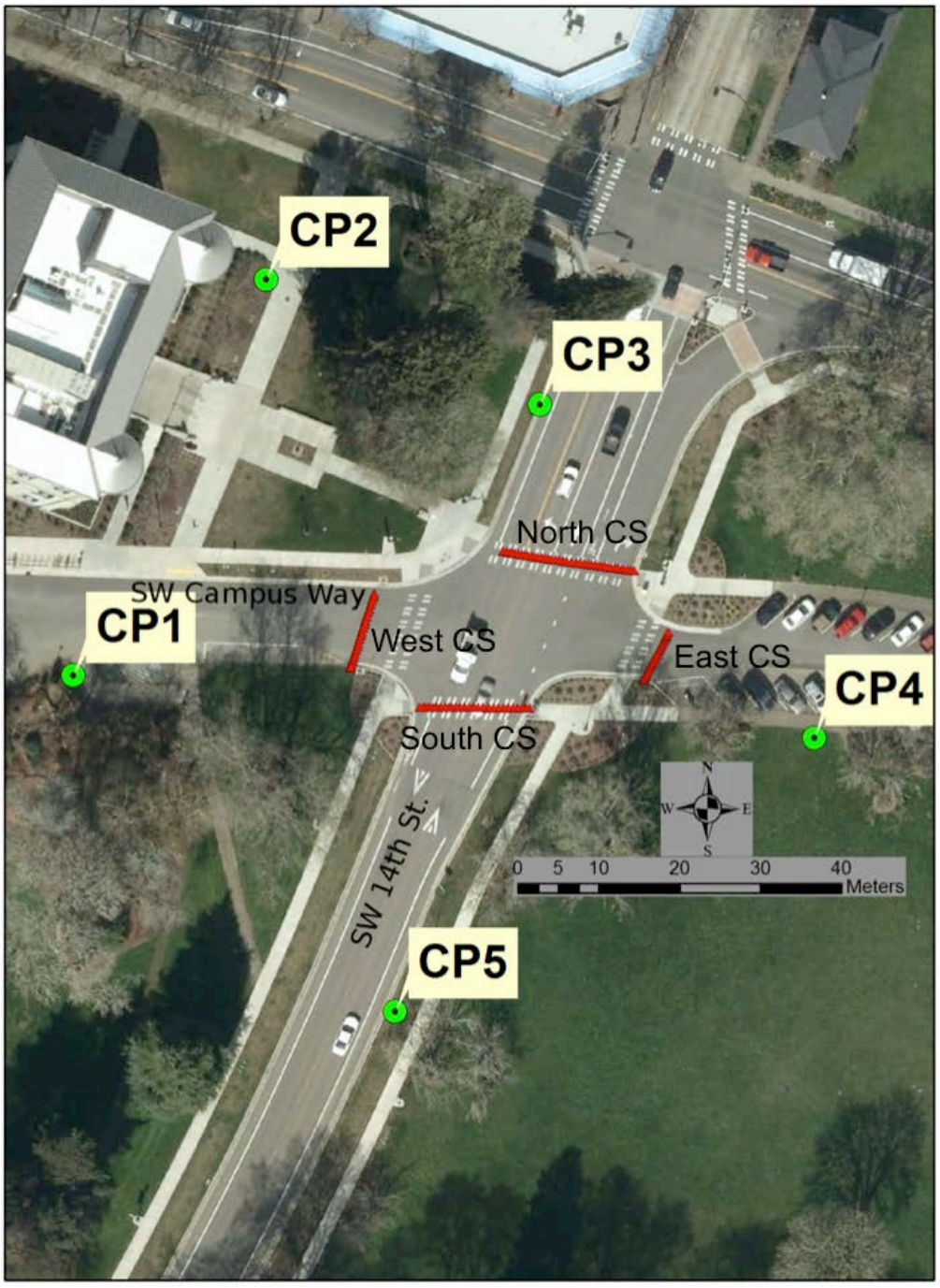

Figure 26. Intersection with a) control points well outside of intersection, and b) cross-sections taken at each leg of intersection

4.3.2 Spreadsheet Implementation

To facilitate implementation of this method, a spreadsheet was created to automate many parts of the analysis. Prior to using the spreadsheet, scan points that correspond to the four cross-sections need to be extracted. The cross-section width of the scan data should be only wide enough to accommodate inclusion of the total station points (*e.g.*, less than 2cm). For the functionality of the spreadsheet, only the roadway slope should be included (*i.e.*, no curb and gutter, although this information could be useful, as described later). Figure 27 shows the total station points plotted with the point cloud of the intersection. The user then inserts all X, Y, Z points for the total station and scan data into the "Raw Data" tab of the spreadsheet.

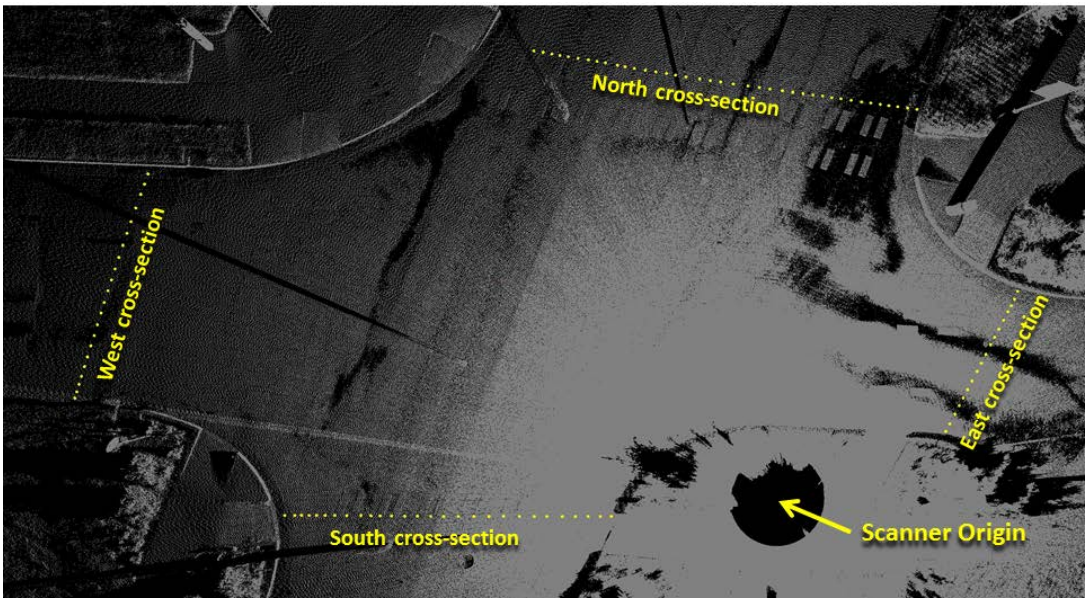

Figure 27. Total station points overlaid within the point cloud.

Once points are inserted for the scan and total station into the “Raw Data” sheet for each of the four cross-sections, they are automatically carried over to the individual leg calculations, titled N-Calcs, S-Calcs, E-Calcs, and W-Calcs. These sheets automatically sort the data, select the minimum easting value and corresponding northing value, and then truncate the scan and total station data to this minimum easting value and corresponding northing value. Using the truncated total station values, the angular rotation from the Cartesian coordinate system (with X-axis equal to zero) is calculated, and then the inverse value is used to rotate the total station and scan points so that they are oriented along the X-axis using the rotation matrix:

$$\begin{bmatrix} X' \\ Y' \end{bmatrix} = \begin{bmatrix} \cos\theta & -\sin\theta \\ \sin\theta & \cos\theta \end{bmatrix} \begin{bmatrix} E \\ N \end{bmatrix} \tag{2}$$

This rotation is applied so that each cross-section is oriented in the same direction so that a direct northing or easting shift can be determined. The translated scan and total station points are then sorted by increasing the X'-values. Note that northing (N) and easting (E) are used for pre-rotation notation and Y' and X' are used for post-rotation notation. The user must then manually determine the crown of the road surface, by finding the high Z-value, and divide the data into a left value for the low X'-values and a right value for the high X'-values. Plots of these values can then be created which permit the user to visualize the relationship between the total station and the

scan data. In addition, translation adjustment parameters are provided for the X' and Z directions, which allow the user to manually translate the total station data to fit the scan data if they are not already in agreement. This magnitude of this shift provides an estimate of the absolute accuracy of the point cloud. If a roadway crown is present in the cross-section, the plots will reflect left and right values for both total station and scan; this distinction orients the view looking from the center of the intersection to the cross-slope leg being analyzed.

4.4 RESULTS

The results of the plotted data for the described intersection can be seen in the following graphs (Figure 28 to Figure 35). All plots display the raw data after rotation has been applied, as well as the slope of each collection of points, and the coefficient of determination (R^2) for the defined slope. Note that the first graph of each series is the raw values, and the second graph depicts shifted cross sections with both the amount and uncertainty of the shift indicated. These shifted graphs are visually manipulated by moving the total station points as a rigid body in both the X' and Z direction for a visual best fit. Once an alignment is found, the graphs are then incremented in a positive and negative direction until they obviously are no longer in visual alignment. This process is then iterated so that the mean of the positive and negative shift is

assigned to the true shift value, and the uncertainty range from this shift value is defined.

A comparison of slope values can be seen in Table 7. Summary of slope values for each cross-sectionTable 7; these slope values are also plotted on each cross-section graph. Note that the west cross-section has a parabolic curve that results in slope comparisons between scan and total station data to have a larger difference than the other cross-sections. In traditional slope measurements, two points typically define the slope of the road; as can be seen by the following graphs utilization of two points may not accurately describe the cross-slope of the roadway surface. Utilization of scan data preserves the variability in cross slope that is lost by using two points to define the cross-slope.

Table 7. Summary of slope values for each cross-section

Cross-Section Slope Summary (%)			
Cross-Section	Total Station Slope	Scan Slope	Difference
North-Left	0.64	0.70	0.06
North-Right	-1.33	-1.40	0.07
South-Left	-0.74	-0.51	0.23
South-Right	-3.04	-3.03	0.01
East	0.24	0.21	0.03
West-Left	1.60	1.65	0.05
West-Right	-5.12	-4.07	1.05

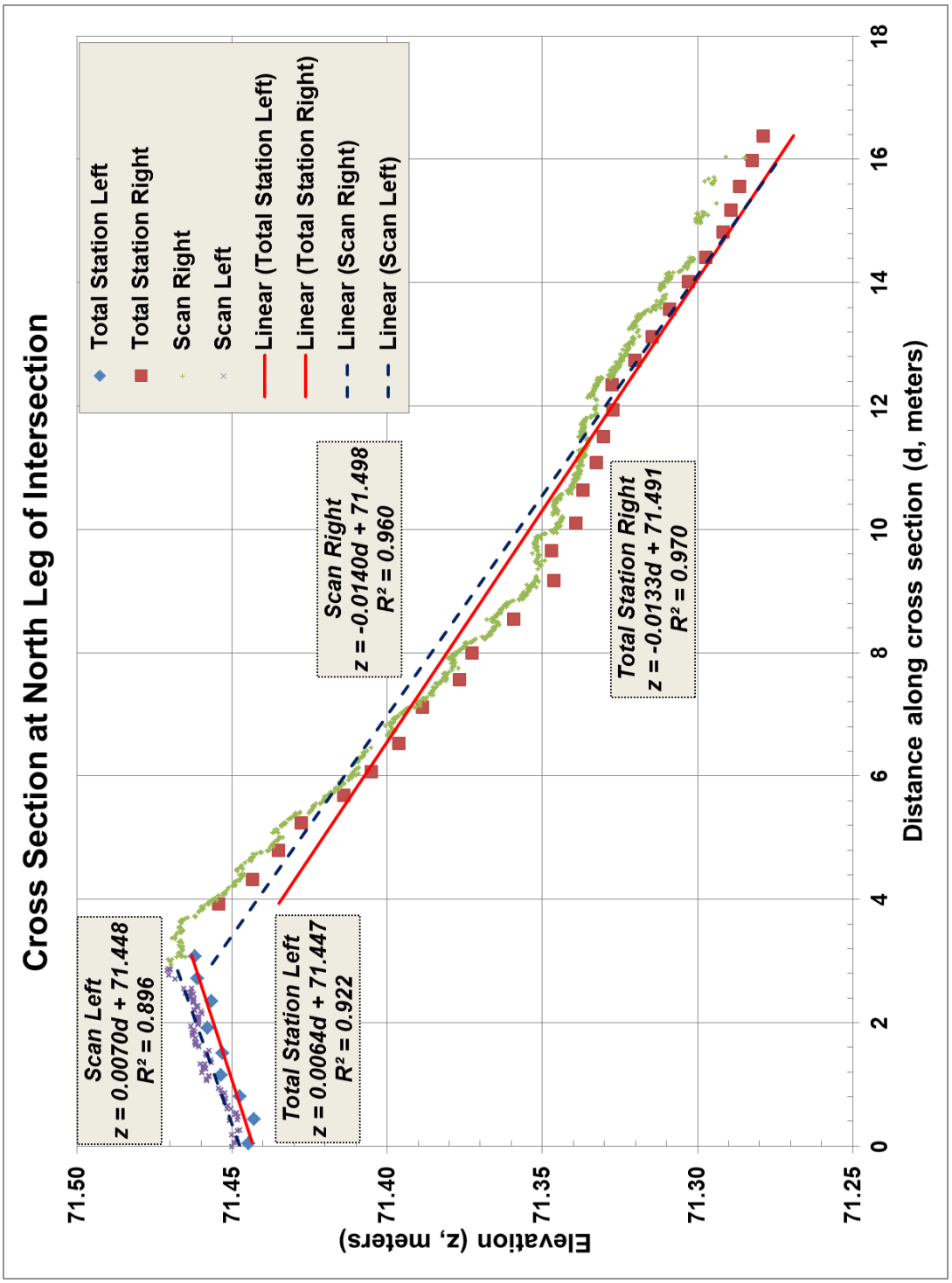

Figure 28. Un-shifted cross-section at north leg of intersection.

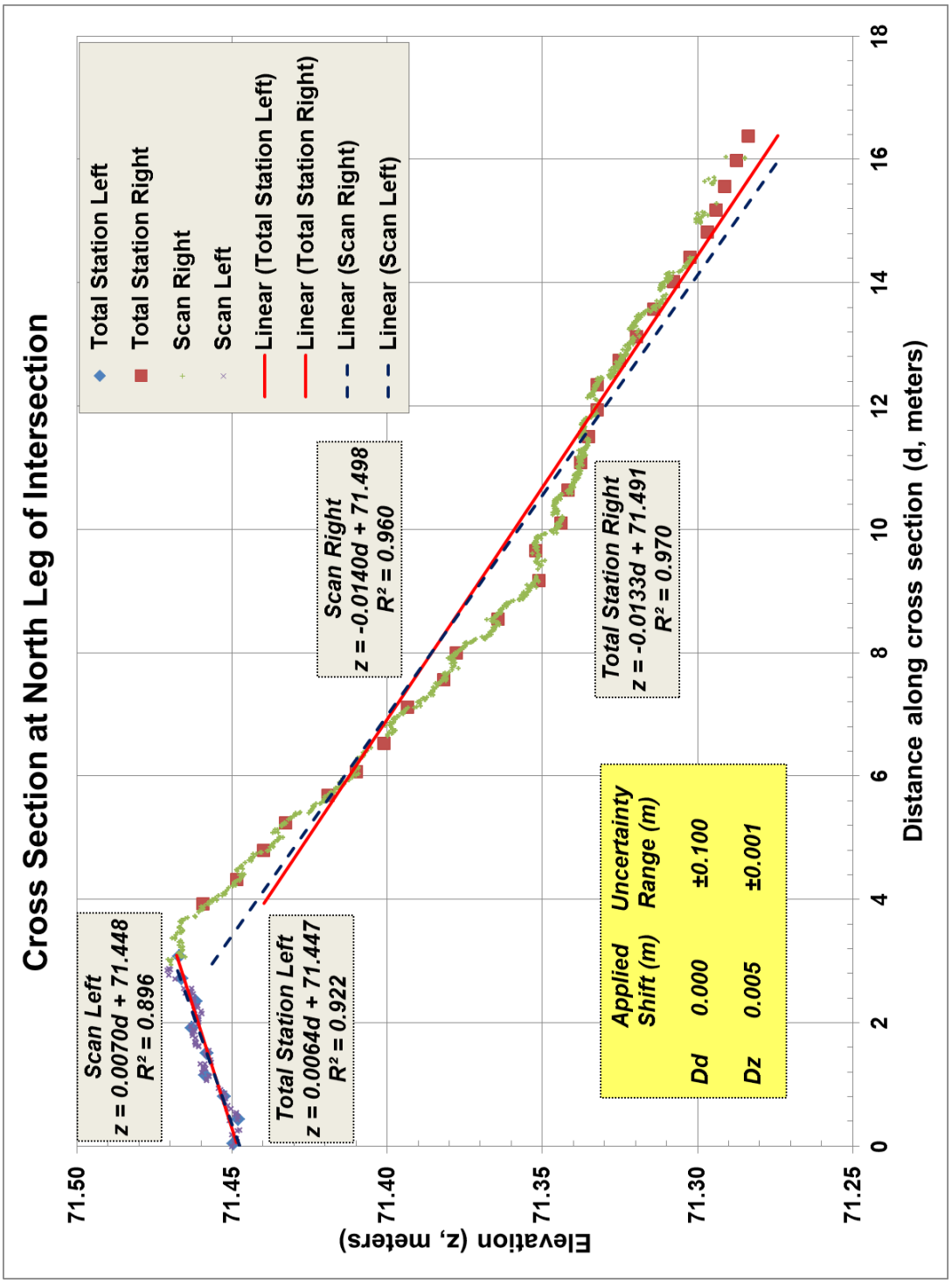

Figure 29. Shifted cross-section at north leg of intersection

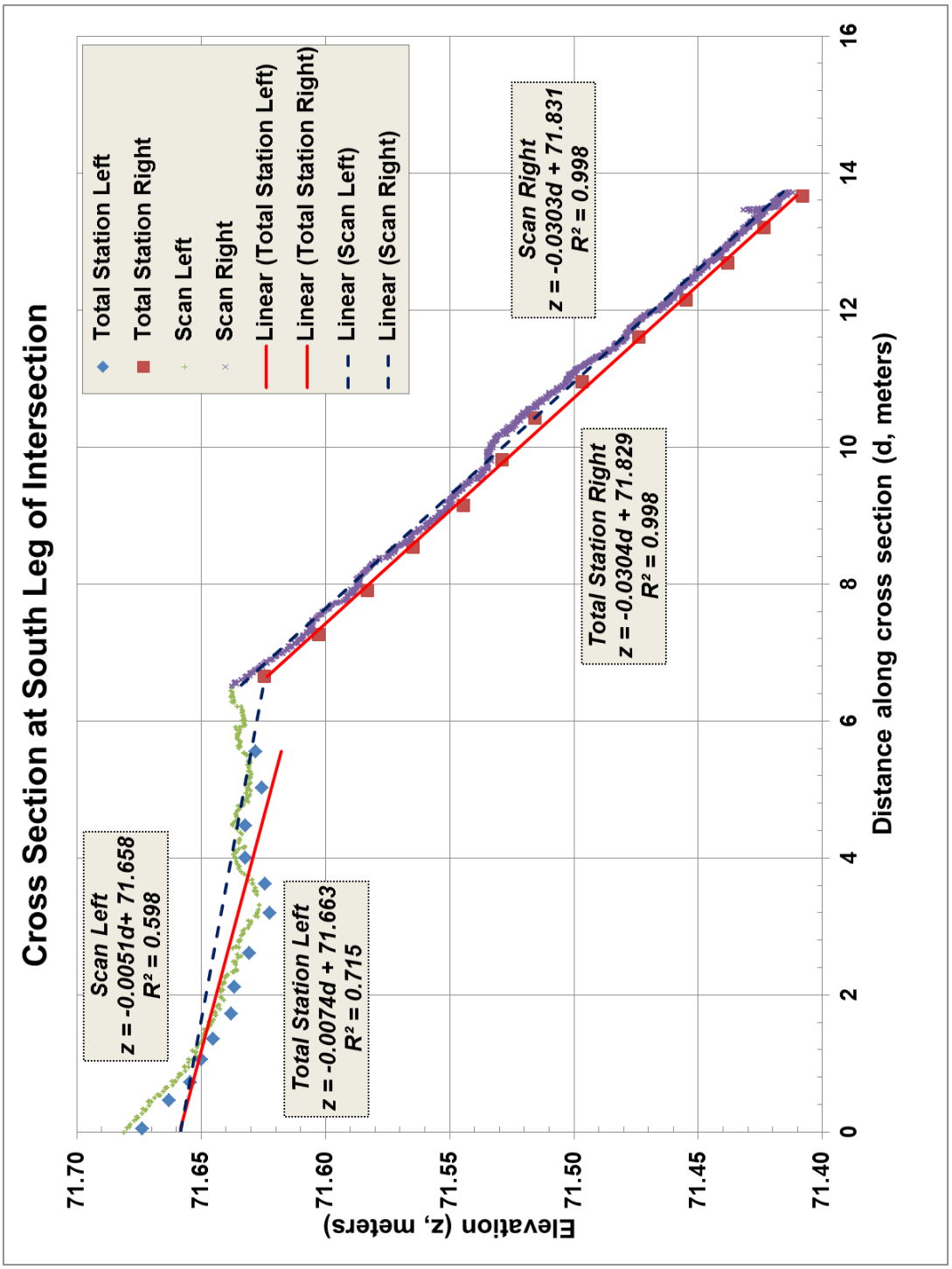

Figure 30. Un-shifted cross-section at south leg of intersection.

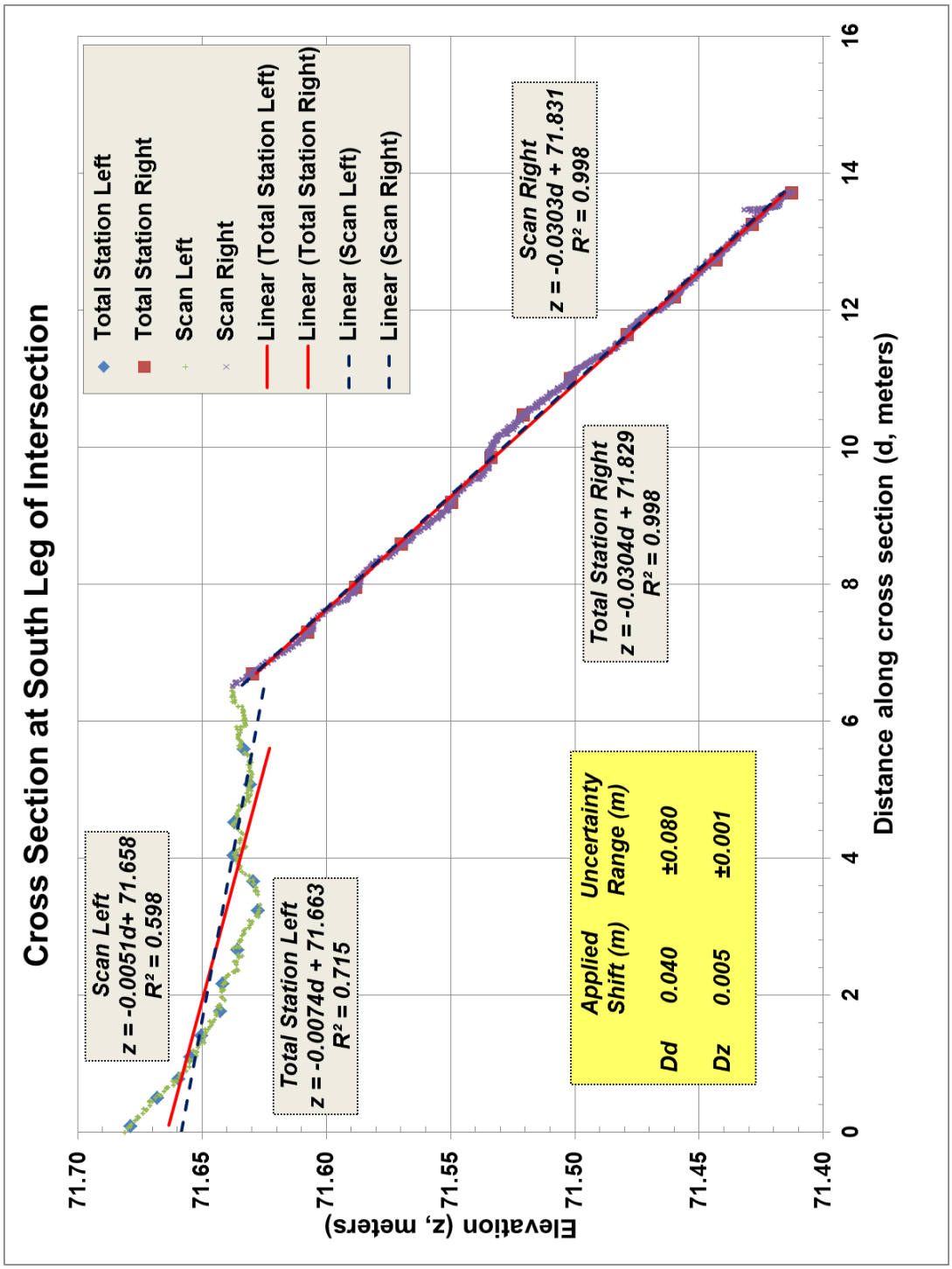

Figure 31. Shifted cross-section at south leg of intersection.

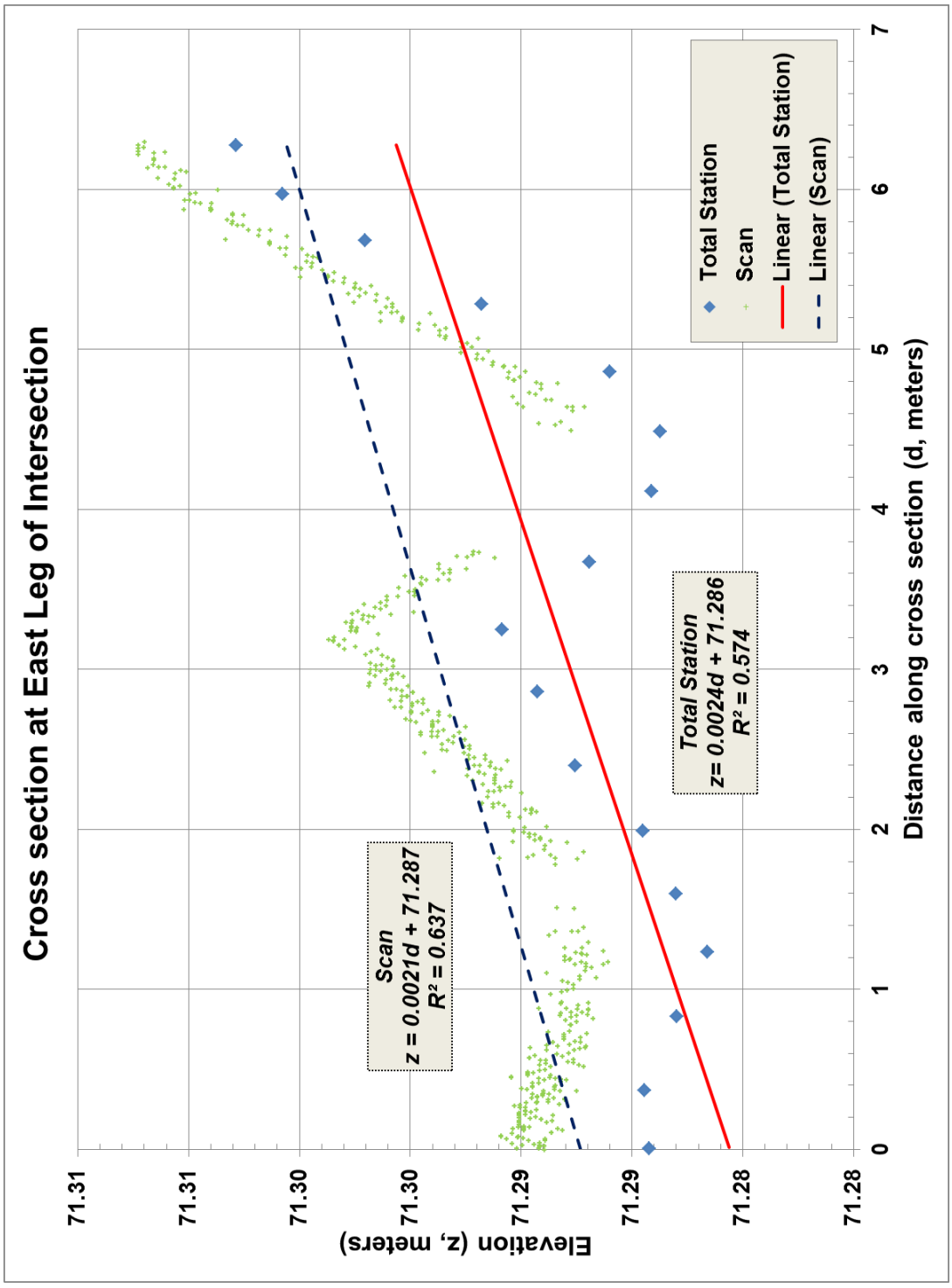

Figure 32. Un-shifted cross-section at east leg of intersection.

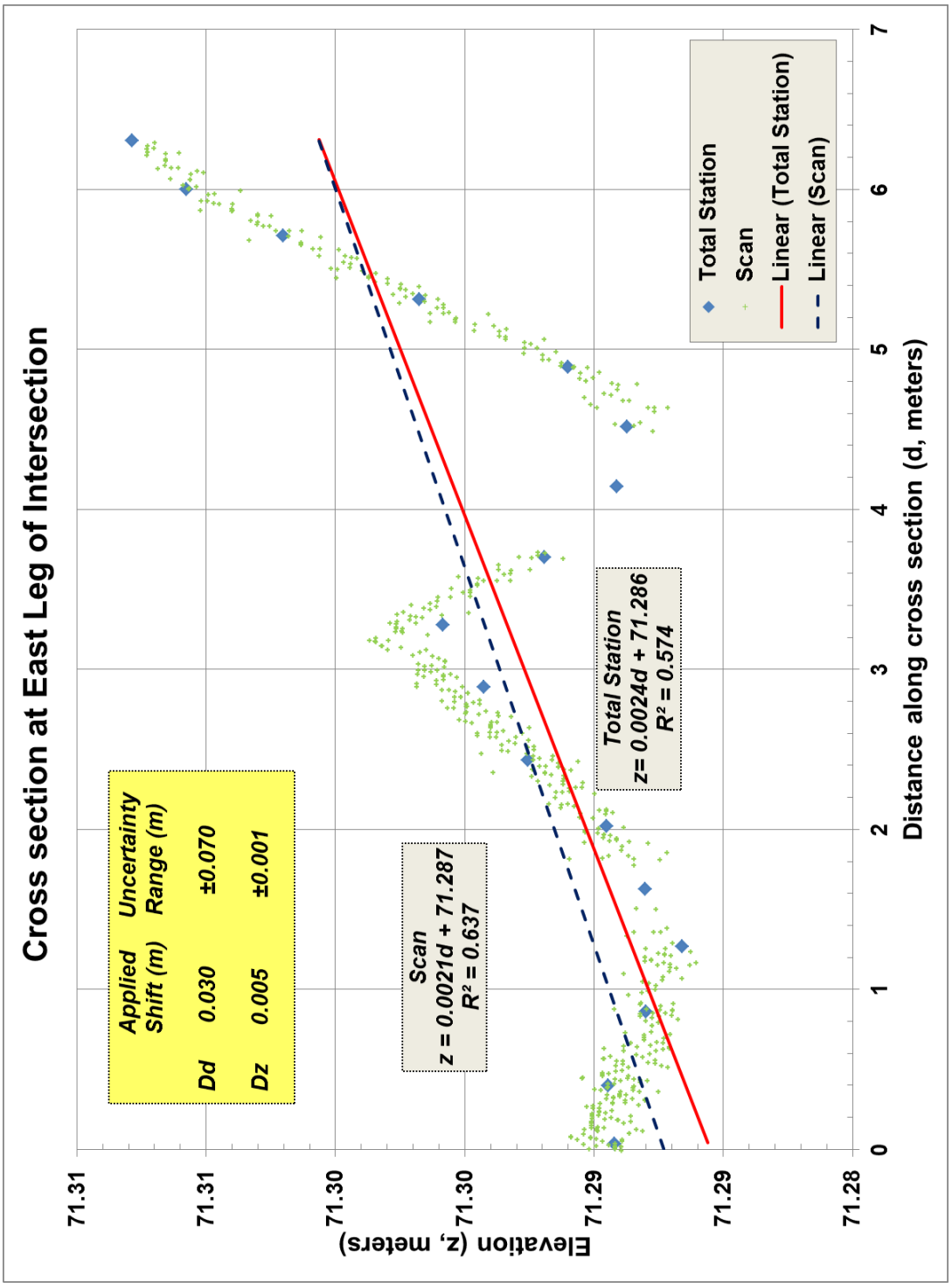

Figure 33. Shifted cross-section at east leg of intersection.

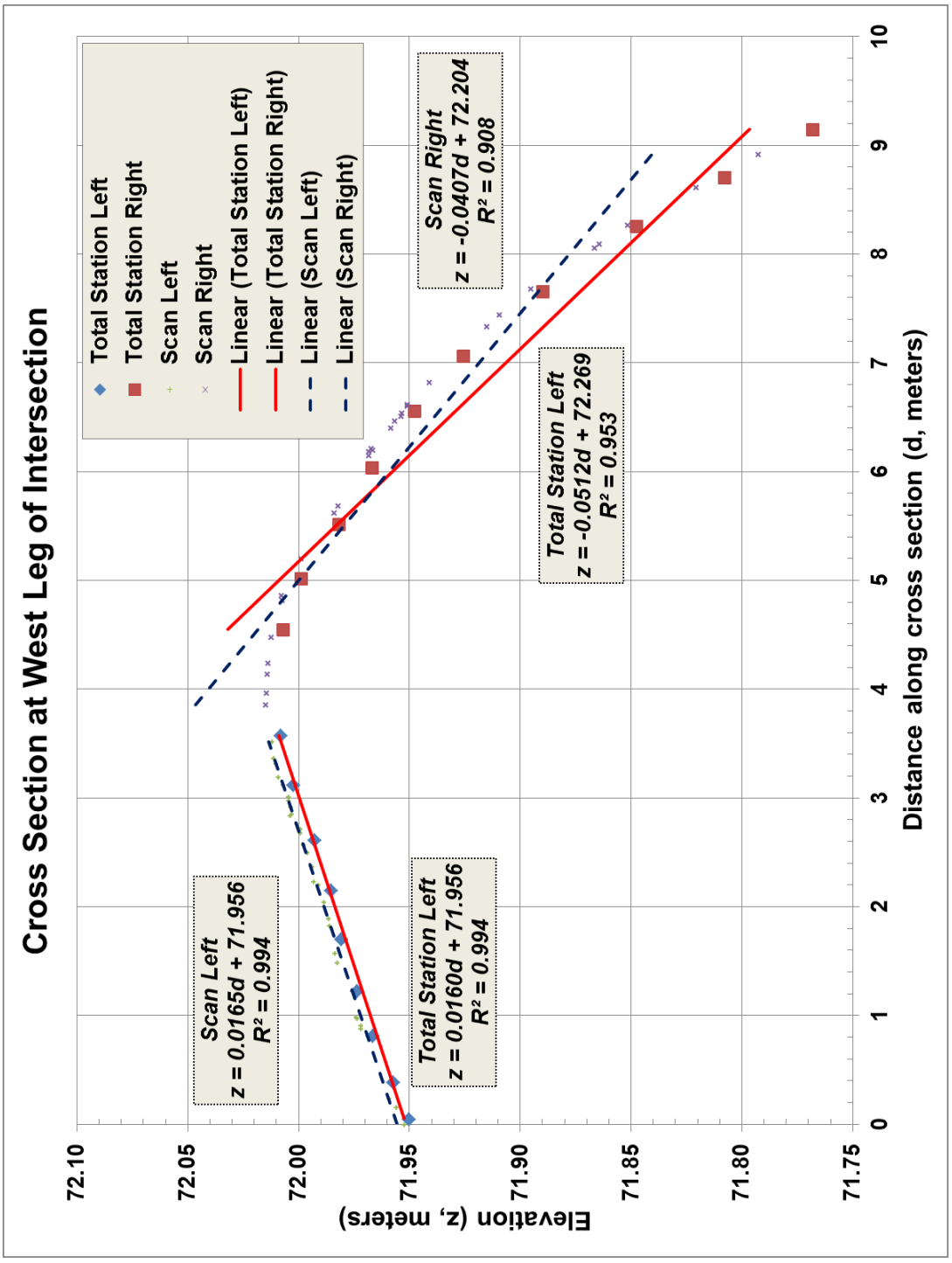

Figure 34. Un-shifted cross-section at west leg of intersection.

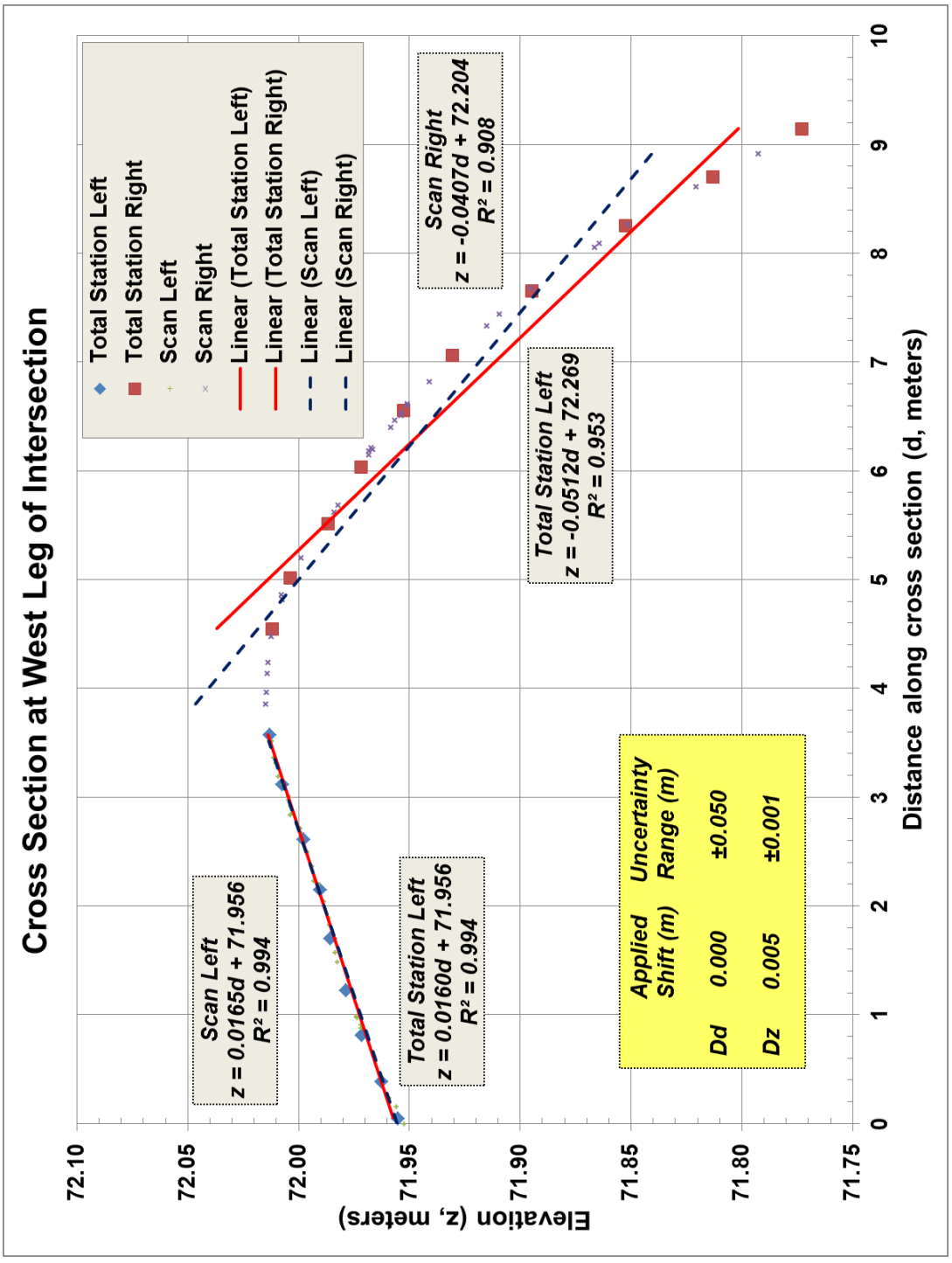

Figure 35. Shifted cross-section at west leg of intersection.

4.5 DISCUSSION

An initial hypothesis was that this methodology would accurately predict the roadway crown, and that this location could be used to verify the scan accuracy. Unfortunately, the roadway crowns were not reliably detected due to the curved geometry of the road surface; the crown location was detected within 1cm vertically and up to 40cm horizontally (Table 8).

Table 8. Slope estimation of roadway crown.

Roadway Crown Location From Intersection Slopes						
Intersection Leg	Total Station		Scan		Difference	
	d (m)	z (m)	d (m)	z (m)	d (m)	z (m)
North	-2.227	71.429	-2.381	71.431	0.154	-0.002
South	-7.249	71.712	-6.868	71.693	-0.381	0.019
West	-4.656	71.877	-4.340	71.884	-0.317	-0.007
Note, east leg did not have a roadway crown						

Visually shifting the cross-sections provided improved accuracy results over locating the roadway crown. The plots produced by this method allow a user to visually compare scan and total station data. As often is the case with scan accuracy, the vertical component is better resolved (~2mm of uncertainty); however, the horizontal component is less certain (~5-10cm of uncertainty). The ability to verify vertical accuracy along a cross section has added benefits over the traditional method of checking individual control points. Primarily, because the cross-section spans the entire width of the road, any off-level scans can be readily detected (*i.e.*, scan points on the left

will sit higher than total station, and scan points on the right would sit lower than total station, or vise-versa). Additionally, because the data is viewed as a large collection of points, outliers or possible scanner malfunctions can be more easily detected by examining slope variations. Table 9 demonstrates that utilizations of four 2D cross-sections can provide a 3D accuracy assessment of the site without requiring higher resolution sampling on targets, which is difficult, if not impossible for MLS.

Table 9. Determined accuracy for test intersection.

Shifted Intersection Values			
Intersection Leg	Δ X (m)	Δ Y (m)	Δ Z (m)
North	0.000	---	0.005
South	0.040	---	0.005
East	---	0.030	0.005
West	---	0.000	0.005
Average	0.020	0.015	0.005
Range	0.040	0.030	0.000

Improvement to the horizontal verification of accuracy could be incorporated into this spreadsheet, which could bring the accuracy down to an estimated ~1-2cm level. This could be accomplished by obtaining the full cross-section including the curb and gutter. Reflectorless shots could be acquired on the vertical curb faces, which could then be exploited in the same manner as the vertical verification of accuracy. Similarly, buildings, retaining walls, and other vertical structures could provide features for validation. In

addition, intersections with a steeper cross-slope permit a better verification of horizontal accuracy, which can be seen by comparing Figure 29 (less cross-slope) and Figure 35 (more cross-slope).

Methods such as the iterative closest point (ICP) algorithm (*e.g.*, Besl and McKay, 1992) could provide statistical verification of both the horizontal and vertical components. The complexity of an ICP algorithm, however, would not permit incorporation into a spreadsheet; this would need to be coded in a more efficient language (*e.g.*, C++). In conjunction with these improvements, one could simultaneously calculate the RMS error of the fit, which enables the verification of the relative (local) accuracy. This could be accomplished by determining the quality of fit of the shifted total station points to the scan data.

4.6 CONCLUSION

The discussed methodology demonstrates a new approach to validate point cloud accuracy using more information than single targets. The vertical component of accuracy using this methodology showed a small level of uncertainty (2mm). Horizontal accuracy is improved over current methods with a 5-10cm level of uncertainty, but could be improved with further refinement to include curb and gutter, which would facilitate an improved visual fit. Additionally, use of an ICP algorithm could remove the need for manual selection of shift parameters, enabling a more rigorous evaluation.

5 OVERALL CONCLUSION

Chapters 2, 3, and 4 discuss many of the different methods that are used to assess the accuracy a LiDAR point cloud. Chapter 2 focuses on MLS systems and how they are used to collect LiDAR data safely and efficiently while still maintaining accuracies nearing that of TLS. Chapter 3 examines different methods of registering TLS point cloud data, and it outlines the time taken and accuracy produced for each method. Chapter 4 provides a methodology for an accuracy assessment for any type of LiDAR data. This methodology was developed, in part, due to the findings in Chapter 2 that demonstrate that there is not an industry standard method used to verify MLS accuracy, particularly horizontal accuracy.

5.1 REVIEW OF APPLICATIONS OF MLS IN TRANSPORTATION

The literature review touches briefly on the basics of LiDAR followed by a more in depth description of current MLS trends, including systems components and software. This review also provides insights on current and emerging applications of MLS for DOTs through industry projects and academic research. An overview of existing quality control procedures used to verify the accuracy of the collected data is presented. A collection of case studies provides a clear description of the advantages of MLS, including an increase in safety and efficiency.

The final portions of the review delve into current challenges the industry is facing, what guidelines currently exist, and what guidelines are needed to streamline the adoption of MLS by DOTs. Most existing guidelines for geospatial data are typically developed for digital terrain modeling using data from a generic source and focused primarily on elevation values. Unfortunately, many of these guidelines do not cover the specific challenges and concerns for LiDAR use. Some have been developed for airborne LiDAR acquisition and processing. However, these do not meet the needs of many DOT applications utilizing MLS, creating a number of gaps that cannot be filled without an in-depth set of guidelines developed specifically for MLS systems. Specifically, guidelines that outline the procedures to provide an accuracy assessment of the point cloud alignment are necessary. This includes control/check point requirements, vehicle trajectory reporting, and various levels of data to account for different accuracy and resolution of data.

5.2 Accuracy Assessment of Geo-Referencing Methodologies for Terrestrial Laser Scan Site Surveys

This study demonstrated key considerations that should be made prior to planning a TLS project, and has provided a TLS surveyor with valuable information regarding time, accuracy, and the risks of error introduction for various geo-referencing methodologies. The three methods and variants that were tested in this study provided very similar accuracy results, however, the

time and equipment used varied significantly between the methods. Time was divided into field processing time and office processing time. A common trend in the data was that more time spent in the field resulted in less time needed for office processing and vise-versa. This is a key consideration as the cost requirements of field time can often time be significantly higher than that of office processing time (*e.g.*, charges for construction delay, road closures, per diem for surveyors, environmental conditions, and traffic).

5.3 3D Positional Error and 2D Slope Evaluation for LiDAR Using Natural Features

The methodology presented in this chapter enables rapid verification of ALS, MLS, or TLS data accuracy over a more inclusive range (as opposed to individual point verifications). The method was specifically designed as a quality assurance check on the absolute accuracy of the point cloud. It has been revealed that fixing the absolute alignment of the point cloud can also provide a means of measuring the relative accuracy of the point cloud. Errors in relative accuracy are often hard to detect in a point cloud, unless they are exceedingly evident, and may go unnoticed until the equipment is sent in for calibration. The ability to verify both relative and absolute horizontal and vertical accuracy to high precision is very important to the laser scanning industry, and this methodology demonstrates that this can be done with an improved level of confidence.

WORKS CITED

3D Laser Mapping, (2011). "3DLM Helps Reduce Motorway Congestion." http://www.3dlasermapping.com/index.php?option=com_content&view=article&id=193:-3d-laser-mapping-helps-reduce-motorway-congestion&catid=7:news&Itemid=39

ASPRS Mobile Mapping Committee, (2011). Unpublished PowerPoint slides from meeting on May 2, 2011.

ASPRS Press Release, (2011). "LAS 1.4 Specification Approved by ASPRS Board." http://www.asprs.org/Press-Releases/LAS-1-4-Specification-Approved-by-ASPRS-Board.html

ASPRS Standards Committee, (2005). The 1st draft of the ASPRS LiDAR Guidelines on Reporting Horizontal Accuracy. (in review), http://www.asprs.org/a/society/committees/standards/Horizontal_Accuracy_Reporting_for_Lidar_Data.pdf

ASPRS Standards Committee, (2010). LASer (LAS) File Format Exchange Activities, http://www.asprs.org/society/committees/standards/LiDAR_exchange_format.html

ASTM E57, (2010). Lib E57: Software Tools for Managing E57 Files, http://www.libe57.org/.

Bae, K.H., and D.D. Lichti, (2006). Automated registration of unorganized point clouds from terrestrial laser scanners. Curtin University of Technology.

Barber, D., J. Mills, and S. Smith-Voysey, (2008). "Geometric validation of a ground-based mobile laser scanning system." *ISPRS Journal of Photogrammetry and Remote Sensing* Vol. 63, no. 1: 128–141.

Barry, K., (2011). "BMW Tests an Autonomous Vehicle." *Wired*, http://www.wired.com/autopia/2011/08/bmw-tests-an-autonomous-vehicle/

Becker, S., and N. Haala, (2007). "Grammar supported facade reconstruction from MLS mapping." *International Archives of Photogrammetry, Remote Sensing and Spatial Information Sciences* Vol. 38: 229–234.

Besl, P.J., and N.D. McKay, (1992). A method for registration of 3-D shapes, *IEEE Transactions on pattern analysis and machine intelligence* 14(2):239-256.

Böhler, W., (2006). “Comparison of 3D laser scanning and other 3D measurement techniques.” *Recording, Modeling, and Visualization of Cultural Heritage,* Baltsavias *et al.*, (eds), Taylor & Francis Group, London, pp. 89-99.

Boehler, W., M. Bordas Vicent, and A. Marbs (2003). “Investigating laser scanner accuracy.” *The International Archives of Photogrammetry, Remote Sensing and Spatial Information Sciences* Vol. 34, no. 5: 696–701.

Brenner, C., (2009). “Extraction of features from mobile laser scanning data for future driver assistance systems.” *Advances in GIScience* : 25–42.

Burtch, Robert., (2006). “Mobile Mapping Systems” *Unpublished Lecture Notes*, http://www.ferris.edu/faculty/burtchr/sure382/lessons/Lesson_4.pdf.

Cahalane, C., T. McCarthy, and C. P Mc Elhinney., (2010). “Mobile mapping system performance–an initial investigation into the effect of vehicle speed on laser scan lines.” *RSPSoc* no. 2005.

California Department of Transportation (CALTRANS), (2011). “Chapter 15, Terrestrial Laser Scanning Specifications.” *Surveys Manual.*

Chang, J.R., K.T. Chang, and D.H. Chen, (2006). “Application of 3D Laser Scanning on Measuring Pavement Roughness.” *Journal of Testing and Evaluation, 34*(2).

Chiang, K.W., Y.S. Huang, M.L. Tsai, and K.H. Chen, (2010). “The Perspective from Asia Concerning the Impact of Compass/Beidou-2 on Future GNSS.” *Survey Review* 42 (315): 3–19.

Chin, A., and M.J. Olsen, (2011). “Comparison of Inertial Profiler measurements with leveling and 3D laser scanning results for pavement profiles.” *Road Profile Users' Group (RPUG) Conference*.

Clancy, S., (2011). “The Importance of Applied Control.” *LiDAR Magazine* Vol. 1, no. 2, http://lidarnews.com/emag/2011/vol1no2/index.html

Duffell, C. G., and D. M. Rudrum, (2005). “Remote Sensing Techniques for Highway Earthworks Assessment.”

Federal Aviation Administration (FAA), (2011). “Standards for Using Remote Sensing Technologies in Airport Surveys, AC 150/5300-17C”. http://www.faa.gov/documentLibrary/media/Advisory_Circular/150_5300_17c.pdf

Federal Geographic Data Committee (FGDC), (1998). “Geospatial Positioning Accuracy Standards Part 3: National Standard for Spatial Data Accuracy”. http://www.fgdc.gov/standards/projects/FGDC-standards-projects/accuracy/part3/chapter3

Glennie, C., (2009). “A kinematic terrestrial LiDAR scanning system.” *In Proceedings of the Transportation Research Board 88th Annual Meeting*, Washington DC, January 11th to 15th, 09–0122.

Glennie, C., (2009). “Kinematic Terrestrial Light-Detection and Ranging System for Scanning.” *Transportation Research Record: Journal of the Transportation Research Board* Vol. 2105, no. 1: 135–141.

Glennie, C., (2007). “Reign of point clouds. A kinematic terrestrial LiDAR scanning system.” *Inside GNSS* Vol. 2, no. 7: 22–31.

Glennie, C., (2007). “Rigorous 3D error analysis of kinematic scanning LiDAR systems.” *Journal of Applied Geodesy* Vol. 1, no. 3: 147–157.

Glennie, C., and D. D Lichti, (2010). “Static Calibration and Analysis of the Velodyne HDL-64E S2 for High Accuracy Mobile Scanning.” *Remote Sensing* Vol. 2, no. 6: 1610–1624.

Grafe, G., (2008). “Kinematic 3D laser scanning for road or railway construction surveys.” *Proceedings of First International Conference on Machine Control and Guidance*.

Graham, L., (2010). “Mobile Mapping Systems Overview.” *Photogrammetric Engineering & Remote Sensing* Vol. 76, no. 3: 222-228.

Haala, N., M. Peter, J. Kremer, and G. Hunter, (2008). “MLS Mapping for 3D Point Cloud Collection in Urban Areas-a Performance Test.” *The International Archives of the Photogrammetry, Remote Sensing and Spatial Information Sciences* Vol. 37: 1119–1127.

Herr, W., (2010). “Unification of Roadway Surface Dimensional Measurements.” *Phoenix Scientific Inc.* http://www.phnx-sci.com/PPS/New_Paradigm_files/New%20Paradiam%202010_0121.pdf

Hiremagalur, J., K. S. Yen, K. Akin, T. Bui, T. A. Lasky, and B. Ravani, (2007). “Creating Standards and Specifications for the Use of Laser Scanning in Caltrans Projects.” *AHMCT Rept.# UCD-ARR-07-06-30-01, Davis*.

Jacobs, G., (2005). “High Definition Surveying & 3D Laser Scanning Uses in Transportation.” *Professional Surveyor Magazine* Vol. 25, no. 4.

Jaselskis, E. J, Z. Gao, R. C Walters, and others, (2005). “Improving transportation projects using laser scanning.” *Journal of construction engineering and management* Vol. 131: 377.

Jaselskis, E. J, Z. Gao, A. Welch, and D. O’Brien, (2003). “Pilot study on laser scanning technology for transportation projects.” In *Proceedings of the 2003 Mid-Continent Transportation Research Symposium*.

Jochem, A., B. Höfle, and M. Rutzinger, (2011). “Extraction of Vertical Walls from Mobile Laser Scanning Data for Solar Potential Assessment.” *Remote Sensing* Vol. 3, no. 4: 650-667.

Kim, J. S, J. C Lee, I. J Kang, S. Y Cha, H. Choi, and T. G Lee, (2008). “Extraction of geometric information on highway using terrestrial laser scanning technology.” *The International Archives of Photogrammetry, Remote Sensing and Spatial Information Sciences,* Vol. 37, no. 5: 539–544.

Knaak, T., (2010). “TopoDOT Calibrated Image Requirements (#1001).” *Certainty 3D*, http://www.certainty3d.com/pdf/technotes/CalibratedImageReq.pdf

Knaak, T., (2012a). “Developing Requirements for Mobile LiDAR Data (#1015).” *Certainty 3D*, http://www.certainty3d.com/pdf/technotes/MobileLiDARProjectRequirements.pdf

Knaak, T., (2012b). “Two perspectives on LiDAR technology market adoption.” *LiDAR News*.

Laefer, D.F., M. Fitzgerald, E.M. Maloney, D. Coyne, D. Lennon, and S.W. Morrish, (2009). “Lateral image degradation in terrestrial laser scanning.” *Structural Engineering International* Vol. 19, no. 2: 184–189.

Mandli Communications. (2011). “MLS Captures Data for Driving Simulator.” *LiDAR News* Vol. 1, no. 18, http://www.lidarnews.com/newsletter/Vol1No18.htm

Mcquat, G.J., (2011). “Feature Extraction Workflows for Urban Mobile-Terrestrial LiDAR Data.” *MS Thesis*, http://qspace.library.queensu.ca/bitstream/1974/6530/1/Mcquat_Gregory_J_201105_MSc.pdf

Meade, M., (2008). “From the Ground Up: Horizontal Accuracy Assesment in LiDAR.” Point of Beginnings Online. http://www.pobonline.com/Articles/Column/BNP_GUID_9-5-2006_A_10000000000000449514

Mendenhall, S. (2011). “Moble Laser Scanning-CALTRANS Evaluates the Technology’s Costs and Benefits.” *CE News* Vol. 23, no 5: 42-43.

Mettenleiter, M., N. Obertreiber, F. Härtl, M. Ehm, J. Baur, and C. Fröhlich, (2008). “3D Laser Scanner as Part of Kinematic Measurement Systems.” *International Conference on Machine Control Guidance*, Vol. 1:1–9.

Miller, P., J. Mills, S. Barr, M. Lim, D. Barber, G. Parkin, B. Clarke, S. Glendinning, and J. Hall, (2008). “Terrestrial laser scanning for assessing the risk of slope instability along transport corridors.” *International Archives of Photogrammetry, Remote Sensing and Spatial Information Sciences* Vol. 37: 495–500.

National Digital Elevation Program (NDEP), (2004). “Guidelines for Digital Elevation Data, Version 1.0”. http://www.ndep.gov/NDEP_Elevation_Guidelines_Ver1_10May2004.pdf

National Oceanic and Atmospheric Administration (NOAA) Coastal Services Center. (2008). “Lidar 101: An Introduction Lidar Technology, Data, and Applications.” Charleston, SC: NOAA Coastal Services Center.

Novak, K., (2011). “How we use LiDAR to Inventory Street Lights in El Paso.” *Transmap Corporation*, http://www.transmap.com/?p=1260

Olsen, M.J., (2011). Putting the pieces together: laser scan geo-referencing, *LiDAR Magazine*, 1(2).

Olsen, M.J., S. Butcher, and E.P. Silvia, (2011). "Real-time change and damage detection of landslides and other earth movements threatening public infrastructure". *OTREC Final Report* 2011-22 and *ODOT Final Report RS* 500-500, 80p

Olsen, M.J., E. Johnstone, F. Kuester, N. Driscoll, S.A. Ashford, and others, (2011). "New Automated Point-Cloud Alignment for Ground-Based Light Detection and Ranging Data of Long Coastal Sections." *Journal of Surveying Engineering* Vol. 137: 14.

Olsen, M.J., E. Johnstone, N. Driscoll, S.A. Ashford, and F. Kuester, (2009). "Terrestrial laser scanning of extended cliff sections in dynamic environments: a parameter analysis." *ASCE Journal of Surveying Engineering* Vol. 135, no. 4: 161-169.

Olsen, M.J., R. Singh, K. Williams, and A. Chin, (2012, In Press). Transportation Applications Subchapter, ASPRS LiDAR Manual.

Persi, F., E. Hoffman, (2006). "Comparing historical and laser scan surveys to identify discrepancies." *Hydrocarbon Processing*, July 2006, 95-97.

Pesci, A., and G. Teza, (2008). Terrestrial laser scanner and retro-reflective targets: an experiment for anomalous effects investigation. *International Journal of Remote Sensing* 29 (19): 5749–5765.

POB, (2010). "Point of Beginnings Laser Scanner Survey," http://laser.jadaproductions.net/default.php

Ray, J. A., and L. Graham. (2008). "New Horizontal Accuracy Assessment Tools and Techniques for Lidar Data." In Proceedings of the ASPRS Annual Conference, Portland Oregon, USA.

Rieger, P., N. Studnicka, M. Pfennigbauer, and G. Zach, (2010). "Boresight alignment method for mobile laser scanning systems." *Journal of Applied Geodesy* Vol. 4, no. 1: 13–21.

Rusinkiewicz, S., and M. Levoy, (2001). Efficient Variants of the ICP Algorithm, *International Conference on 3D Digital Imaging and Modeling.* Los Alamitos, CA, USA: IEEE Computer Society. doi:http://doi.ieeecomputersociety.org/10.1109/IM.2001.924423.

Rybka, R., (2011). “Down-to-Earth LiDAR” *LiDAR News*. Vol 1, No 2, http://www.lidarnews.com/newsletter/Vol1No2.htm

Samberg, A., (2007). “An implementation of the ASPRS LAS standard.” *IAPRS Volume, XXXVI,-Part3/W* 52.

Silvia, E.P., and M.J. Olsen, (In Press). To Level or Not to Level: Laser Scanner Inclination Sensor Stability and Application. *Journal of Surveying Engineering*. doi:http://dx.doi.org/10.1061/(ASCE)SU.1943-5428.0000072.

Singh, R., (2009). “Engineering Automation, Key Concepts for a 25 Year Time Horizon.” V3, ODOT report.

Soudarissanane, S., R. Lindenbergh, M. Menenti, and P. Teunissen, (2011). “Scanning Geometry: Influencing Factor on the Quality of Terrestrial Laser Scanning Points.” *ISPRS Journal of Photogrammetry and Remote Sensing* 66 (4) (July): 389-399. doi:10.1016/j.isprsjprs.2011.01.005.

Tang, P., D. Huber, and B. Akinci., (2011). “Characterization of laser scanners and algorithms for detecting flatness defects on concrete surfaces.” *Journal of Computing in Civil Engineering* Vol. 25: 31.

Tao, C., R. Li, and M. A Chapman., (1998). “Automatic reconstruction of road centerlines from mobile mapping image sequences.” *Photogrammetric Engineering and Remote Sensing* Vol. 64, no. 7: 709–716.

Toth, C. K., (2009). “R&D of MLS mapping and future trends.” In *Proceeding of ASPRS 2009 Annual Conference (Baltimore, Maryland).*

Transportation Research Board, (2011). “Guidelines for the Use of Mobile LIDAR in Transportation Applications.” *NCHRP 15-44* http://apps.trb.org/cmsfeed/TRBNetProjectDisplay.asp?ProjectID=2972

U.S. Geological Survey (USGS) National Geospatial Program Lidar Guidelines and Base Specification, (2010). Version 13-ILMF 2010. http://lidar.cr.usgs.gov/USGS-NGP%20Lidar%20Guidelines%20and%20Base%20Specification%20v13%28ILMF%29.pdf

Ussyshkin, V., (2009). “Mobile Laser Scanning Technology for Surveying Application: From Data Collection to End Products.” *Proceeding of FIG*

Working Week 2009, Surveyors Key Role in Accelerated Development, Eilat, Israel.

Ussyshkin, R. V, and M. Boba., (2008). “Performance characterization of a MLS system: Expected and unexpected variables.” In *ASPRS Conference Proceedings, Portland, Oregon, USA*. Vol. 27.

Vaaja, M., J. Hyyppä, A. Kukko, H. Kaartinen, H. Hyyppä, and P. Alho, (2011). “Mapping Topography Changes and Elevation Accuracies Using a Mobile Laser Scanner.” *Remote Sensing* Vol. 3, no. 3: 587-600.

Vincent, R., and M. Ecker. (2010). “Light Detection and Ranging (LiDAR) Technology Evaluation.” Missouri Department of Transportation.

Yen, K.S., K. Akin, A. Lofton, B. Ravani, and T.A. Lasky, (2010). “Using Mobile Laser Scanning to Produce Digital Terrain Models of Pavement Surfaces.” AHMCT Research Center

Yen, K. S., B. Ravani, and T.A. Lasky, (2011). “LiDAR for Data Efficiency.” AHMCT Research Center.

Vosselman, G., H. G Maas, and others, (2010). *Airborne and terrestrial laser scanning*. Scotland: Whittles. Print.

Yoo, H. J., F. Goulette, J. Senpauroca, and G. Lepere, (2010). “Analysis and Improvement of Laser Terrestrial Mobile Mapping Systems Configurations.” *International Archives of Photogrammetry, Remote Sensing and Spatial Information Sciences* Vol. 38, no. 5.

Young, A.P., M.J. Olsen, N. Driscoll, R.E. Flick, R. Gutierrez, R.T. Guza, E. Johnstone, and F. Kuester, (2010). “Comparison of Airborne and Terrestrial Lidar Estimates of Seacliff Erosion in Southern California.” *Photogrammetric Engineering and Remote Sensing* 76 (4): 421–427.

Yousif, H., J. Li, M. Chapman, and Y. Shu, (2010). “Accuracy Enhancement of Terrestrial MLS Data Using Theory of Assimilation.” *International Archives of Photogrammetry, Remote Sensing and Spatial Information Sciences* Vol. 38, no. 5.

Zampa, F., and D. Conforti, (2009). “Mapping with MLS.” *GIM International* Vol. 23, no. 4: 35–37.

APPENDICES

APPENDIX A – GLOSSARY OF TERMS FOR THE REVIEW OF MLS IN TRANSPORTATION

Many of the following definitions have been extracted from the ASTM Designation: E2544-10, they have been cited (ASTM) after the definition. It should be noted that ASTM has gathered standard terminology from sources including: ASTM Standard E456, ASME Standard B89.4.19, ISO Standard 11146-1 and VIM, and NIST/SEMATECH Standard. In addition, ASTM E2544-10 provides greater detail and discussion about the following terminology.

Term:	Definition:
2D	Two-dimensional. Typically referring to data that has been mapped to a plane such as a map, plan view, or profile.
2.5D	Two and a half dimensional. This typically refers to the situation where a horizontal coordinate system and vertical coordinate system are separated. Generally, in this case, there is one elevation point for a given XY coordinate. Generally most DTMs are 2.5D.
3D	Three-dimensional. In a 3D Cartesian coordinate system (XYZ), there can be multiple Z values at any given XY coordinate.
3D imaging system	A non-contact measurement instrument used to produce a 3D representation (for example, a point cloud) of an object or a site. (ASTM)
Accuracy of measurement	Closeness of the agreement between the result of a measurement and a true value of the measurand. (ASTM)
Alignment	The process of aligning adjoining scans to each other, see registration.

ALS (aerial laser scan)	Laser scans that are captured from and aerial platform such as an airplane or helicopter.
Artifacts	Erroneous points in a scan that do not accurately depict the objects intended to be measured.
As-built	Refers to a survey of a project after construction.
ASCII (American standard code for information interchange)	A code used to store and transfer information between computers consisting of 128 characters.
ASTM (American Society for Testing Materials)	Agency which provides a consensus of terminology and/or specifications for testing through international volunteers.
Azimuth	An angular measurement of the scanners facing direction to north.
Beam divergence	The increase in beam width as the distance from scan origin increases.
Beam width	The extent of the irradiance distribution in a cross section of a laser beam (in a direction orthogonal to its propagation path) at a distance away from the origin. (ASTM)
Birds	Refers to actual birds captured in a scan or artificial points in sky. See artifacts.

Boresight	In MLS systems this term refers to the rotation of the laser scanner frame to align with the body frame of the IMU.
CAD\CADD (computer aided design and drafting)	The use of computer technology to design, draw, model, and analyze objects before creation in the real world.
Calibration	Set of operations that establish, under specified conditions, the relationship between values of quantities indicated by a measuring instrument or measuring system, or values represented by a material measure or a reference material, and the corresponding values realized by standards. (ASTM)
Change detection	Use of remote sensing data to analyze how the attributes of a region change over a period of time.
Consolidated vertical accuracy	A verification of vertical accuracy for several types of ground cover, which consists of bare, open ground, and other types of land cover.
Control network	A collection of identifiable points (visible or inferable), with stated coordinate uncertainties, in a single coordinate system. (ASTM)
Control point	An identifiable point which is a member of a control network. (ASTM)

CORS (continuously operating reference station)	Satellite receives that are continuously operating in a fixed location to provide highly accurate positional location for use in applications such as RTK GPS.
Cross section	A 2D planar slice of the 3D point cloud.
Decimation	A method of lowering point density in a point cloud.
DEM (Digital Elevation Model)	A DTM which has been more heavily focused on elevation values only.
Density	The number of points per unit area, can also be expressed as the average distance between points in a point cloud.
Detail Scan	A scan, or portion of scan, that is performed at higher resolution. Often a detail scan of targets will be used for better alignment.
DGPS (differential GPS/GNSS)	Use of ground-based reference stations to correct for pseudo range ambiguities in GPS/GNSS signals
DHM (digital height model)	A DEM that utilizes ground surface as a zero elevation to gain height values above ground level, commonly used for tree heights in forestry applications.
Discrete pulse	A method by which a scanner records returning pulses as a series of discrete values.

DMI (distance measuring instrument)	A device that physically measures distance traveled along the ground surface.
DSM (digital surface model)	A DEM that has not had surface features removed, vegetation and structures are preserved.
DTM (Digital Terrain Model)	A digital representation of ground surface topography, usually consisting of a grid and triangulated irregular network (TIN).
E57	A binary file format that has been specifically developed by the American Society for Testing and Materials to improve efficiency and compatibility of working with LiDAR data.
Echoes	Used to describe all reflected returns to the scanner from an emitted laser pulse, see first return, last return, multiple returns.
EDM (electronic distance measurement)	Devices that use infra-red or laser light to accurately measure distance by measuring the time-of-flight of the light.
Ephemeris	The flight path that a satellite takes through space.
Error (of measurement)	Result of a measurement minus a true value of the measurand. (ASTM)

Fast static	Result of a measurement minus a true value of the measurand. (ASTM)
Field of View (FOV)	The angular extent within which objects are measurable by a device such as an optical instrument without user intervention. (ASTM)
Filtering	The removal of points from a point cloud, often to reduce the density.
First Return	For a given emitted pulse, it is the first reflected signal that is detected by a 3D imaging system, time-of-flight (TOF) type, for a given sampling position, that is, azimuth and elevation angle. (ASTM)
Footprint	See beam width.
Full waveform	A method of recording the full returning waveform of a laser scan to permit more advanced processing than in a discrete pulse method.
Fundamental vertical accuracy	A verification of vertical accuracy using only ground control check points in a location on bare, open ground with a high probability of LiDAR sensor detection.
GDOP (geometric dilution of precision)	See PDOP (positional dilution of precision).

Geo-reference	The process of assigning a coordinate system and location information to a point or points in space.
GIS (geographic information system)	A computing program designed to analyze spatial data.
GNSS (global navigation satellite system)	A satellite system with global coverage that provides autonomous geo-spatial positioning. Includes the United States' GPS system, Russia's GLONASS, and will include China's COMPASS and Europe's Galileo.
GPS (global positioning system)	A GNSS system put into use by the United States.
Grid	A point cloud that has been reduced by assigning points into equally distributed cells, typically used as a form of DEM generation.
Ground	Used to describe the physical ground surface with any occluding material removed such as vegetation and structures
HDOP (horizontal dilution of precision)	An indicator of how well a satellite receiver can be horizontally located in 3D space based on the geometry of over-head satellites.

ICP (iterative closest point) algorithm	A software algorithm commonly used to register adjoining point clouds by iteratively minimizing the distance between paired or corresponding points in the cloud.
IMU (Inertial Measurement Unit)	A device which utilizes a combination of gyroscopes and accelerometers to provide velocity and orientation information.
INS (Inertial Navigation System)	Not applicable to mobile mapping, see IMU.
Instrument origin	Point from which all instrument measurements are referenced, that is, origin of the instrument coordinate reference frame (0, 0, 0). (ASTM)
Intensity	The quantity of laser energy measured at the scanner after light is reflected and returned from a surface. Typically scaled from 0 to 1, 0 to 255, or 0 to 65535.
LAS	A binary file format that has been specifically developed by the American Society for Photogrammetry and Remote Sensing (ASPRS) to improve efficiency and compatibility of working with LiDAR data between software packages. Current version: 1.4.
Last return	For a given emitted pulse, it is the last reflected signal that is detected by a 3D imaging system, time-of-flight (TOF) type, for a given sampling position, that is, azimuth and elevation angle. (ASTM)

Lever Arm	In MLS systems this term refers to the difference in origin of the laser scanner frame and the body frame of the IMU.
LiDAR	Light Detection And Ranging, a method of measuring the flight time of a beam of light to calculate range.
Line scan	Constraining the Z-rotation of a laser scanner so that vehicular or platform motion results in linear scan swaths through a corridor.
Local	A coordinate system that is referenced using the laser scanner location as the origin of the point cloud.
MLS (mobile laser scan)	A mobile system capable of collection of geo-referenced remotely sensed data, utilizing the use of at least one LiDAR scanner.
MMS (mobile mapping system)	A mobile system capable of collection of geo-referenced remotely sensed data, typically using imagery based sensors.
Multiple returns	The signals returned to a single detector element from simultaneously-illuminated multiple surfaces resulting from a single laser pulse. (ASTM)
Noise	See artifacts
Occlusions	Areas within a point cloud that are void of measurements due to objects blocking the scanners line of sight.

On-the-fly	1) A mode of mobile mapping that utilizes continuous movement of the mapping platform while collecting data. 2) Processing of scan data in real time.
OPUS (online positioning user service)	A service provided by the National Oceanic and Atmospheric Administration (NOAA), which allows GPS users to increase the accuracy of collected GPS point locations using through post processing.
Overview Scan	A low resolution scan, may be used to select areas specific areas within a scan which need to be scanned at higher resolution.
Panoramic scan	Allowing the scanner head to rotate in the Z-axis up to 360°.
Parallax	The apparent displacement of a distant object in relation to a nearer as viewed from different locations.
PDOP (positional dilution of precision)	An indicator of how well a satellite receiver can be located in 3D space based on the geometry of over-head satellites.
Phantom points	See artifacts
Phase-based	A method of measuring distance by observing the phase shift of a laser's sinusoidally modulated waveform, and the reflected return from a surface. Used over smaller ranges with a higher data collection rate.

Pitch	Refers to the rotation about the Y axis in a Cartesian coordinate system.
Pits	Refers to artificial points captured below the ground surface. See artifacts.
Point Cloud	A collection of data points in 3D space (frequently in the hundreds of thousands), for example as obtained using a 3D imaging system. (ASTM)
Polar coordinates	A coordinate system that locates points in space by defining an angle and a distance from a fixed reference pole.
Post spacing	Elevation or z-values at evenly spaced grid intervals in the horizontal or 'x' and 'y' direction. In airborne LiDAR, the nominal post spacing is defined as the typical separation distance between points.
PPK (post-processed kinematic)	A method of improving GPS receiver positioning by using a precisely calculated post-flight ephemeris instead of the pre-flight predicted ephemeris.
Precision	Closeness of agreement between independent test results obtained under stipulated conditions. (ASTM)
Random error	Result of a measurement minus the mean that would result from an infinite number of measurements of the same measurand carried out under repeatability conditions. (ASTM)

Range resolution	The distance, in units of length, between a point in space and an origin fixed to the 3D imaging system that is measuring that point. (ASTM)
Range	The distance, in units of length, between a point in space and an origin fixed to the 3D imaging system that is measuring that point. (ASTM)
Rapid static	Collection of 15 minutes to 2 hours of GPS data over a point location which is then submitted to OPUS for accuracy enhancement via post processing.
Raw scan data	Collection of 15 minutes to 2 hours of GPS data over a point location which is then submitted to OPUS for accuracy enhancement via post processing.
Reference frame	The coordinate system or location that is used to refer to an object or point location.
Reflectance	A measure of how much light is reflected off a surface compared to how much initially hit the surface.
Registration	The process of determining and applying to two or more datasets the transformations that locate each dataset in a common coordinate system so that the datasets are aligned relative to each other. (ASTM)

Repeatability (of results of measurements)	Closeness of the agreement between the results of successive measurements of the same measurand carried out under the same conditions of measurement. (ASTM)
Resolution	The degree of detail which can be seen. See density.
Rigid body transformation	Refers to the translation and rotation of a point cloud in which the point cloud is treated as a rigid body that has no deformation of the points with relation to other points in the cloud.
RMS(E) (root mean square (error))	An indicator of precision by measuring the differences of an estimated or modeled object to the values of the physically observed object.
Roll	Refers to the rotation about the X axis in a Cartesian coordinate system.
Rotation matrix	A matrix that is used in linear algebra to rotate a point in 3D space.
RTK (real time kinematic)	An enhancement to satellite navigation that utilized carrier phase measurements for better positioning; allows for GPS corrections in real time.
Scan	The result of a LiDAR scanner, often interchangeable with point cloud.
Spot size	See beam width

Static	Collection of 2 hours to 48 hours of GPS data over a point location which is then submitted to OPUS for accuracy enhancement via post processing.
Stop-and-go	A simplified mode of mobile mapping that utilizes non-continuous movement of the mobile mapping platform, data points are only collected while the platform is stationary.
Subsample	A lower density of points, or a small collection of points taken from a larger sample.
Supplemental vertical accuracy	A verification of vertical accuracy over ground cover that does not consist of bare, open ground.
Systematic error	Mean that would result from an infinite number of measurements of the same measurand carried out under repeatability conditions minus a true value of the measurand. (ASTM)
TIN (Triangulated Irregular Network)	A type of DTM created by generating triangles to connect points that are irregularly spaced. The three points that form each triangle are used to create a plane that is used for interpolation (typically for elevation) between the points.
Time-of-flight	A method of measuring distance by observing the time it takes for a laser beam to travel from the scanner, reflect off a surface, and return to the scanner.

TLS (terrestrial laser scan)	Laser scans that take place from a momentarily fixed platform, typically tripod based.
Transformation matrix	A matrix that is used in linear algebra to translate, without rotation, a point in 3D space.
Uncertainty of measurement	Parameter, associated with the result of a measurement, that characterizes the dispersion of the values that could reasonably be attributed to the measurand. (ASTM)
Validation	Verification that data meets certain criteria.
VDOP (vertical dilution of precision)	An indicator of how well a satellite receiver can be vertically located in 3D space based on the geometry of over-head satellites.
Voids	Areas within a point cloud which were not well detailed, typically due to blocking of the scanner line of sight.
VRS (virtual reference station)	A method of assigning a virtual base station near the survey location to permit RTK corrections along short baselines.
XYZRGBI	Any combination of these letters may be used to define a scanner file format, represented by X, Y, and Z point coordinates, (R)ed, (G)reen, (B)lue color values assigned to the point, and (I)ntensity value assigned to the point.

Yaw	Refers to the rotation about the Z axis in a Cartesian coordinate system.

APPENDIX B – INDIVIDUAL TARGET TRANSFORMATION PARAMETERS FOR CHAPTER 3

Retro-target								
Scan Position	Overall Std. Deviation (m)	Std. deviation X (m)	Std. deviation Y (m)	Std. deviation Z (m)	Std. deviation ϕ (m)	Std. deviation ν (m)	Std. deviation ψ (m)	Corresponding points
1	0.0033	0.0015	0.0032	0.0083	0.0011	0.0028	0.0017	5
2	0.0048	0.0051	0.0022	0.0079	0.0018	0.0028	0.0025	6
3	0.0028	0.0014	0.003	0.0051	0.0009	0.0011	0.0019	6
4	0.0036	0.0045	0.0017	0.0108	0.0013	0.003	0.0027	6

Paper target								
Scan Position	Overall Std. Deviation (m)	Std. deviation X (m)	Std. deviation Y (m)	Std. deviation Z (m)	Std. deviation ϕ (m)	Std. deviation ν (m)	Std. deviation ψ (m)	Corresponding points
1	0.0077	0.0035	0.0076	0.0195	0.0025	0.0066	0.0041	5
2	0.0116	0.0137	0.0054	0.0224	0.0046	0.0088	0.0064	5
3	0.0066	0.0034	0.007	0.0121	0.0022	0.0025	0.0045	6
4	0.0093	0.0132	0.005	0.0435	0.0035	0.0115	0.0116	5

APPENDIX C – CONDENSED INSTRUCTIONS FOR SLOPE AND VISUAL SHIFT QUALITY ASSURANCE SPREADSHEET

Field Procedures

1. Collect total station cross-sections within the region of the point cloud.
    a. Take measurements ~1ft in a straight line (use laser or chalk line) at each leg of the intersection.
    b. Avoid pavement patches, roadway rutting, and transition zones within the intersection.
2. Take measurements to geo-referencing control.

Processing Procedures

1. Overlay the total station points within the point cloud.
2. Define a plane for each linear collection of total station points.
3. Set the plane width only wide enough to encompass all total station points ~1inch if collection was done with a laser or chalk line.
4. Extract the scan points that correspond to the total station points (*i.e.*, not the whole plane; only the points along the cross-slope of the roadway that correspond to the width of the roadway curb-to-curb.

Spreadsheet Procedures

1. Ensure the spreadsheet Raw Data tab is void of all data.
2. Paste in scan and total station points for each leg of the intersection. Note that north, south, east, west orientation does not matter it is used for consistent directionality.
3. Data will be carried over to the N,S,E,W-Calcs tabs.

4. In each N,S,E,W-Calcs tab verify that the Total Station X' values contain no negative values.
    a. If negatives are found, total station points are outside of the scan bounding box, manually remove these points.
5. Carry X' and Y' values for the scan and total station to their respective columns titled Scan, sort increasing X, and TS, sort increasing X (Column AE-AJ). Also, carry over the original Z-values for the scan and total station.
6. Sort column AE-AG, and column AH-AJ by increasing X' values
7. Select the high Z-value in each of these groupings and indicate the X'Y'Z values
    a. The high Z-value should be the crown of the road, view the plot at row 38 column Z to verify that the roadway has a crown that would be the high Z-value.
8. Update the plots by selecting all scan and total station left data as that which lies above the selected high Z from step 7.
9. Plot the right section by selecting all values that lie below the high Z-value from step 7.
10. Use the highlighted yellow box indicating delta X and Z to shift the data into a visual alignment.
    a. These shift values provide an indication of horizontal and vertical accuracy. Note that horizontal accuracy of this shift is applicable to how the shift would have occurred in the original coordinate system.

APPENDIX D – DIGITAL ACCESS TO SLOPE AND VISUAL SHIFT QUALITY ASSURANCE SPREADSHEET